

THE CONTRIBUTION OF RECENTLY-ASSIMILATED
CARBON TO SOIL RESPIRATION

by

Andrew Burton Moyes

A dissertation submitted to the faculty of
The University of Utah
in partial fulfillment of the requirements for the degree of

Doctor of Philosophy

Department of Biology

The University of Utah

August 2010

Copyright © Andrew Burton Moyes 2010

All Rights Reserved

The University of Utah Graduate School

STATEMENT OF DISSERTATION APPROVAL

The dissertation of Andrew Burton
has been approved by the following supervisory committee members:

David R. . Chair May 6, 2010

Thure E. . Member May 6, 2010

James R. . Member

K. Solomon . Member May 6, 2010

John S. . Member May 6, 2010

and by . Chair of
the Department of

and by Charles A. Wight, Dean of The Graduate School.

ABSTRACT

The aim of the research reported in this dissertation was to define and quantify the contribution of recent photosynthetic carbon uptake to spatial and temporal patterns of CO_2 respiration from soils. Carbon dioxide is produced in soils primarily by roots and heterotrophic bacteria and fungi. Roots use carbon from recent photosynthesis or storage for growth, maintenance, and nutrient uptake, and a large fraction of soil microorganisms live in close proximity to roots and consume short-lived tissues and root exudates. Thus, both of these components largely depend on carbon that has been assimilated only hours to months before. Therefore, it was expected that seasonal patterns of uptake and use of carbon associated with particular vegetation types would be primary drivers of spatial and temporal variability in soil respiration. However, it was also expected that these general patterns would be mediated by environmental conditions.

I conducted a multiyear analysis of soil CO_2 production in a Rocky Mountain meadow and found that respiration during spring and summer months was tightly coupled to growth of meadow vegetation. In three consecutive summers, soil respiration rates rose with increasing aboveground plant biomass, peaked just before meadow vegetation started to senesce (apparent as a cessation of soil moisture depletion), and then decreased despite continued increases in soil temperature.

I compared seasonal soil respiration patterns in adjacent meadow and riparian tree vegetation zones and found that plant phenology was a stronger driver of seasonal and

spatial variability in soil respiration than soil temperature or extractable soil organic carbon or microbial biomass carbon.

I developed a method to assess the carbon isotope ratio ($\delta^{13}\text{C}$) of CO_2 in fine-scale soil profiles for determination of $\delta^{13}\text{C}$ of CO_2 respired by the composite of all soil sources. I applied this method and continuous open soil chambers in a root exclusion (trenching) experiment to analyze the effect of root activity on seasonal patterns of rates and $\delta^{13}\text{C}$ of CO_2 production in soil. Presence of roots accounted for ~75% of soil respiration in the summer, and this source was about 1 ‰ enriched in ^{13}C relative to summer heterotrophic respiration in trenched plots.

TABLE OF CONTENTS

ABSTRACT.....	iii
LIST OF FIGURES.....	vii
ACKNOWLEDGEMENTS.....	x
Chapter	
1. INTRODUCTION.....	1
The Chapters.....	4
2. SEASONALITY OF TEMPERATURE, MOISTURE, AND SUBSTRATE CONTROLS ON SOIL RESPIRATION IN A ROCKY MOUNTAIN MEADOW.....	6
Abstract.....	6
Introduction.....	7
Methods.....	10
Results.....	16
Discussion.....	19
3. PLANT PHENOLOGY REGULATES SEASONAL VARIATION OF SOIL RESPIRATION ALONG ROCKY MOUNTAIN TREE-MEADOW TRANSECTS.....	32
Abstract.....	32
Introduction.....	33
Methods.....	36
Results.....	43
Discussion.....	46
Conclusions.....	54

4. DIFFUSIVE FRACTIONATION COMPLICATES ISOTOPIC PARTITIONING OF AUTOTROPHIC AND HETEROTROPHIC SOURCES OF SOIL RESPIRATION.....	63
Abstract.....	63
Introduction.....	64
Methods.....	67
Results.....	80
Discussion.....	83
Conclusions.....	93
 APPENDIX: AN INJECTION METHOD FOR MEASURING THE CARBON ISOTOPE CONTENT OF SOIL CARBON DIOXIDE AND SOIL RESPIRATION WITH A TUNABLE DIODE LASER ABSORPTION SPECTROMETER.....	103
 REFERENCES.....	111

LIST OF FIGURES

Figure

- 2.1 Soil temperature (a), volumetric water content (θ , b), snow depth (c), and CO₂ (d), and modeled surface CO₂ flux (e) vs. time for the entire study period.....26
- 2.2 Vertical profiles of CO₂ within the soil measured at specific dates during the 2005/06 (a) and 2006/07 (b) winters, shown to highlight the interannual differences.....27
- 2.3 Parameterization and validation of diffusion model.....28
- 2.4 Daily means of volumetric water content at 10 cm (a), soil temperature at 10 cm (b), calculated CO₂ production rate for soil within the 0-22 (c) and 22-48 (d) cm ranges of soil depth, modeled CO₂ surface flux (e), and cumulative respired carbon (f) for each growing season during the study.....29
- 2.5 Modeled surface CO₂ flux vs. soil temperature at 10 cm for each of the three complete growing seasons of the study (left panels). Each season was divided into three periods, with the first division (day 169) identified by the maximum respiration rate from averaged model results for all three years (middle right panel), and the second division (day 213) identified as the average seasonal maximum soil temperature at 10 cm (upper right panel). These divisions are shown as vertical dotted lines in the upper right panels. The lower right plot is a schematic representation of the relationship between CO₂ flux and soil temperature over the course of each of the three periods.....30
- 2.6 Slopes of change in soil T at 10 cm (a), surface CO₂ flux (b), and volumetric water content (θ) at 10 cm (c) for successive 5-day windows of daily-averaged data from all years.....31

3.1	Schematic showing tree-meadow transect positions for soil chamber, gas well, soil organic carbon (SOC), and microbial biomass carbon (MBC) measurements.....	55
3.2	Soil temperature (a) and volumetric water content (θ , b) at 10 cm depth within the meadow during 2006.....	56
3.3	Photographs taken looking northwest from a central position in the meadow, showing phenological status of trees and meadow vegetation on the five intensive sampling dates in 2006.....	57
3.4	Top row: Point measurements of CO ₂ fluxes vs. transect position relative to the canopy dripline (see Figure 3.1) of each tree, volumetric water content (θ) over 0-20 cm depth (via moisture probe (2005) or gravimetric measurements (2006)), and soil temperature at 10 cm. Vertical column: CO ₂ flux, volumetric water content (as above), and soil temperature at 10 cm plotted vs. transect position relative to the canopy dripline. Lower right panel: relationship between soil moisture and temperature at 10 cm.....	58
3.5	Extractable microbial biomass carbon ((a), MBC), extractable soil organic carbon ((b), SOC), and modeled surface CO ₂ flux (c) vs. transect position for each of the five intensive sampling periods (separated by vertical dotted lines). (d), model results of CO ₂ production with depth for each transect position during each sampling period.....	59
3.6	Calculated rates of production of CO ₂ within the top 10 cm of soil for each transect position vs. extractable microbial biomass carbon (MBC, (a)) and extractable soil organic carbon (SOC, (b)) from 10 cm-deep soil cores.....	60
3.7	Modeled surface CO ₂ flux for each of the five intensive sampling dates (numbers) vs. soil temperature ((a), and (b)) and volumetric water content (θ , (c) and (d)) at 10 cm. Plots (a) and (c) are data from 1.5 m transect positions (under tree canopies) and (c) and (d) are data from 9 m positions (in open meadow).....	61
3.8	Soil carbon dioxide at 20 cm depth vs. transect position over sampling dates throughout the 2006 growing season.....	62

4.1	Overhead view of plot setup showing one of six replicate plot pairs under individual boxelder trees.....	95
4.2	Temperature, soil respiration fluxes, and $\delta^{13}\text{C}$ of soil respiration for trenched and untrenched plots during the study period.....	96
4.3	Carbon isotope ratio of soil-respired CO_2 derived from soil gas profiles (\circ) and three-hour means from open chambers (\bullet) on individual plots with (top two panels) and without (bottom two panels) roots during 2008.....	97
4.4	Comparison of fluxes and $\delta^{13}\text{C}$ of soil-respired CO_2 using two method combinations: afternoon closed chamber flux measurements vs. $\delta^{13}\text{C}$ of soil respired CO_2 from gas profile-derived Keeling plots (a), and daily average fluxes vs. $\delta^{13}\text{C}$ of soil-respired CO_2 from open chambers (b). (c) Bulk $\delta^{13}\text{C}$ values from sieved soils (soil with roots and rock pieces removed, from the +Roots or the – Roots plots) and plant tissues (open symbols) and the $\delta^{13}\text{C}$ of their respired CO_2 (closed symbols).....	98
4.5	$\delta^{13}\text{C}$ of soil respiration from open chamber measurements from each of the four collars during days 220 – 235 of 2008, showing differences in diel $\delta^{13}\text{C}$ variability.....	99
4.6	Open chamber data from the plot 1 pair of untrenched (+ Roots) and trenched (- Roots) treatments, averaged from days 215–224, 2008.....	100
4.7	Diel variation in $\delta^{13}\text{C}$ of soil respiration plotted against soil respiration flux (a) and the coefficient of variation of the respiration flux (b).....	101
4.8	Diel variation in $\delta^{13}\text{C}$ of soil respiration plotted against soil respiration flux (a), the coefficient of variation of the respiration flux (b), and the depth of zero production (c, $z_{R=0}$). Panels (a) and (b) contain data from the current study, model results, and results from 4 published studies for comparison. Model results on all panels were obtained from 320 model simulations (including data beyond the axes limits of (a) and (b)).....	102

ACKNOWLEDGEMENTS

I would like to thank my advisor, Dave Bowling, for his incredible mentorship, his inexhaustible and unwavering support, and for his enthusiasm for my research and my scientific development. Dave provided the structure and feedback necessary for me to make progress through my dissertation research and graduate school, but always with just the right balance of freedom to find my own solutions and encouragement to believe that I could. I have felt tremendously fortunate to have had such an advisor, for many reasons beyond (but certainly including) the fact that he shares my unusual fondness for great salsa and hot peppers. I would also like to thank the rest of my committee for their ideas and feedback at committee meetings and whenever I approached them for help.

I have appreciated the support of my family throughout my graduate studies. Thanks especially to my wife Angel for helping me through stressful moments, such as preparing presentations, traveling for meetings, staying up late writing, or spending irregular hours in the field whenever the weather and plant conditions were right. I would like to thank the members of the Bowling lab for discussions and assistance with projects. In particular, Sarah Gaines helped with an immense amount of data collection in the field and lab work, for which I am extremely grateful. Tim Jackson and Kevin Hultine helped with setting up instrumentation and Susan Bush helped me dig root exclusion trenches at the experimental garden. Andy Schauer, Craig Cook, and Mike Lott provided technical assistance with instrumentation. I am also grateful for funding

from teaching assistantships from the University of Utah Biology Department, research assistantships from Jim Ehleringer and Dave Bowling, and the A. Herbert and Marian W. Gold Scholarship. The appendix was published with permission from Rapid Communications in Mass Spectrometry.

CHAPTER 1

INTRODUCTION

There is currently a clear impetus among the scientific community to understand the global carbon cycle. Burning of fossil fuels is adding an estimated 6.3 Gt (6,300,000,000 metric tons) of carbon to the atmosphere every year (Schimel et al. 2001). While fossil fuel combustion has increased atmospheric carbon dioxide concentrations to levels unprecedented in the last 400,000 years (Petit et al. 1999), this efflux is much smaller than the 120 Gt estimated to come from the respiration of Earth ecosystems (Schimel 1995). More than half of this respiration flux, about 75 Gt, comes from the soil (Schlesinger and Andrews 2000). The balance between these very large sources of CO₂ and uptake by all vegetation on the globe (also about 120 Gt/yr) determines the rate and direction of change in atmospheric CO₂ concentrations (Schulze 2006). Due to the complexity of factors affecting these processes, the relative increase in atmospheric CO₂ from one year to the next can be highly variable (Keeling et al. 1995, Schimel et al. 2001).

Soils currently store two to three times as much carbon as exists in the atmosphere (Schimel 1995, Davidson et al. 2000). There is a general concern that feedbacks between CO₂ concentrations and rising temperatures will lead to accelerated rates of respiration of these stores, exacerbating the current CO₂ rise attributed to fossil fuel combustion (Knorr et al. 2005).

Concern about a warming-CO₂ feedback loop stems from the long understanding of temperature as a driver of respiration. Increasing temperatures can offset the net balance of photosynthesis and respiration through direct stimulation of metabolic activity (Fang and Moncrieff 2001, Luo et al. 2001), melting frozen soils at high latitudes containing accumulated carbon (Goulden et al. 1998, Hirsch et al. 2002b), or changing the timing of snowmelt and initiation of the growing season (Monson et al. 2005). However, temperature is only one factor contributing to variability in soil respiration.

Recent work has uncovered rapid links between photosynthesis and soil respiration. An isotopic CO₂ label applied to the upper canopy of beech trees in Switzerland measurably affected the isotopic composition of soil air within weeks (Steinmann et al. 2004b). Clipping and shading treatments on tallgrass prairie species were shown to cause rapid and significant reductions of soil surface fluxes around the plants (Bremer et al. 1998, Craine et al. 1998, Wan and Luo 2003). A study in which a large section of trees in a forest was girdled (cut around the perimeter of the trunks to stop the flow of sugars downward to roots through the phloem) found a reduction of soil respiration by about 37% within 5 days (Hogberg et al. 2001). Within 2 months, soil respiration was less than half of what it had been before the girdling treatment.

The contribution of roots to soil surface fluxes has been investigated directly with trenching experiments. The fraction of total respiration from rhizosphere components has been found to be 30-60% in a French beech forest (Epron et al. 2001), 25 and 65% for young and old stands in a larch plantation, respectively (Jiang et al. 2005), 49-57% in a Japanese cedar forest (Ohashi et al. 2000), and 27-71% in a Japanese deciduous forest (Lee et al. 2003). These annual values do not reflect the variable contributions associated

with season; during the growing season they may be much higher (Hanson et al. 2000). Campbell et al. (2004) found that variability in respiration in a wide variety of Oregon forests was best predicted by the amount of living fine roots.

The connection between assimilation and soil respiration has also been observed following periods when weather conditions are favorable for photosynthesis (Bowling et al. 2002b, Ekblad et al. 2005). These studies found that forest soil respiration is primarily derived from carbon assimilated approximately 1 week prior to respiration measured on a given day or night. The 1-week period between changing conditions and a measured respiration response coincides with the time of translocation of photosynthates from leaves to roots. These findings contribute to a growing interpretation that respiration in soils is driven largely by root respiration and decomposition of labile, young sources.

Over the course of a year in temperate ecosystems, seasonal patterns of productivity related to plant phenology and functional types (e.g., trees vs. annuals) and spatial patterns of plant distribution will lead to variations in supply of substrate for soil respiration. This supply and its utilization will also be constrained by environmental variations in weather, soil temperature, moisture, and soil physical and chemical properties. The relative importance of these variables in ecosystems over time needs to be defined in order to understand and model the respiratory flux of ecosystems (Reichstein et al. 2003, Del Grosso et al. 2005). An accurate estimation of this flux is a necessary part of understanding and interpreting the overall carbon balance of ecosystems and feedbacks to increasing atmospheric CO₂.

The primary goal of the research described in this thesis was to test the hypothesis that variation in primary productivity is a central driver of seasonal and spatial variability in soil respiration. Studies were designed to consider the dominant variables leading to variation in soil respiration, with the central goal of understanding links between productivity and respiration in soils. One option for study is to manipulate conditions to provide variation in each parameter individually. Another is to capture as much natural variation as possible and look for “natural experiments” within which single parameters vary. In an effort to understand soil respiration in the larger context, my research made use of both approaches.

The Chapters

Chapter 2 describes a study conducted to determine soil respiration continuously at a single location in a Rocky Mountain meadow over a 3.5-year period. Soil respiration in the meadow followed three phases over the year: 1) spring, when soil respiration increased with meadow plant growth; 2) midsummer, when soil respiration decreased with senescence of meadow plants despite increasing soil temperatures; and 3), fall, when soil respiration was enhanced by litter inputs and stimulated by fall rains, but decreased with temperature.

Chapter 3 investigates the role of plant type and phenology on spatial and seasonal patterns of soil respiration in two growing seasons (2005 and 2006). A dense growth of a nitrogen-fixing forb was associated with high soil respiration in 2005. In 2006 seasonal patterns of soil respiration were related to differences in meadow and tree

phenology, which was a stronger driver of soil respiration than soil organic carbon and microbial biomass carbon.

Chapter 4 details a trenching experiment, in which seasonal contributions of rhizospheric and heterotrophic sources of soil CO₂ production were examined, as well as the natural abundance variability in carbon isotope ratios of CO₂ respired by these sources. Summer respiration was decreased by 75% by trenching to remove roots. Carbon isotope ratio variability in respired CO₂ was related to presence of roots, seasonal changes in heterotrophic respiration, and diel fluctuations driven by transient diffusive fractionation.

The appendix outlines a novel method developed to determine the carbon isotope ratio of carbon dioxide from soil gas profiles using a tunable diode laser absorption spectrometer. This new method was applied in the study described in chapter 4 to investigate carbon isotope ratio variability of soil respiration components.

CHAPTER 2

SEASONALITY OF TEMPERATURE, MOISTURE, AND

SUBSTRATE CONTROLS ON SOIL RESPIRATION

IN A ROCKY MOUNTAIN MEADOW

Abstract

In seasonally drought-stressed ecosystems, soil moisture and plant phenology can have large impacts on the apparent temperature sensitivity of soil respiration. To understand how soil respiration will impact ecosystem carbon balance in changing environments it is necessary to evaluate the interannual variability of seasonal drivers of soil respiration over multiple years. We investigated the seasonal importance of soil temperature, moisture, and plant phenology on soil respiration in a meadow in the mountains of northern Utah, USA, characterized by seasonal shifts between cold, wet winters and hot, dry summers. We calculated shallow and deep soil CO₂ production and surface fluxes using continuous measurements of soil profiles of CO₂, temperature, and moisture over a 3.5-year period (2005-2008). Soil respiration in all years reached a maximum just before soil moisture became limiting and meadow vegetation senesced. The timing of meadow senescence varied between years with amount of winter and spring precipitation, but on average occurred about 45 days before soil temperatures peaked. Soil respiration fluxes then decreased until the arrival of substantial fall rains.

Years with earlier fall rains were associated with larger sustained increases in soil respiration than years with rains occurring later. Physical effects of winter snow and ice impacted winter and spring flux rates by mediating the loss of CO₂ stored in deep soil horizons. Early spring surface CO₂ fluxes were apparently enhanced several-fold during one year by efflux of CO₂ which had accumulated in the soil pores beneath a winter surface ice layer. The dependence of temperature sensitivity of soil respiration on soil moisture and plant phenology suggests that soil carbon storage at this site is probably less dependent on projected changes in temperature than on future variations in amount and timing of precipitation, which are more difficult to predict.

Introduction

Soil temperature is a first-order control of soil respiration, and a recent meta-analysis of published soil respiration fluxes found that respiration rates have been increasing globally with air temperature over the last 50 years (Bond-Lamberty and Thomson 2010). For a limited number of sites a single empirical temperature relationship is adequate to describe variation in soil respiration over daily to annual time scales (Lloyd and Taylor 1994, Fang and Moncrieff 2001). In the majority of locations where water or other limitations constrain biological activity, simple temperature relationships fail to capture seasonal variability in soil respiration. Further, soil temperature and other variables such as soil moisture often covary, making it difficult to quantify their individual effects on soil respiration (Davidson et al. 1998, Davidson et al. 2006). The large body of soil and ecosystem respiration literature that has accumulated in the last two decades has revealed that responses of respiration fluxes to environmental

changes are sensitive to complex, site-specific interdependencies between abiotic conditions and plant and soil microbial interactions (Wardle et al. 2004, Ryan and Law 2005, Davidson and Janssens 2006, Kuzyakov 2006, Subke et al. 2006, Paterson et al. 2009).

Low soil moisture availability can limit soil respiration by reducing plant assimilation of carbon for phloem transport to roots and the rhizosphere, or limiting access to soil carbon for heterotrophic microorganisms. Often a consistent, site-specific soil moisture limitation may be identified, and a model incorporating soil moisture and temperature can be fit to explain soil respiration variability over the year (Savage and Davidson 2001, Xu and Qi 2001, Boroken et al. 2002, Palmroth et al. 2005, Curiel Yuste et al. 2007). However, responses to drought and precipitation may vary substantially from year to year (Savage and Davidson 2001, Fierer et al. 2005, Irvine et al. 2008). Rapid soil moisture increases associated with seasonal drought-ending precipitation can immediately raise soil carbon availability to heterotrophic microorganisms and fuel a burst of microbial respiration (reviewed by Boroken and Matzner 2009). In arid ecosystems, rain pulses can stimulate widely varying amounts of soil respiration, depending on pulse size and timing, soil texture, and the status of plants and soil microbes at the time of precipitation (Austin et al. 2004).

On long timescales and over regional spatial scales, soil respiration corresponds with primary productivity (Raich 1992, Janssens et al. 2001), and autotrophic and heterotrophic sources of soil respiration are positively correlated (Bond-Lamberty et al. 2004). Substrate availability for root and rhizosphere respiration depends on the supply of photosynthate and use of stored carbon, which vary with plant type and environmental

conditions. For example, in a seasonally dry ponderosa pine forest, seasonal (Irvine et al. 2005) and interannual variability in soil respiration over a 6-year period (Irvine et al. 2008) was shown to correspond with variability in ecosystem primary productivity. Seasonal changes in carbon assimilation or the utilization of stored carbon have been shown to cause large fluctuations in the apparent temperature sensitivity (Q_{10}) of soil respiration (Janssens and Pilegaard 2003, Curiel Yuste et al. 2004, Savage et al. 2009). This dependence of soil respiration on input of recently-fixed carbon results in part from root and rhizosphere respiration and in part through stimulation of decomposition by rhizodeposition (Kuzyakov et al. 2000). Annual and seasonal inputs of detritus to heterotrophic organisms also may vary widely, as pulses associated with above- and below-ground dieback and litter production are also dependent on plants and their environment. While the fast-cycling component of soil respiration (root and rhizosphere respiration and decomposition of fresh litter) is largely dependent on inputs of substrate and thus variability in assimilation (Boone et al. 1998, Lavigne et al. 2003), feedbacks between atmospheric CO_2 , environmental changes, and net ecosystem carbon balance depend on changes in storage of more stable soil organic carbon (Kuzyakov 2006). There is evidence that any increases in net primary productivity of ecosystems due to elevated atmospheric CO_2 may lead to enhanced mineralization of old soil organic matter, especially in nitrogen-poor soils (Sulzman et al. 2005, Paterson et al. 2009).

Thus, the controls on soil respiration depend on site-specific details on a wide range of temporal scales (Bardgett et al. 2005), and research is needed to predict soil respiration responses to environmental changes via dynamic abiotic and biotic interactions. Long-term data sets are necessary to define these relationships, as

interannual variability leads to incorrect conclusions drawn from individual years, and years with unusual conditions (e.g., El Niño years) can have a disproportionate impact on long-term carbon balance for sites (Fierer et al. 2005). Unfortunately, relatively few long-term (multi-year) studies are available characterizing seasonal and interannual patterns of soil respiration and its biotic and abiotic drivers. We conducted a study to determine the seasonal importance of temperature, moisture, and substrate supply to soil respiration in an herbaceous meadow in the Wasatch Mountains of northern Utah. The Great Basin site is beyond the reach of summer rain from the North American monsoon, and experiences cold, snowy winters and hot, dry summers (Ehleringer et al. 1992).

Methods

Site description

Field measurements were made in a 4.3 ha meadow in Red Butte Canyon (111°47'46.83"W, 40°47'20.78"N, 1758 m elevation) above Salt Lake City, Utah, USA. The meadow sits on a flat, open area of deep soil accumulated by downslope erosion of the steep, rocky canyon hillsides. A perennial stream runs along one side of the meadow, which is surrounded by boxelder (*Acer negundo*) and bigtooth maple (*Acer grandidentatum*) trees. The understory meadow vegetation primarily consists of native and introduced herbaceous perennials and annuals. Mean annual precipitation at the site is about 500 mm, mostly falling in winter, and soils are loamy, deep, and well-drained (Ehleringer et al. 1992). Additional site details were described by Hultine et al. (2007).

Automated CO₂, moisture, and temperature profile measurements

Sensors and gas inlets were installed near the center of the meadow in June 2004 for measurement of vertical profiles of CO₂, temperature, and water content. A pit with a surface area of ~0.5 m² was hand-excavated to 50 cm depth. The surface soil horizons were placed to the side of the pit in large, intact pieces and were replaced with minimal disturbance after the pit was backfilled. Soil moisture sensors (CS615, Campbell Scientific, Logan UT, USA), thermocouples (Type T), and gas inlets were installed horizontally at 3, 10, 22, and 48 cm depths into intact soil through the wall of the pit, in non-overlapping positions. The gas inlets consisted of a 25.5 cm length of 5 mm ID PTFE tubing (International Polymer Engineering, Tempe AZ, USA) within a protective length of 1.3 cm OD perforated polyethylene tubing. The PTFE tubing allowed diffusion of gases but prevented liquid water from being sampled, and was attached to sample tubing using 6.35 mm barb fittings with a cap at the distal end. The proximal end was fitted with a reducing union attached to a 2 m length of 1.6 mm diameter stainless steel tubing. The fittings were held in place at the ends of the protective tubing with epoxy adhesive. Gas inlets were inserted through the pit wall by drilling pilot holes and tapping capped inlets into place gently with a mallet, before removing the caps and attaching the sample tubing. The tubing and sensor wires were bundled and covered above ground until the measurement system was installed at the site the following summer.

A soil gas measurement system was built similar to the design of Hirsch et al. (2002a), but expanded to sample seven gas inlet lines, four soil moisture probes, and four thermocouples on a regular schedule. Each gas inlet measurement cycle lasted 14 min, with 2 min for each of the seven inlet lines in the following order: calibration gas 1,

calibration gas 2, +5 cm (just above the soil), -3 cm, -10 cm, -22 cm, and -48 cm. A rotary valve (EMTCSD10MWM, Valco Instruments CO. Inc., Houston TX, USA) was used to cycle between inlet lines. Flow was driven by a pump (KNF Neuberger Inc., Trenton NJ, USA) or cylinder pressure (calibrations) and controlled downstream of an infrared gas analyzer (IRGA, LI-820, Li-Cor Biosciences, Lincoln NE, USA) to 50 sccm by a mass flow controller (1179A, MKS Instruments, Andover MA, USA). Flow for each gas source was stopped after 75 s to allow the gas in the measurement cell to return to ambient pressure, and data from the final 10 s were averaged. Ten minutes prior to each measurement cycle a solenoid valve was opened to flow pure nitrogen gas at 100 sccm through a counterflow exchange tube (MD-050-12, Perma Pure LLC, Toms River NJ, USA), which was used to dry soil gas prior to introduction to the IRGA, and the solenoid valve was then closed at the end of each cycle to conserve gas. Additional solenoid valves were used for calibration gases (WMO-traceable CO₂ in air standards). All sample flows were filtered to 2 μm (Alltech, Deerfield IL, USA).

The enclosure was connected to the buried inlet tubes and sensor wires on July 20, 2005, more than a year after the inlets were buried. The seven gas inlets and buried temperature and moisture sensors were measured every 1-4 hours, depending on seasonally available sunlight used for power. Measurements continued, with some interruptions due to power loss and blockage of flow in winter (probably related to freezing water in inlet tubes), until late November of 2008. An ultrasonic snow depth sensor (Judd Communications, Salt Lake City UT, USA) was installed in the meadow near the soil profile measurements during each winter period.

Laboratory measurements of soil tortuosity

Soil gas tortuosity factors were calculated from diffusion coefficients of artificially-induced CO₂ fluxes through soil cores at variable moisture contents. To check for spatial variability in soil properties, soil cores were collected from two locations at 10 cm depth intervals to 50 cm in the meadow using 10 cm diameter PVC tubing. Soil was held in place inside the tubing with a metal screen. Soil cores were brought to the laboratory and wetted to field capacity. A series of measurements of induced CO₂ fluxes were made over the maximum range of water contents of the cores (field capacity to oven dried) to identify tortuosity vs. air-filled porosity functions for each core, following Jassal et al. (2005). Soil moisture within the cores was allowed to equilibrate between incremental changes in wetness by sealing each core inside a plastic bag for at least one week. Total porosity of soil cores was calculated from dry mass, assuming a particle density of 2.65 g cm⁻³. Air-filled porosity was calculated by subtracting the volume of water ((wet mass – dry mass)/water density) from the total pore space in each core during measurements.

Model calculation of fluxes and production

Molar density of CO₂ (μmol m⁻³) in the meadow soil profile was calculated from CO₂ mole fraction and temperature profile data. A second-order polynomial function was fit to each set of CO₂ molar density data vs. depth for each measurement cycle from the field sampling system. The first derivative of this function was calculated for the surface (depth = 0) and each measurement depth, and these values were used as the CO₂ gradients (dC/dz) in flux calculations following Fick's first law of diffusion:

$$F = D * \frac{dC}{dz} \quad 2.1$$

where F is the flux of CO₂ across a horizontal plane at each measurement depth (μmol m⁻² s⁻¹), and D is the diffusion coefficient. Diffusion coefficients of CO₂ were calculated for each measurement depth and time following:

$$D = D_o * \xi \quad 2.2$$

with D_o being the diffusivity of CO₂ in air, given by:

$$D_o = D_{ao} * \left(\frac{T}{293.15} \right)^{1.75} * \left(\frac{101.3}{P} \right) \quad 2.3$$

where P is 82 kPa (local atmospheric pressure for the site) and T is the soil temperature at the relevant depth and time (Massman 1998). D_{ao} is 15.7 mm² s⁻¹, the reference value for CO₂ diffusivity in air at 293.15 K and 101.3 kPa. ξ is a tortuosity factor, which was calculated using the power function fit to soil core data from the laboratory diffusion experiment (Jassal et al. 2005). This relationship was not different between soil depths or the two meadow positions sampled (shown later), so the following function derived from the entire data set was used:

$$\xi = 0.95 * \varepsilon^{1.93} \quad 2.4$$

where ε is the air-filled porosity calculated for each soil measurement depth and time from total porosity and volumetric water content. Rates of production of CO₂ (μmol m⁻³

s^{-1}) within depth intervals between measurements were calculated as the difference in CO_2 fluxes across the upper and lower depth limits divided by the difference in depth.

Open chamber system

An open chamber system was built and installed at the meadow site to measure surface fluxes for comparison with diffusion modeling results. The chamber designed following Rayment and Jarvis (1997) and was placed on bare soil near the soil profile measurements during the period between July 10 and November 9, 2008. The chamber remained in a single position until rain events, and after each rain it would be moved to another bare soil location within two meters of the profile measurements. The system was controlled by a datalogger (CR5000, Campbell Scientific, Logan UT, USA), programmed to sample every fourth day to conserve solar power. On sampling days a pump (KNF Neuberger, Trenton NJ, USA) was turned on at midnight and remained running for 24 hours, continuously pulling air through the chamber at 1.5 sLpm and from the inlet flow of the chamber at 500 sccm. A second pump was used to pull subsample flows at 150 sccm individually from the chamber inlet and outlet flows through an IRGA (LI-800, Lic-Cor Biosciences, Lincoln NE, USA). The chamber was measured every two hours beginning at 1 am, and each cycle of measurements was preceded by calibration. Switching between all gas measurements was controlled using solenoid valves (Clippard Instrument Laboratory, Inc., Cincinnati OH, USA), and all flows were set manually using variable area flow meters (Gilmont Instruments, Barrington IL, USA). Flows were stopped prior to all CO_2 measurements to allow the measurement cell to come to atmospheric pressure. The dilution effect of water vapor in inlet and outlet flows was

examined by placing a humidity sensor (HMP45A, Vaisala, Woburn MA, USA) in line upstream of the IRGA. Dilution effects on calculated CO₂ fluxes were determined to be minimal (< 5%).

Soil respiration flux rates were calculated using:

$$Flux = \frac{(C_o - C_i) * Flow}{A} \quad 2.5$$

where C_o and C_i are the mole fractions of CO₂ in the inlet and outlet flows from the chambers, “Flow” is the number of moles of air passing through the chamber per second, and A is the soil surface area enclosed by the chamber.

Results

Soil temperatures varied between 0 and 30 °C annually, with maximum seasonal and diel temperature variability near the soil surface (Fig. 2.1a). Temperatures in the soil under snow cover (Fig. 2.1c) slowly declined over the winter and remained just above freezing. Soil moisture was consistently highest in the cold months of the year, and then decreased during spring/summer following snow melt (Fig. 2.1b, c). Summer depletion of soil moisture was greatest near the soil surface. The timing and magnitude of late summer and fall precipitation events varied from year to year.

Carbon dioxide increased with depth and varied seasonally (Fig. 2.1d), with highest mole fractions measured in mid June, about 1.5 months before soil temperature reached the seasonal maximum. Additional CO₂ peaks occurred in the soil following summer and fall rain events. Profiles of CO₂ under snow cover varied between winters.

In winter 2005/06, CO₂ diffused out of the soil and through the snow, until the entire measured profile was nearly the same as in the atmosphere, suggesting very low CO₂ production under snow (Fig. 2.1c,d; 2.2a). In winter 2006/07, an ice layer formed in the snowpack just above the soil, limiting diffusion of CO₂ from the soil to the atmosphere. Mole fractions increased in the shallow soil under this layer as equilibration occurred with CO₂ stored in deeper layers. Above the ice, but within the snow (+5 cm inlet), CO₂ was decoupled from the soil profile and reflected mole fractions similar to the convectively-mixed air above the snow (Fig. 2.1c). By the time the ice and snow melted (Apr. 4), an inverted CO₂ gradient was apparent in the measured profile (Fig. 2.2b), indicating shallow soil winter CO₂ production was occurring and producing a net downward CO₂ flux.

Modeled surface fluxes during the growing season (days 100 to 330) peaked sharply in mid June for all years at around 6 $\mu\text{mol m}^{-2} \text{s}^{-1}$ (Fig. 2.1e). Surface fluxes increased steeply during spring, and decreased more gradually over summer and fall, with additional, smaller peaks appearing after rain events. These model results incorporate the composite measured tortuosity relationship with air-filled porosity from all soil cores (Eqn. 2.4), which was similar to relationships published by Millington (1959) and Jassal et al. (2005) (Fig. 2.3a). Soil respiration patterns within the study period were not strongly affected by choosing one of these other tortuosity functions (data not shown). Model results were similar to measured surface fluxes for the period in summer/fall 2008 when both methods were applied simultaneously (Fig. 2.3b, c), though the amplitude of diel flux variability was larger in chamber observations than was produced by the model. For this reason daily means were used in many subsequent analyses.

Daily CO₂ production was generally larger over the 0-22 cm depth interval than from 22-48 cm (Fig. 2.4), and the sum of these sources accounted for nearly all of the surface flux, suggesting that very little CO₂ production occurred below 48 cm. Model results indicated late summer production spikes occurring after rains at both depth intervals, though often these rain events did not penetrate deep into the soil (Fig. 2.1b). Soil moisture reached similar seasonal summer minima at 10 cm for all years studied, and modeled shallow soil CO₂ production and surface CO₂ flux peaks were synchronized with the drawdown of spring soil moisture and not the seasonal pattern of soil temperature (Fig. 2.4). Though there were seasonal differences in fluxes between years, cumulative soil-respired carbon was similar for the three complete growing seasons measured, with total C respired being consistently near 600 g m⁻² (Fig. 2.4f).

The relationship between soil temperature and soil respiration for each year followed three different trajectories for three consistent periods throughout the season (Fig. 2.5). In the first period (P. 1, days 100-169), soil respiration increased steeply with soil temperature; while in the second (P. 2, days 170-213), soil temperature continued to increase while soil respiration decreased; and in period 3 (P. 3, days 214-330), soil temperature and soil respiration decreased together. The transitions between these phases were evident in the slopes of change (first derivatives) of temperature, surface flux, and soil moisture calculated for sets of five consecutive days, averaged across all years of this study (Fig. 2.6). While large variations in temperature, moisture, and respiration fluxes associated with synoptic weather events during periods 1 and 3 were apparent after averaging all years, the consistently warm and dry conditions during period 2

corresponded with a relatively smooth increase in the average slope of soil moisture depletion towards zero.

Discussion

At the beginning of the growing season (day 100), meadow vegetation was emerging from seed and perennating buds, and thus supply of recent photosynthate to roots and the rhizosphere was likely minimal. Meadow plants grew rapidly during period 1, using soil moisture available from melted snow and spring rains. Metabolism of recent photosynthate transported belowground during rapid growth of meadow vegetation was likely primarily responsible for the steep increase in soil respiration during this period (Craine et al. 1999, Wan and Luo 2003). At the point when the CO₂ surface flux peaked and began to decrease sharply, the rate of soil moisture depletion at 10 cm reached a maximum (most negative $d\theta/dt$ in Fig. 2.6c), and then rapidly slowed down. This slowing of the rate of soil moisture loss is attributable to a sharp decrease in transpiration flux of water out of the soil as meadow vegetation senesced (Moyes and Bowling in prep-a). Meadow senescence, defined functionally here by the slowing of soil moisture depletion, was associated with an abrupt change from increasing to decreasing soil respiration (Fig. 2.6b), though soil temperatures continued to increase (Fig. 2.6a). The linkage observed between inferred plant water use and respiration implies that soil respiration during this period was strongly associated with plant activity. This result may be unique to shallow-rooted herbaceous ecosystems, as microbial respiration is likely more sensitive to drying surface soils than respiration from the rhizosphere of deeply-rooted plants. Drought limits heterotrophic respiration disproportionately in sites where a

large proportion of heterotrophic respiration is produced in surface litter (Borken et al. 2006, Savage et al. 2009), though no litter layer was present during summer at our site. The similarity of minimum soil moisture at 10 cm during summers of all years (Fig. 2.4a) likely reflects a physiological limitation of meadow vegetation at this site to grow or persist at the corresponding minimum water potential for this soil (Sperry 2000). The timing of peak CO₂ production in shallow soil from year to year appeared tightly linked to the timing of drawdown of soil moisture to this threshold value (at 10 cm), with wetter winters (e.g., 2008) corresponding with later and larger peaks in CO₂ production and fluxes (Fig. 2.4).

During period 2, soil respiration was increasingly substrate limited as photosynthetic assimilation decreased, and carbon allocation may have been directed towards reproduction for annual plants. This midsummer depression of soil respiration is similar to that observed in oak savannas and other regions where herbaceous vegetation senesces during similarly hot and dry summers (Fierer et al. 2005, Tang and Baldocchi 2005). During soil moisture depletion, soil carbon would have become progressively less available to microorganisms via diffusive limitation on transport of substrate and extracellular enzymes (Davidson and Janssens 2006). It is unknown whether soil water potentials reached a limiting threshold for microbial activity during summer, as has been observed in laboratory studies (Skopp et al. 1990, Howard and Howard 1993). The large increase in soil respiration following summer and fall rains after soil temperatures peaked (within period 3) was most likely due to stimulated heterotrophic respiration, including decomposition of labile carbon from dead and dying plant tissues (Saetre and Stark 2005, Borken and Matzner 2009, Chen et al. 2009), although growth of a limited set of plants

waw observed in response to fall rains. Some of the initial respiratory increase after re-wetting may have been due to mineralization of intracellular solutes during microbial adjustments to the rapid change in osmotic conditions (Fierer and Schimel 2003). The respiration responses to these events between years varied with the timing of precipitation and soil temperature, which declined relatively smoothly over this period (Fig. 2.1a, 4b). Earlier summer/fall rains were associated with larger increases in respiratory production and surface fluxes than later rains, presumably due to higher soil temperatures (Fig. 2.4, 2.5). Respiration increases following precipitation during the dry season have been shown to account for a large percentage of total soil respiration at moisture-limited sites (Xu et al. 2004, Sponseller 2007). For example, growing season soil respiration was increased by 16.5% in a ponderosa pine plantation due to summer rain (Misson et al. 2006). In that study respiration in trenched plots only showed a 1% response to the same events, and summer rain-induced respiration was attributed to decomposition of fresh root litter and stimulated root activity, depending on the timing of precipitation. Similarly, in the current study timing of rain events appeared to be as important as rainfall amount. Relatively early rains within period 3 compensated for relatively lower soil respiration during period 1 in 2008 vs. 2006 (Fig. 2.5, 2.6), leading to similar total amounts of carbon respired for the growing season in both years. Larger rain events occurred in the fall of each of the other three years studied, but the increase in respiration following rain consistently decreased with time during the season (Fig. 2.4, 2.5). However, there may be a threshold amount of water necessary to induce respiration, as very small rains during high soil temperatures (around day 220) in all 4 years did not stimulate soil respiration substantially, according to model results (Fig. 2.4). Respiratory

responses to small rain events are difficult to quantify and were probably not correctly captured by our steady state model. Small midsummer rains did wet surface soils briefly before being lost to evapotranspiration (Fig. 2.1b), and led to increased soil CO₂ (Fig. 2.1d). However, in model calculations the decrease in the diffusion coefficient due to wetting almost entirely offset the increase in CO₂ gradients, leading to a minimal increase in the calculated surface flux. Deep soil production of CO₂ (22-48 cm) appeared to increase somewhat in response to these shallow moisture increases (Fig. 2.4), but these model results are most likely an artifact of the change in the shape of the CO₂ profile and the coarse discretization of soil diffusion coefficients and CO₂ gradients used to calculate production. Larger increases in respiratory CO₂ production below 22 cm following larger rains (usually occurring after day240 (Fig. 2.4)) could reasonably have been due to percolation of rain water relieving drought stress and bringing dissolved organic carbon to these depths.

At the end of period 3, soil respiration rates were higher for a given temperature than rates associated with the same temperatures during period 1 (Fig. 2.5). Both of these seasonal phases were associated with similarly high soil moisture. The greater respiration in fall than spring may be due to the greater amount of soil carbon available for decomposition in fall due to litter input from senescent plant tissues above- and belowground. Soil carbon extractions from this site over the 2006 growing season showed a fall peak in dissolved organic carbon (Moyes and Bowling in prep-a). Lower respiration rates in spring with adequate moisture and similar temperatures imply that at the time of green up of the meadow in spring, heterotrophic soil respiration was substrate-limited. One exception to this pattern was spring 2007, when early spring

respiration rates for a given temperature were as high as rates during the fall (Fig. 2.5). However, the 2007 growing season followed the unique winter within this study when CO₂ accumulated in soil pores beneath an ice layer (Fig. 2.1, 2.2). As soils at the site were extremely deep, with unsaturated, porous soil extending for several meters (data not shown), some of the uniquely high spring flux in 2007 could have been due to the efflux of CO₂ stored in the soil from winter and the previous growing season (2006). This conclusion was supported by the decreasing offset between high CO₂ surface fluxes (and production attributed to both depth intervals) in 2007 and those of other years over the first few weeks after snow melt (Fig. 2.4e). Alternatively, if below normal rates of decomposition occurred during winter 2006/07, these higher flux rates could have been associated with decomposition of residual litter. The accumulation of CO₂ in the soil during this winter (Fig. 2.1, 2.2) does not indicate that heterotrophic soil respiration was limited under the snow, for example by reduced oxygen supply via diffusion through the ice layer and soil with high water content (Fig. 2.1).

Soil respiration peaked earlier in the season than soil temperature (Fig. 2.1, 2.4), leading to a seasonal hysteresis in the soil respiration vs. soil temperature relationship (Fig. 2.5). This recurrent annual pattern was the result of the particular seasonal relationships between soil temperature, moisture, and substrate supply to roots and soil heterotrophs for this site. Contrasting hysteresis patterns between soil CO₂ fluxes and soil T with time have been observed in different ecosystems where the interactions between plants, soil microorganisms, and climate lead to different seasonal limitations on soil respiration (Borken et al. 1999, Moren and Lindroth 2000, Xu and Qi 2001, Jassal et al. 2008). The spring and summer relationships between growth and senescence of

meadow vegetation with decreasing soil moisture and increasing soil temperature in the current study were similar to reports from herbaceous ecosystems with strong summer soil moisture limitations, such as grasslands in Mediterranean climates (Tang and Baldocchi 2005, Curiel Yuste et al. 2007). As in Mediterranean ecosystems (Fierer et al. 2005, de Dato et al. 2010), the amount and timing of winter and spring precipitation at our site was probably a stronger driver of soil respiration than variability in summer temperatures. However, initiation of growth of meadow vegetation at our site occurred several months later in the year (April) than occurs in Mediterranean sites with milder winters. At our Rocky Mountain site there was a long period (~9 months) between plant senescence in midsummer and the productive period of plant growth in the following year when heterotrophic respiration was assumed to be the primary soil CO₂ source. During much of this heterotrophically-dominated period, soil moisture was near field capacity (Fig. 2.1). Higher rates of soil respiration in fall vs. spring at similar soil temperatures (Fig. 2.5) were attributed to a decrease in substrate availability for decomposition. Our results were similar from three separate growing seasons, providing some sense of the inter-annual consistency of seasonal drivers of soil respiration at this site.

Cumulative soil respiration during the growing season (63% of the year from day 100 to 330) ranged from 559-633 gC m⁻² y⁻¹, which was higher than the value of 442 ±78 reported for annual periods in temperate grasslands by Raich and Schlesinger (1992), and more similar to the value for temperate deciduous forests of 647 ±51 gC m⁻² y⁻¹. Heterotrophic respiration at this site may be enhanced by carbon subsidies (litterfall) from the surrounding deciduous trees. Respiration under snow during winter likely

contributed a substantial amount to the annual soil CO₂ flux, as insulation by the snowpack kept soil temperatures above 0 °C (Fig. 2.1), with liquid water available to soil organisms (Hubbard et al. 2005). Measurements of winter soil respiration were limited in the current study, but there was evidence that some CO₂ production was occurring under snow (Fig. 2.2). Notably, the difference in fall and spring relationships between respiration and soil T (Fig. 2.5) was attributed to heterotrophic respiration depleting soil carbon over the winter period, leaving microbial communities substrate limited in spring. This interpretation is consistent with glucose addition experiments in winter showing microbial respiration under snow to be carbon limited (Brooks et al. 2005). It appeared that fall and winter decomposition had diminished the carbon inputs from each growing season by the time of the following spring, so that the net change in carbon stocks may have been near zero for each annual cycle. A bleached and compressed litter layer was present immediately after each snowmelt, but then disintegrated and almost entirely disappeared by the time of emergence and growth of vegetation. No permanent litter layer or thatch remained on the soil surface at this site into summer. Winter decomposition of annual litter inputs at this site is likely high due to the litter quality of its herbaceous cover and relatively warm and moist conditions. This contrasts with sites with more recalcitrant litter, where winter decomposition consumes a smaller fraction of litter biomass, such as 60% in an aspen woodland (Coxson and Parkinson 1987), or 10-16% in a coniferous forest (Kueppers and Harte 2005). While these results suggest that interannual variability in aboveground production at this site may be balanced by decomposition, further study is necessary to determine whether slow turnover soil carbon pools are impacted by seasonal transitions between plant growth and decomposition.

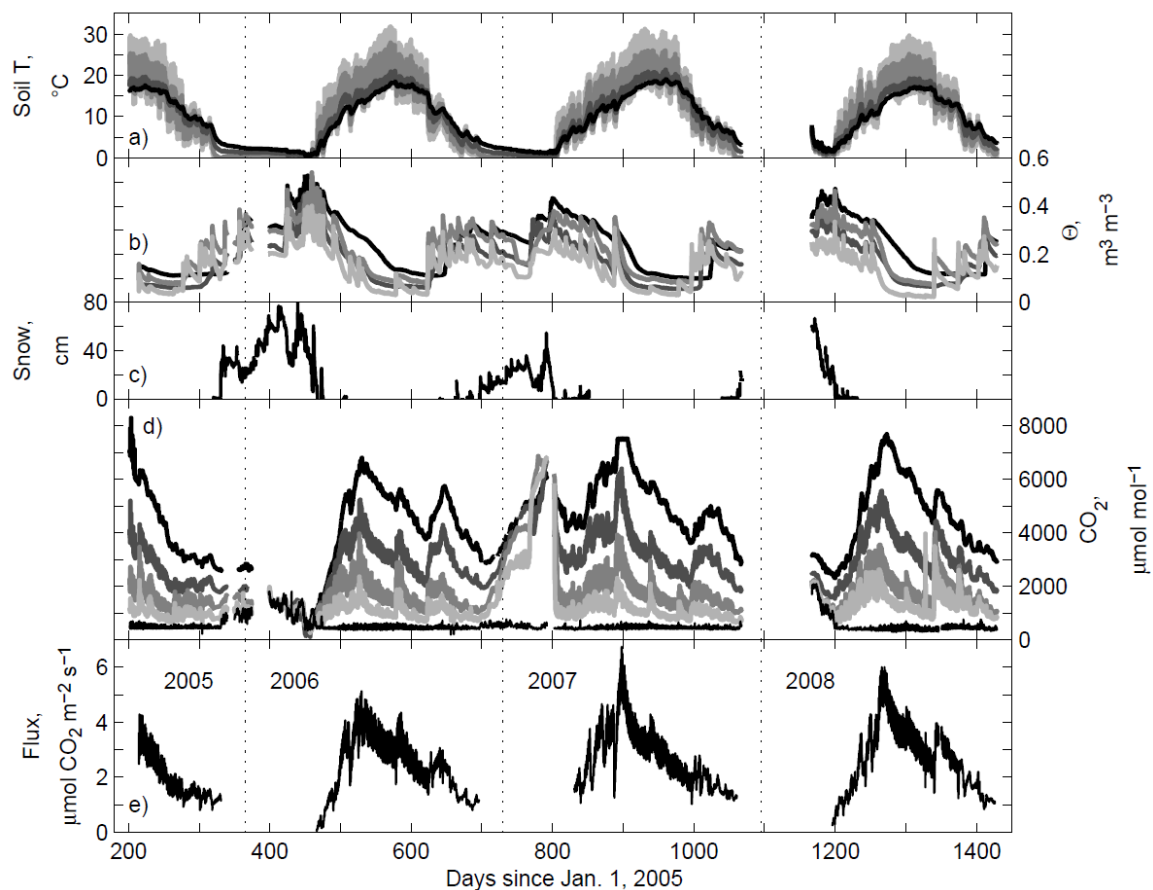


Figure 2.1: Soil temperature (a), volumetric water content (θ , b), snow depth (c), and CO_2 (d), and modeled surface CO_2 flux (e) vs. time for the entire study period. In panels a-d, data from within the soil are shown as thick lines shaded from lightest to darkest for depths of 3, 10, 22, and 48 cm. Mole fraction of CO_2 from 5 cm above the soil surface is shown in (d) as a thin black line. Vertical dashed lines indicate the beginning of each calendar year.

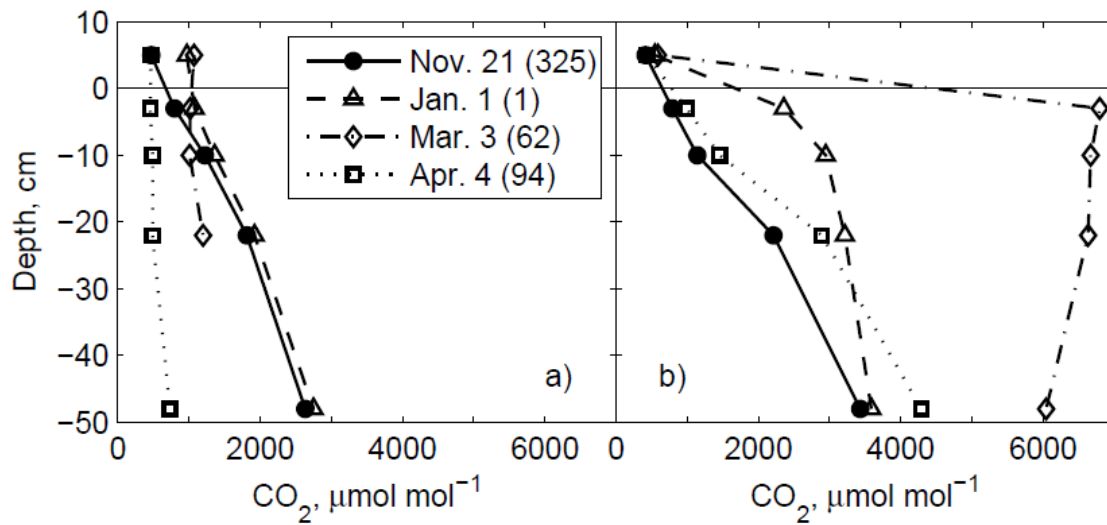


Figure 2.2: Vertical profiles of CO_2 within the soil measured at specific dates during the 2005/06 (a) and 2006/07 (b) winters, shown to highlight the interannual differences. Dates and day of year are indicated in the legend.

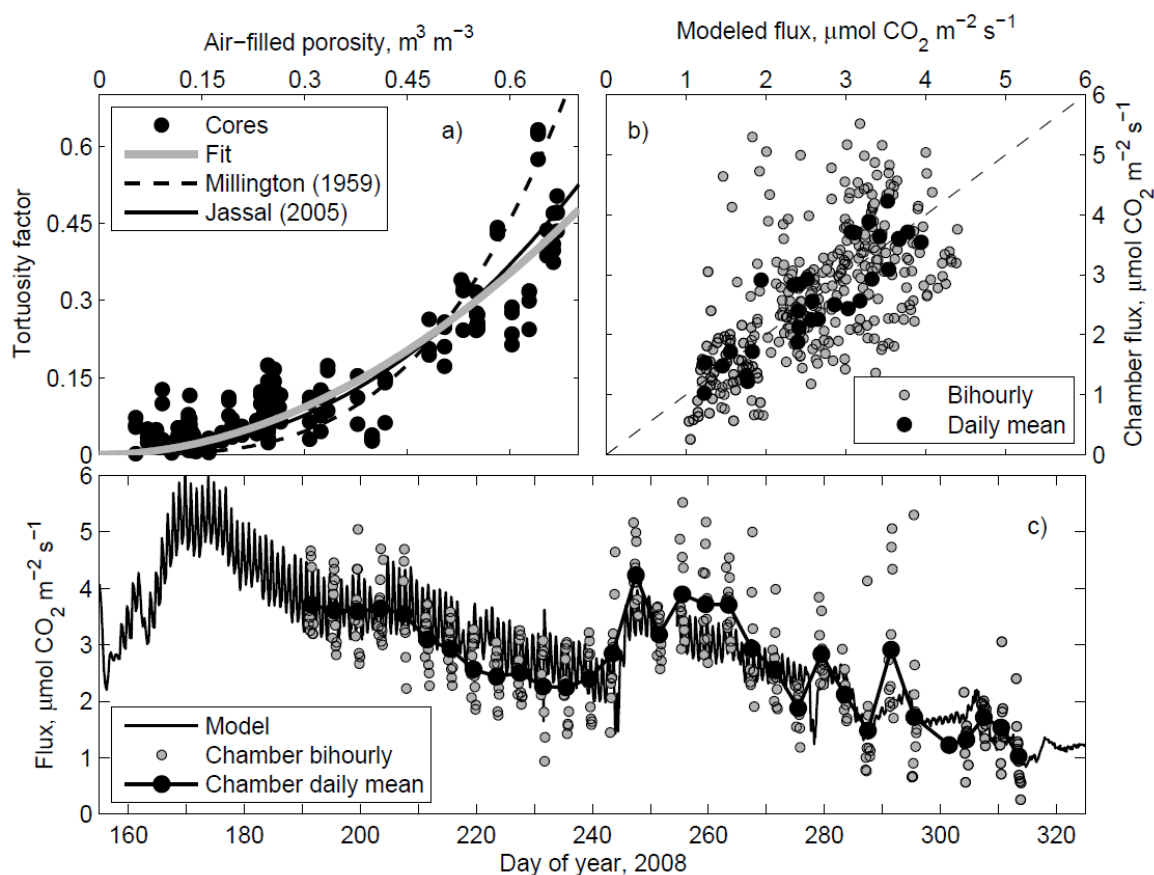


Figure 2.3: Parameterization and validation of diffusion model. (a) Calculated tortuosity factors from laboratory measurements of soil cores evaluated over a range of air-filled porosities, with the fit power function (Eqn. 2.4) and relationships published by Millington (1959) and Jassal et. al (2005) presented for comparison. (b) Comparison of surface fluxes calculated with the model and measured with an open soil chamber placed on top of the soil near the buried soil gas inlets. Model results and chamber data are shown for each of the bihourly chamber measurement periods, in addition to daily mean fluxes for both methods. The 1:1 line is shown for comparison. (c) Time series of modeled surface fluxes and bihourly and daily mean open soil chamber measurements during summer and fall 2008.

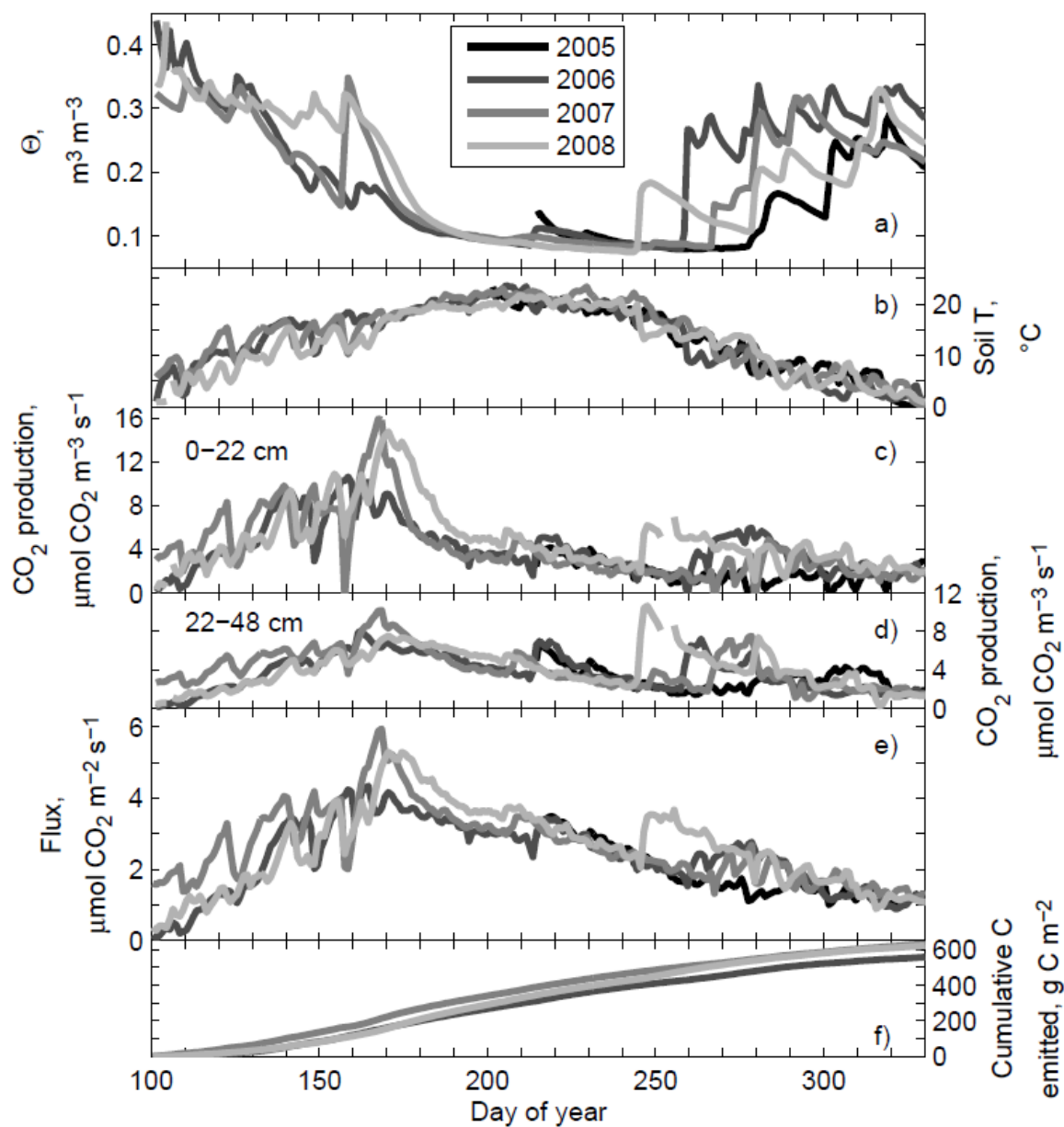


Figure 2.4: Daily means of volumetric water content at 10 cm (a), soil temperature at 10 cm (b), calculated CO₂ production rate for soil within the 0-22 (c) and 22-48 (d) cm ranges of soil depth, modeled CO₂ surface flux (e), and cumulative respired carbon (f) for each growing season during the study. Data from 2005 are not shown in (f) because measurements began late within that year.

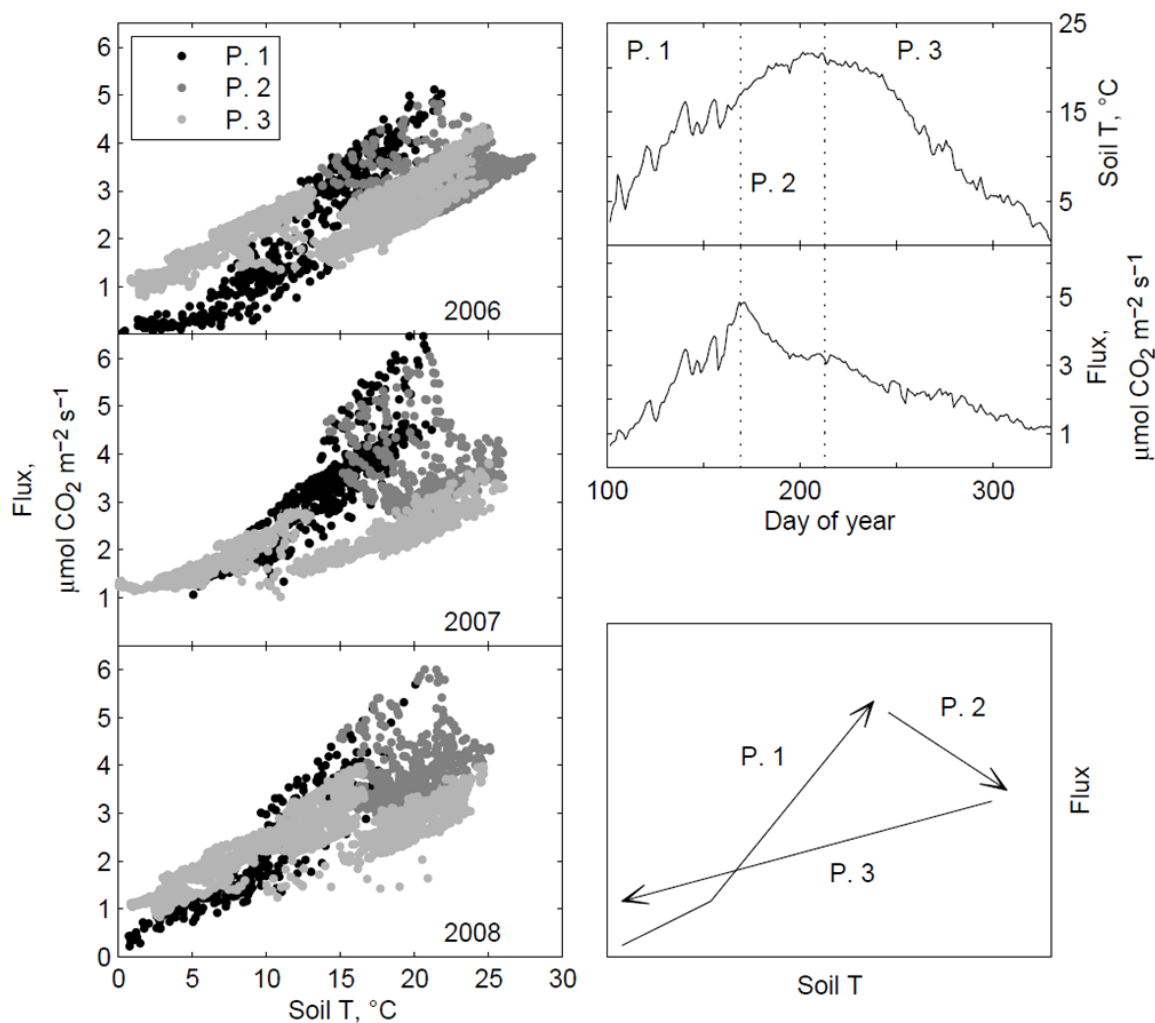


Figure 2.5: Modeled surface CO₂ flux vs. soil temperature at 10 cm for each of the 3 complete growing seasons of the study (left panels). Each season was divided into 3 periods, with the first division (day 169) identified by the maximum respiration rate from averaged model results for all 3 years (middle right panel), and the second division (day 213) identified as the average seasonal maximum soil temperature at 10 cm (upper right panel). These divisions are shown as vertical dotted lines in the upper right panels. The lower right plot is a schematic representation of the relationship between CO₂ flux and soil temperature over the course of each of the three periods.

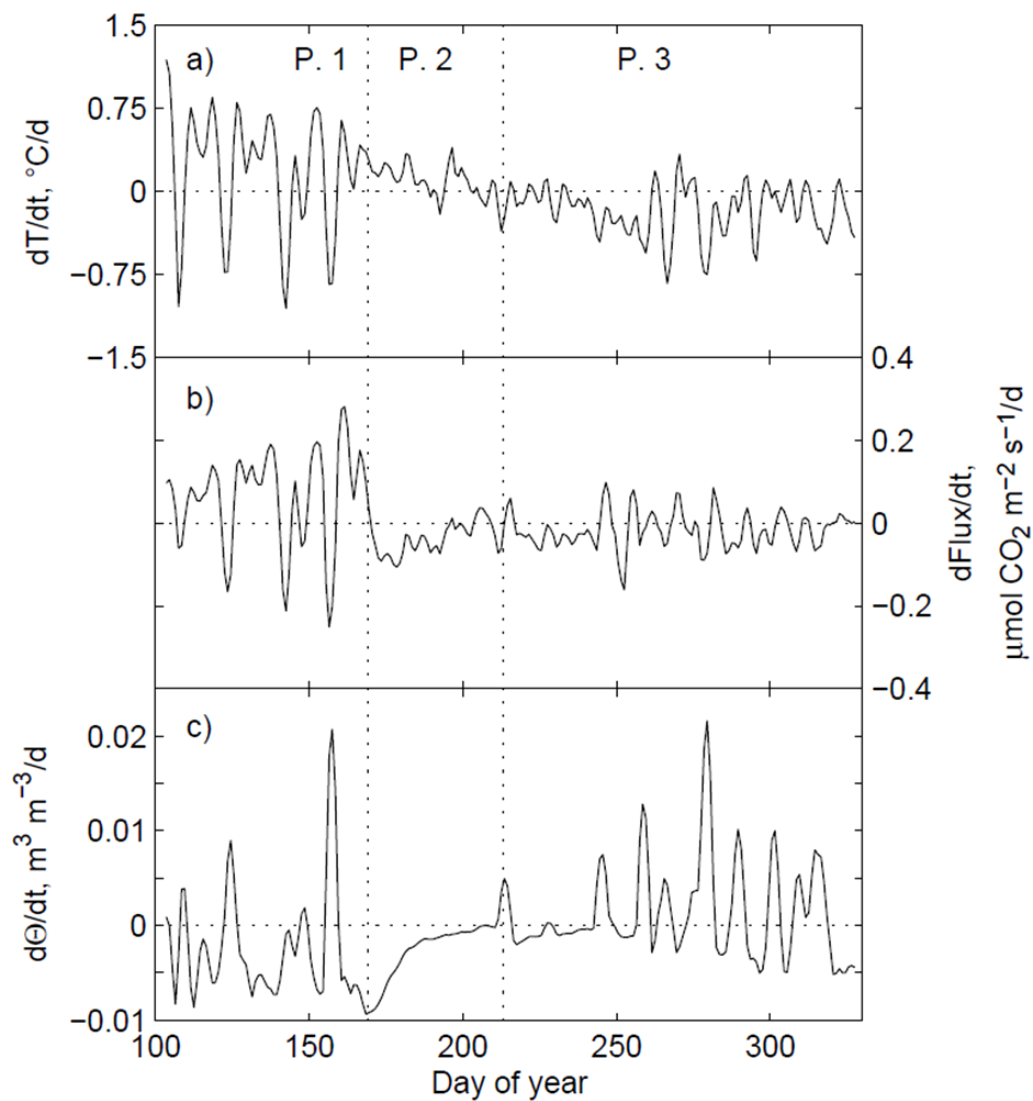


Figure 2.6: Slopes of change in soil T at 10 cm (a), surface CO_2 flux (b), and volumetric water content (θ) at 10 cm (c) for successive 5-day windows of daily-averaged data from all years. Values above zero indicate increasing slopes and values below zero indicate decreasing slopes. Averaged slopes change sporadically due to weather events during individual years in periods 1 and 3, but are more consistent during P.2, when soil temperature continued to increase ((a), line decreases to zero), fluxes peaked and began to decrease ((b), line crosses zero), and soil moisture depletion ended ((c), line increases to zero).

CHAPTER 3

PLANT PHENOLOGY REGULATES SEASONAL VARIATION

OF SOIL RESPIRATION ALONG ROCKY MOUNTAIN

TREE-MEADOW TRANSECTS

Abstract

Spatial variability in soil respiration results from the presence of contrasting vegetation types interspersed on the landscape. We compared seasonal patterns of soil respiration along transects from under deciduous riparian trees to within an adjacent meadow in the Rocky Mountains. We hypothesized that plant traits (phenology, growth form, growth rates, etc.) would be associated with seasonal differences in soil respiration under trees and in the meadow. In 2005 a large flush of the N-fixing forb *Melilotus officinalis* emerged in the meadow and under trees and produced a dense canopy >1 m tall. Soil respiration fluxes in summer of 2005 were greater than measurements in 2006 at all transect positions. In 2006, meadow vegetation was similar to typical years with a low abundance of *M. officinalis*, and in this year soil respiration fluxes were reduced overall, with larger fluxes under trees than in the meadow during summer. The timing of plant phenological events such as growth and senescence of aboveground biomass corresponded with seasonal and spatial variability of soil respiration in the two vegetation types. Soil respiration under trees was consistently near $5 \mu\text{mol m}^{-2} \text{s}^{-1}$ from spring

before leaf out until just before leaves began to change color and abscise. Contrary to other studies, high spring respiration under trees was not correlated with either microbial biomass or soil organic carbon extractions. Soil respiration in the meadow increased from 2.1 to 3.2 $\mu\text{mol m}^{-2} \text{s}^{-1}$ between spring and early summer. Summer soil moisture was depleted to a larger extent at shallow depths in the meadow than under trees, and soil temperatures were higher in the meadow in summer. Warm and dry soil conditions in midsummer led to meadow senescence and reduced soil CO_2 fluxes. Soil respiration rates in late fall after dormancy of trees and meadow vegetation were 1.3 and 0.7 $\mu\text{mol m}^{-2} \text{s}^{-1}$ under trees and in the meadow, respectively. Calculated production of CO_2 with depth under trees was higher than production in the meadow to 50 cm during spring and summer, presumably due to deeper root distributions of trees.

Introduction

Plant traits impact soil carbon cycling by affecting both inputs and outputs. For example, one broad functional characteristic with strong implications for soil carbon balance is plant relative growth rate. Fast-growing species typically produce large inputs of readily-decomposable plant material, generally at the cost of lifespan, while slow-growing plants typically allocate more carbon to defense and structural tissues, and produce smaller inputs of longer-lasting, nutrient-poor litter (Raich and Tufekcioglu 2000, Chapin 2003, De Deyn et al. 2008). Root litter quality has a similarly strong effect on decomposition rates (Silver and Miya 2001), and root and leaf litter quality are largely independent (Craine et al. 2005, Hobbie et al. 2010). Exudation of carbon-rich compounds such as sugars by roots depends largely on plant assimilation rates (Jones et

al. 2004), and the consequent “priming effect” of root exudation on microbial mineralization of soil carbon can be positive or negative, depending on soil biota and the relative quality of exudates vs. soil organic matter (Kuzuyakov and Cheng 2004, Dijkstra et al. 2006, Paterson et al. 2009). Plants can also increase or reduce soil carbon storage via changes in carbon balance associated with exotic species invasions and altered frequency of disturbance such as fire (see reviews by Chapin 2003, De Deyn et al. 2008). Introduced nitrogen-fixing species can change both nitrogen and carbon cycling, especially in N-limited ecosystems (Vitousek et al. 1987).

Transects between adjacent vegetation types provide a way to assess the importance of vegetation in mediating soil respiration, because climatic and edaphic conditions are largely similar across transect positions (Raich and Tufekcioglu 2000). In most ecosystems a variety of plant types coexist by exploiting contrasting competitive strategies (Grime 1997, Tilman et al. 2001). Differences in vegetation can lead to spatial and temporal variability in rates of assimilation and transport of carbon belowground, litter production, and soil microclimate (temperature and moisture), and thus can impact variability in both autotrophic and heterotrophic soil respiration (De Deyn et al. 2008).

Spatial variability in soil respiration associated with vegetation gradients may be driven by differences in plant uptake and transfer of carbon belowground. For example, soil respiration associated with deciduous tree cover was shown to increase dramatically with photosynthesis in midsummer, while respiration under nearby coniferous trees was associated with lower and more stable soil respiration rates throughout the year (Curiel Yuste et al. 2005b). Comparisons between adjacent grasslands and trees have shown decreasing (Tang et al. 2005) and increasing (Raich and Tufekcioglu 2000) soil

respiration rates with distance from trees. In these two examples, opposing directional differences in soil respiration between trees and grasslands were attributed to different rates of plant carbon assimilation and transport belowground. The contrasting relative rates of productivity and soil respiration between trees and grasslands at these sites were probably due to overriding interactions of vegetation and climate (e.g., Mediterranean vs. temperate trees and grasslands). Thus, differences in soil respiration associated with plant productivity between particular plant types are not independent of abiotic controls, and may vary with geographic region and climatic fluctuations.

Variability in soil respiration between vegetation types may also be caused by localized inputs of litter and microclimate effects of plants. In a subalpine forest, spatial variability in heterotrophic respiration associated with concentrations of needle litter beneath conifer trees was the strongest predictor of spatial differences in soil respiration (Scott-Denton et al. 2003). Decreasing needle litter and fine root density corresponded with a 20% decrease in soil respiration with distance from trees in another high-elevation forest (Wieser 2004). A recent study in Utah rangelands found that differences in vegetation (trees, sagebrush, grasses) led to variability in soil respiration on the landscape by affecting microclimate and litter quality (Olsen and Van Miegroet 2009). Alternatively, abiotic variables such as weather conditions may be more important than vegetation gradients in determining soil respiration rates at some sites (Kelliher et al. 1999).

In this study, we sought to characterize the relative importance of vegetation on seasonal patterns of soil respiration in a Rocky Mountain canyon bottom with deep and relatively uniform soil. We compared soil respiration patterns under deciduous riparian

trees and in an herbaceous grass/forb meadow, with the expectation that differences in plant growth form, phenology, and litter quality would lead to differences in seasonal patterns of soil respiration at tree and meadow locations. We examined the influence of vegetation type, soil temperature, soil moisture, and extractable soil organic carbon and microbial biomass carbon on soil CO₂ production along transects from under trees into the meadow over two growing seasons. To our knowledge this was the first comparison of soil respiration within these vegetation types in the Great Basin region with winter-dominated precipitation inputs and warm, dry summers.

Methods

Site description

The study was conducted around the perimeter of a meadow within Red Butte Canyon (111°47'47"W, 40°47'21"N, 1758 m elevation) near Salt Lake City, Utah, USA. The meadow was surrounded on all sides by boxelder (*Acer negundo*) and bigtooth maple (*Acer grandidentatum*) trees, with water birch (*Betula occidentalis*) and red osier dogwood (*Cornus sericea*) also present along the riparian zone. In 2005, the meadow was dominated by a dense growth of yellow sweetclover (*Melilotus officinalis*), which is a nitrogen-fixing legume (Schubert and Evans 1976). The flush of this species in 2005 was an unusual occurrence based on the experience of the authors at this site. Presence of yellow sweetclover was reduced to <5% cover in 2006 (visually estimated, data not shown), when the meadow vegetation comprised a variety of native and introduced grasses and forbs more consistent with the species composition of typical growing seasons in this meadow. In 2006 there were relatively high abundances of orchard grass

(*Dactylis glomerata*), blue wildrye (*Elymus glaucus*), rye brome (*Bromus secalinus*), milfoil yarrow (*Achillea millefolium*), dalmation toadflax (*Linaria dalmatica*), and houndstongue (*Cynoglossum officinale*). A perennial stream flowed between the trees growing along the western side of the meadow. Under trees near the stream, false Solomon's seal (*Smilacina stellata*) was abundant. The site received about 500 mm of precipitation annually, which primarily arrived in winter (Ehleringer et al. 1992). Soils were loamy, deep, and well-drained. Additional site details are available in Moyes and Bowling (in prep-b).

Trees surrounding the meadow access groundwater throughout the growing season (Dawson and Ehleringer 1991), while the herbaceous perennials and annuals in the understory meadow vegetation primarily make use of shallower soil moisture. The meadow was known *a priori* to cycle between cool, wet soils in spring following fall rains and snowmelt and relatively warm and dry soils in summer, and it was also known that meadow vegetation typically senesced in midsummer before tree leaves began to change color. Ten transects were established, running 9 m towards the center of the meadow from the bases of ten selected boxelder (8, 4m/4fm) and bigtooth maple (2) trees positioned around the perimeter of the meadow (Fig.3.1). We conducted regular measurements of soil respiration along these transects in the 2005 and 2006 growing seasons. To characterize seasonal patterns of soil respiration and its drivers across the vegetation gradient, five time periods were selected for intensive measurements (days 117, 167, 201, 236, and 307) in 2006, including soil respiration, soil CO₂, gravimetric water content, and temperature profiles for modeling production with depth, and soil organic carbon and microbial biomass carbon extractions. These periods were chosen to

encompass the range of soil moisture and temperature conditions occurring at the site (Fig. 3.2), and the phenological cycles of the two vegetation types (Fig. 3.3).

Soil chamber measurements

Positions for soil respiration measurements on the tree/meadow transects were chosen to obtain one measurement with a maximum effect of tree proximity, one measurement impacted by the meadow, and one intermediate position. In 2005, respiration collars were placed at 3, 6, and 9 m from tree trunks (Fig. 3.1). In 2006, the decision was made to move two of the collars towards the tree trunks, and measurements were made at 1.5, 3, and 9 m. To account for these changes and for differences in tree diameter (canopies ranged from 3.2 to 8 m in diameter), soil respiration measurement positions are presented relative to the canopy dripline (Fig. 3.1). Soil respiration collars (10 cm diameter polyvinylchloride) were installed in spring of both years at least 2 days before measurements began, and were kept free of live plant stems. Soil respiration within the collars was measured using a portable gas exchange system connected to a closed soil chamber (Li-6400 and 6400-09, Licor Biosciences, Lincoln NE, USA). Collars were measured every 1-2 weeks between May 23 (day 143) and August 27 (239) in 2005, and from April 27 (117) to November 3 (307) in 2006. The 2006 measurements included the five intensive sampling periods. During each soil respiration flux measurement a soil temperature probe was inserted 10 cm into the soil near the respiration collar and this temperature was recorded. In 2005 a soil moisture probe (Hydrosense, Campbell Scientific, Logan UT, USA) was used to measure volumetric water content of the top 20 cm with each flux chamber measurement. In 2006, soil

moisture was only measured on the five intensive sampling dates, and was done gravimetrically, as described below.

In-situ soil CO₂

Gas wells consisting of 6.35 mm OD stainless steel tubing attached to straight unions (SS-400-6, Swagelok, Solon, OH) containing septa (Microsep F-138, Alltech, Deerfield, IL, USA) were installed on April 21, 2006. Gas wells were and tapped into the ground vertically from the surface (without digging) using a rubber mallet, with a steel rod temporarily placed within each tube during installation to prevent clogging with soil. At 1.5, 3, and 9 m transect positions on 6 of the 10 transects, vertical profiles of gas wells were installed with open buried ends at 5, 10, 20, 23.5, 38.5, and 48.5 cm depths. Additional 20 cm-deep gas wells were installed so that all 10 transects contained 20 cm wells at all 1.5, 3, 6, and 9 m positions (Fig. 3.1). Gas wells were sampled on 10 dates from April 27 to November 3, 2006, including the five intensive sampling periods. Mole fraction of CO₂ was measured from each well by sampling gas via the septum with a gas-tight syringe (050035 (A-2), Pressure-Lok, VICI, Baton Rouge, LA) and injecting 0.5 mL at ambient pressure into a circulating, CO₂-free air loop, just upstream of an infrared gas analyzer (LI-7000, Licor Biosciences, Lincoln NE, USA), as described by Davidson and Trumbore (1995). Calibration of injection peak areas was performed by measuring injection standards in the field before and after gas well samples. Standards were prepared in the laboratory as volumetric combinations of CO₂-free air and pure CO₂, as described by Moyes et al. (2010).

Soil moisture and temperature profiles for modeling

Soil moisture and temperature profiles to 50 cm were required for calculating CO₂ fluxes and production from soil CO₂ data. During the five intensive sampling periods soil cores were collected using a bucket auger at the 1, 3, and 9 m transect positions in 10-cm depth increments to 50 cm for gravimetric determination of water content. Initial mass of cores was measured in the field with a digital scale and samples were dried in an oven at 60 °C in the lab before measuring dry mass on the same scale. Volumetric water content (θ , m³ m⁻³) was calculated by assuming a soil particle density of 2.65 g/cm³. Profiles of θ were calculated from the samples by fitting a third-order polynomial to average sample depth and water content data.

Soil temperature profiles were measured with type T thermocouples buried at 3, 10, 22, and 48 cm in the center of the meadow. Quadratic functions were fit to temperature profile data from the same time of day for the same dates that gas wells were measured. Soil probe temperature data collected at 10 cm during soil respiration measurements (described above) were used to calculate a temperature offset function for each gas well cluster transect position. This was done to account for spatial variability in shallow soil temperatures along each transect. Temperatures at 48 cm depth at all transect positions were assumed to match the thermocouple measurement from the central meadow position, and each temperature offset function was a linear fit through the difference in temperature measured at 10 cm. This offset was subtracted from the quadratic fit line of meadow soil temperature vs. depth to give a smooth temperature profile for each transect position and sampling date.

Model of CO₂ fluxes and production

Gas well CO₂ data were used to calculate quadratic functions of CO₂ molar density (μmol m⁻³) vs. depth. The first derivative of this function was used to calculate CO₂ gradients (dC/dz) for use in flux calculations for the soil surface CO₂ flux and vertical fluxes of CO₂ across horizontal planes within the soil. Fluxes (F) were calculated using Fick's first law of diffusion:

$$F = -D * \frac{dC}{dz} \quad 3.1$$

where D is the diffusion coefficient. Diffusion coefficients of CO₂ were calculated for each sampling date and modeled depth using soil moisture and temperature profiles. D was calculated following:

$$D = D_o * \xi \quad 3.2$$

with D_o being the diffusivity of CO₂ in air, given by:

$$D_o = D_{ao} * \left(\frac{T}{293.15} \right)^{1.75} * \left(\frac{101.3}{P} \right) \quad 3.3$$

(Massman 1998), where P is 82 kPa (local atmospheric pressure for the site), T is the soil temperature at the relevant depth and time, and D_{ao} is 15.7 mm² s⁻¹, the reference value for CO₂ diffusivity in air at 293.15 K and 101.3 kPa. ξ is a tortuosity factor, which was calculated from a laboratory diffusion experiment using soil cores (Moyes and Bowling in prep-b). Tortuosity vs. air-filled porosity functions were calculated from soil cores collected from 10 cm depth increments to 50 cm at two positions at the site (central

meadow and under tree). Tortuosity factors were calculated from CO₂ fluxes induced through the cores over the range of water contents from field capacity (maximum water held against gravity in each core) to oven-dried at 60 °C. The relationship between tortuosity and air-filled porosity was similar among soil depths and the two transect end positions sampled. The tortuosity factor was best represented by:

$$\xi = 0.95 * \varepsilon^{1.93} \quad 3.4$$

where ε is the air-filled porosity calculated for each soil measurement depth and time from total porosity and volumetric water content.

Fluxes were calculated at 10 cm intervals from the surface (0 cm) to -50 cm for each of the 18 profile locations (6 transects, 3 positions) and sampling date. Rates of production of CO₂ ($\mu\text{mol m}^{-3} \text{s}^{-1}$) within depth intervals between calculated fluxes (e.g. 0-10 cm, 10-20 cm, etc.) were calculated as the difference in CO₂ fluxes across the upper and lower depth limits of each interval, divided by the difference in depth (0.1 m). Modeled surface fluxes and production at each depth interval for each transect position (1.5, 3, and 9 m) are reported as averages from the six transects.

Soil organic carbon and microbial biomass carbon

Soil cores were collected at 1.5, 3, and 9 m transect positions during each of the five intensive sampling periods. Cores were obtained by inserting a 5 cm diameter bulb planter to 10 cm and then digging it out from the side. Cored soil was transferred at field moisture to a 2-mm sieve and particles passing through were mixed thoroughly by shaking. Two 5 g samples were weighed and placed into separate 25 mL sample tubes.

An additional soil sample was placed in a paper envelope, which was sealed and weighed. Envelopes were oven dried and the difference in wet and dry mass was used to adjust to dry soil mass. To extract soil organic carbon (SOC) one of the paired 25 mL tubes was filled with a 0.5 M potassium sulfate solution. To extract microbial biomass carbon (MBC), the other paired tube was incubated with chloroform by placing cotton at the top of the tube, dousing with 2 mL 100% chloroform, and then sealing the tube. Chloroform was allowed to vaporize and diffuse through each soil sample for 2 days. Then the cotton was removed and the vial was filled with the 0.5 M potassium sulfate solution. Sample solutions were filtered (No. 4, Whatman International LTD, Maidstone, UK) and stored at -18 °C until measurement with a total organic carbon analyzer (TOC 3201, Shimadzu, Columbia MD, USA). Blanks were made using the same procedure, but omitting soil. Carbon amounts in unfumigated samples were taken to represent “extractable SOC”, and “extractable MBC” was calculated by subtracting these measurements from each paired fumigated sample.

Results

Soil moisture and soil temperature were strongly correlated over the measurement periods in 2005 and 2006, though soil moisture was slightly higher and soil temperature slightly lower under tree canopies (distance from dripline < 0) than out in the open meadow during the warm and dry summer periods (Fig. 3.4). The N-fixing, European legume *Melilotus officinalis* grew densely in 2005 to over 1 m in height throughout the meadow and under trees. Dense growth of this forb was associated with high measured soil respiration fluxes in spring and summer of 2005 (Fig. 3.4, triangles). In 2006 *M.*

officinalis was a minor component of percent cover, and meadow vegetation consisted of a variety of shorter and less dense grasses and forbs. Spring soil respiration rates in 2006 (Fig. 3.4, circles) were decreased by nearly 50% relative to 2005, but showed similar spatial and seasonal variability. This difference in soil respiration between years was larger than differences associated with transect positions within years. During warm summer months of both years, soil respiration decreased with low soil moisture and high soil temperatures.

Modeled CO₂ fluxes were higher under trees (1.5 m) than at the 3 and 9 m transect positions until the final intensive sampling period (day 307), when soil respiration calculated by the model reached its seasonal minimum at all transect positions (Fig. 3.5c). Model results for soil respiration surface fluxes were similar for the 3 and 9 m positions throughout the year. At day 117 (April 27) the meadow vegetation had just recently begun to germinate or resprout and trees were just about to flower (trees of the two riparian tree species flower just before leaf out). However, by this time calculated surface fluxes for the 1.5 m transect positions were already 4.4 ± 0.5 (SEM) $\mu\text{mol m}^{-2} \text{s}^{-1}$, 77% of the seasonal maximum of $5.7 \pm 0.5 \mu\text{mol m}^{-2} \text{s}^{-1}$ (measured on day 201), whereas fluxes at the 9 m (meadow) position increased from 2.1 ± 0.3 to $3.2 \pm 0.5 \mu\text{mol m}^{-2} \text{s}^{-1}$ following this date. Modeled surface fluxes from meadow profile measurements on day 167 were similar to results from an automated soil CO₂ profile system running concurrently near the center of the meadow (Moyes and Bowling in prep-b). The modeled fluxes from continuously measured profiles showed a decrease on days 160-170 from the seasonal maximum of around $4.5 \mu\text{mol m}^{-2} \text{s}^{-1}$, which coincided with short-term cooling due to a storm system. In the current study, the timing of intensive

measurements during this relatively cool period meant that the seasonal maximum soil respiration flux was probably missed at the meadow transect positions, and would have been more similar to the value of $4.5 \mu\text{mol m}^{-2} \text{s}^{-1}$ measured at the central meadow location in the same summer. Production of CO_2 within the soil was generally greatest near the surface (Fig. 3.5d). Carbon dioxide production throughout the profile was greater at the 1.5 m transect position at all sampling dates except day 307. At this date, similar rates of total production were found for all transect positions, though the location of maximum respiratory production was deeper in the soil at 1.5 m than at the other two transect positions.

Extractable soil organic carbon (SOC) in the upper 10 cm of soil was greater at the end of the growing season than in spring for all transect positions, and was generally higher closer to trees than at the 9 m meadow position (Fig. 3.5b). Extractable microbial biomass carbon (MBC) showed the opposite trend, being highest in spring when the majority of extracted soil carbon was found as microbial biomass. Microbial biomass differences between transect positions were variable throughout the season. Consistent relationships were not found between MBC or SOC and the modeled surface CO_2 flux (data not shown), or the CO_2 production rate found for the same 0-10 cm interval of soil where carbon extraction samples were taken (Fig. 3.6). Microbial biomass carbon explained 8% of the variability in production between 0-10 cm, while SOC explained less than 1%. However, if data from day 307 are interpreted as outliers driven by unusually low soil temperatures and removed from the analysis, SOC explains 22% of the variability in soil CO_2 production in the top 10 cm.

Seasonal comparisons of soil respiration vs. soil temperature and soil moisture during the intensive study periods reflected contrasting seasonal patterns for data from under trees and in the meadow (Fig. 3.7). The progression through the growing season of fluxes, soil moisture, and soil temperature at the transect ends (Fig. 3.7) and their potential interactions with seasonal plant traits are discussed below. Soil CO₂ at 20 cm depth decreased with distance from tree on all sample dates (Fig. 3.8), with additional variability associated with seasonality and rain events. The arrival of fall rain on day 259 (Fig. 3.2) led to increased soil CO₂ at 20 cm (Fig. 3.8), which was primarily an effect of the addition of soil water on the diffusion coefficient, as surface CO₂ fluxes (Fig. 3.4, 3.5c) and soil CO₂ production (Fig. 3.5d) remained seasonally low on day 307. Between days 100 and 250, the shapes of the soil CO₂ curves at 1.5 and 9 m positions mirrored the differences in plant phenology: soil CO₂ under trees (1 m) was relatively high from the first measurement period through day 236, after which the time leaves dropped (yellowing began at ~ day 265), while soil CO₂ in the meadow (9 m) rapidly increased in spring and then decreased over summer and fall after senescence of meadow vegetation (Fig. 3.8).

Discussion

Soil respiration in relation to plant type and phenology

The meadow vegetation during 2005 was unique compared to other years in the six growing seasons from 2004 to 2009 (personal observation) because yellow sweetclover (*Melilotus officinalis*) emerged and created a dense canopy greater than 1 m tall. In other years during 2004-2009, this species was a relatively small fraction of

percent cover (<5% by visual estimation). It is unknown why this species emerged densely this year forming nearly a monoculture, or what the effect of its litter and potential nitrogen input to the soil via root endosymbiont fixation may have been on carbon fluxes in subsequent years. The rapid and dense growth of *M. officinalis* during 2005 corresponded with unusually high soil respiration fluxes shown in Figure 3.4 (triangles), including measurements near $\sim 20 \mu\text{mol m}^{-2} \text{s}^{-1}$. The correspondence of interannual variability in meadow vegetation and soil respiration suggested that plant functional types contribute to potentially large differences soil carbon fluxes.

In 2006, seasonal variability in soil respiration (Fig. 3.4, 3.5, 3.7) and soil CO_2 (Fig. 3.8) in the two vegetation types studied corresponded most consistently with differences in plant phenology during the growing season. Similar results were reported from a study conducted in an oak savanna in California examining transects of soil respiration from under deciduous oaks to open herbaceous understory vegetation (Tang and Baldocchi 2005). Consistent with our results, soil respiration was higher under trees than in the understory during wet spring and dry summer conditions. Trees continued to be active into the summer in both studies, presumably due to access to deeper soil moisture.

In spring (day 117) soil respiration under trees (1.5 m) was already near the seasonal maximum, although leaves had not yet begun to emerge. This may have been due to root growth and/or a microbial response to root exudation. While spring priming of microbial activity under trees has been associated with a winter exudation of SOC in a subalpine forest (Scott-Denton et al. 2005), at the time of our first measurements, MBC was at a seasonal high value while SOC was seasonally low (Fig. 3.5). Additionally,

MBC was similarly high in the meadow and under trees despite differences in soil respiration between these locations. Thus, there was no evidence that a localized pulse of exudation by tree roots in the upper 10 cm of soil was responsible for increased soil respiration rates under trees in spring. It appears more likely that the high respiration under the leafless trees at this time was due to root growth from stored carbon. However, microbial biomass does not necessarily relate to microbial respiration, and the possibility of a less abundant, but highly-active active microbial community under trees on day 117 cannot be excluded. A trenching study conducted with boxelder trees transplanted into an experimental garden from the same population as the current study showed that roots were of primary importance for high soil respiration rates in spring (Moyes et al. in review); however soil respiration increased at that site at the same time as leaf expansion. The profiles of CO₂ production with depth do not indicate substantial respiration from deeper soils where SOC and MBC samples were not collected (Fig. 3.5d). Spring root growth of trees at this site is consistent with the congeneric *Acer saccharum* in northeastern USA, which produced shallow fine roots maximally in spring (April/May) before leaf expansion (Hendrick and Pregitzer 1996). Our interpretation of root activity being a direct source of respiration before leaves appear is also consistent with results of Misson et al. (2006), in which a large spring increase in soil respiration was associated with initiation of growth of ponderosa pine roots before the growth of needles. Root growth has been shown to precede canopy growth in ecosystems where cold soil temperatures do not limit spring root growth (Burke and Raynal 1994, Hendrick and Pregitzer 1996), or to coincide with leaf growth (King et al. 2002). The timing of fine

root production varies between years for some species, probably in relation to soil temperature and nutrient availability (Fahey and Hughes 1994).

Meadow vegetation (9 m transect position) grew between the first and second intensive sampling periods (days 117-167), when the meadow was greenest (Fig 3.3). This growth corresponded with a decrease in soil moisture attributed to uptake by meadow vegetation and an increase in soil respiration (Fig. 3.7d). The increase in fluxes and decrease in soil moisture in the meadow were apparent despite lower soil temperature on sampling day 167 than 117, due to a passing weather system which partially re-wet the soil a few days earlier (Fig. 3.2, 3.7b). The increase in soil respiration despite decreased soil temperatures between days 117 and 167 highlights the potential importance of plant phenology in controlling soil respiration, presumably by impacting the supply of carbon belowground.

After day 167 soil temperature continued to increase, although soil respiration rates changed little at either the tree and meadow positions over days 167, 201, and 236 (Fig. 3.7a, b). While meadow vegetation had begun to senesce soon after day 167 (Fig. 3.3), tree leaves showed no sign of dormancy until approximately day 265, when yellowing was initially apparent (not shown). Modeled soil respiration under trees remained higher than at other transect positions until after leaves fell (Fig. 3.5). Soil moisture was similar on days 201 and 236 in the meadow (Fig. 3.2, 3.7d), and similar rates of soil respiration between these dates may have been sustained by use of carbon accumulated earlier in the season. There may have been a supply of recently-senesced leaf and root litter fueling decomposition, which would have compensated for the reduced supply of carbon transported to roots. Surviving, but senescent grasses and forbs

may have been allocating relatively more carbon to reproduction aboveground than belowground at this time. However, SOC and MBC measurements did not indicate a large increase in available carbon or microbial biomass in the meadow during this period (Fig. 3.5a, b). Under trees, soil organic carbon increased by day 236 (Fig. 3.5), which was unexpected because leaves had not begun to fall by this date (Fig. 3.3). This may have been due to root exudation or root death (Hendrick and Pregitzer 1996), though no coincident increase in soil respiration was observed (Fig. 3.5). It is possible that respiration rates remained similar because a decrease in root respiration was offset by an increase in heterotrophic respiration of root and mycorrhizal fungal litter. Extractable soil organic carbon at all transect positions was near the measured seasonal maximum on day 307 when respiration fluxes had substantially decreased (Fig. 3.4, 3.5, 3.7). At this time, soil moisture was high (Fig. 3.4, 3.7), and soil respiration was low and most likely limited because of low soil temperatures and the dormant status of tree and meadow vegetation.

CO₂ production with depth

Respiratory CO₂ production was higher under trees at depths below 10 cm than at the other transect positions throughout the study (Fig. 3.5d). Much of this difference can likely be explained by the differences in rooting depths of the trees and meadow vegetation. Boxelder trees are known to root to at least 4 m depth (Canadell et al. 1996), while grassland plants typically root to a maximum depth of ~2.5 m, with exponentially decreasing root densities from the surface (Jackson et al. 1996). Production of CO₂ was generally greatest near the surface (Fig. 3.5d), where root density and soil carbon content

were observed to be highest during soil coring (data not shown), and where maximum daily soil temperature would have occurred. Profiles of CO₂ production under trees in fall were an exception to this pattern, when production between 10 and 30 cm depth was found to exceed that near the surface. This result was somewhat perplexing, as it is difficult to speculate why surface CO₂ production near the surface was depressed under trees in fall relative to the other transect positions.

Comparison of model and chamber fluxes

Chamber fluxes in 2006 were more variable than model results (Fig. 3.4 and 3.5c), and this difference was possibly due to non-steady state conditions between soil CO₂ profiles and production. Our model required the assumption that the soil CO₂ profile was in continuous equilibrium with production, which may not have been the case. Spatial variability in soil respiration on the scale of meters is sometimes very high (Nakayama 1990, Goulden et al. 1996, Rayment and Jarvis 2000, Xu and Qi 2001), and this variability may have been muted in the soil profile modeling approach.

Soil respiration and MBC and SOC

It should be noted that our extractions made no distinction of SOC quality (e.g. decomposability), which is known to vary across similar vegetation gradients in the same geographic region (Van Miegroet et al. 2005, Olsen and Van Miegroet 2009), or microbial identity or function, which are independent of microbial biomass. These limitations notwithstanding, soil organic carbon and microbial biomass carbon did not correspond consistently with variability in soil respiration in our site, even when considering only the top 10 cm of soil where soil was collected for SOC and MBC

extractions (Fig. 3.6). This result contrasts with a study of paired riparian and meadow vegetation zones along streams in Oregon, USA, where higher soil respiration rates were associated with greater organic carbon, phosphorus, and mineralizable nitrogen in soils under riparian trees (Griffiths et al. 1997). Microbial biomass was also found to correspond strongly with soil respiration in a ponderosa pine plantation, although other potential respiration drivers were found to covary with MBC and could not be excluded (Xu and Qi 2001). We did observe high extractable MBC in soil in spring, when soil respiration under trees was high before leaf out and initiation of photosynthetic uptake (Fig. 3.5). While other researchers have made the connection between heterotrophic activity stimulated by root exudation and early spring soil respiration (Scott-Denton et al. 2005), the presence of similar MBC amount in the meadow and under trees, but lower respiration rates in the meadow points to another cause. The change in soil carbon between seasonally high MBC in spring and SOC in fall in the current study suggests that winter decomposition at the site may lead to metabolism of litter and proliferation of the microbial community, as has been observed in other sites with winter snow (Coxson and Parkinson 1987, Brooks et al. 2005, Kueppers and Harte 2005). This conclusion was supported for our meadow location in a separate study which compared fall and spring relationships between soil respiration and temperature (Moyes and Bowling in prep-b). Higher respiration rates in fall vs. spring for a given temperature were attributed to higher substrate availability for heterotrophic respiration, as soil moisture was similar and green plant biomass was minimal during these periods.

Plant effects on microclimate

Plant functional type (tree vs. meadow) also influenced soil microclimate. Shallow soil moisture was higher under trees than in the meadow throughout the warm season (Fig. 3.4; 3.7c, d). This was probably due in part to use of deeper soil moisture by these trees and to cooler soil temperatures due to shading by the canopy (Fig. 3.4). Understory vegetation below trees would also have experienced less light and heat energy, which may have reduced its water use relative to plants in the open meadow. Hydraulic redistribution of water in this case is unlikely, since it was not observed in a study evaluating stable isotopes of stem water of trees at this site (Phillips and Ehleringer 1995). A comparable effect of within-site vegetation on microclimate was seen in a northern Utah study of high-elevation tree islands surrounded by open meadow (Van Miegroet et al. 2000). Shading by trees on the perimeter delayed the melting of snow and reduced soil moisture loss and temperatures in the adjacent meadow during summer. A comparison of soils beneath deciduous and conifer trees found that soil temperatures were higher under deciduous trees while they were without shading leaves (Palmroth et al. 2005). In the current study, the deciduous trees had little impact on snowmelt, as they were without leaves until mid-spring, but dense tree canopies did reduce drying and heating of shallow soils during the summer months (Fig. 3.4). However, soil moisture and temperature were strongly correlated throughout the year across all transect positions, and this seasonal effect was stronger than spatial variability due to vegetation (Fig. 3.4). Soil respiration was limited by the combination of high soil temperatures and low soil moisture (Fig. 3.4), and these conditions corresponded with midsummer senescence of meadow vegetation (Fig. 3.1).

Conclusions

Variability in soil respiration in a Rocky Mountain ecotone between riparian trees and an open meadow was observed to correspond strongly with vegetation type and phenology. An unusual proliferation of a nitrogen-fixing forb in the meadow and under trees in 2005 was associated with a doubling of spring and summer respiration rates. In 2006, spatial differences in respiration, soil temperature, and soil moisture were associated with observed (growth and senescence) and interpreted (root growth) phenological events. These vegetation-associated factors corresponded more strongly with variability in soil respiration than soil organic carbon or microbial biomass carbon. Soil respiration at this site thus appears to be primarily dependent on inputs of fast-cycling carbon from plants.

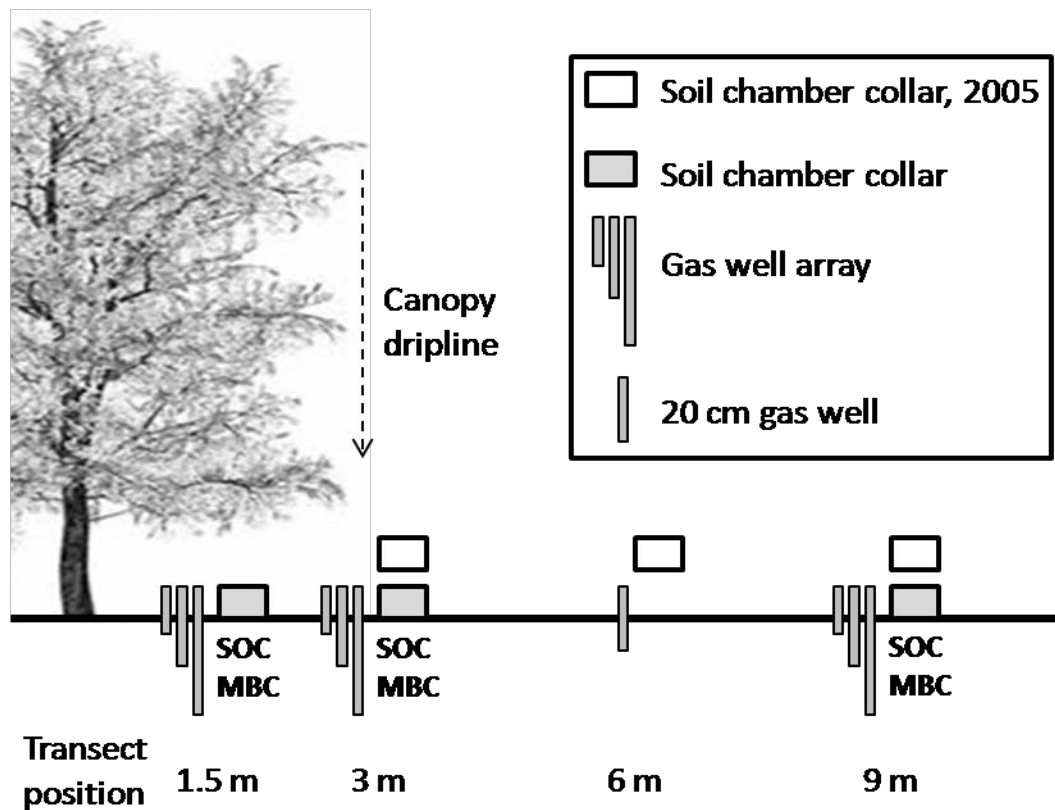


Figure 3.1: Schematic showing tree-meadow transect positions for soil chamber, gas well, soil organic carbon (SOC), and microbial biomass carbon (MBC) measurements. Open rectangles represent soil chamber measurement positions in 2005. All other measurements occurred exclusively in 2006. The canopy dripline is also shown, as some data are presented relative to this position to account for differences in tree size.

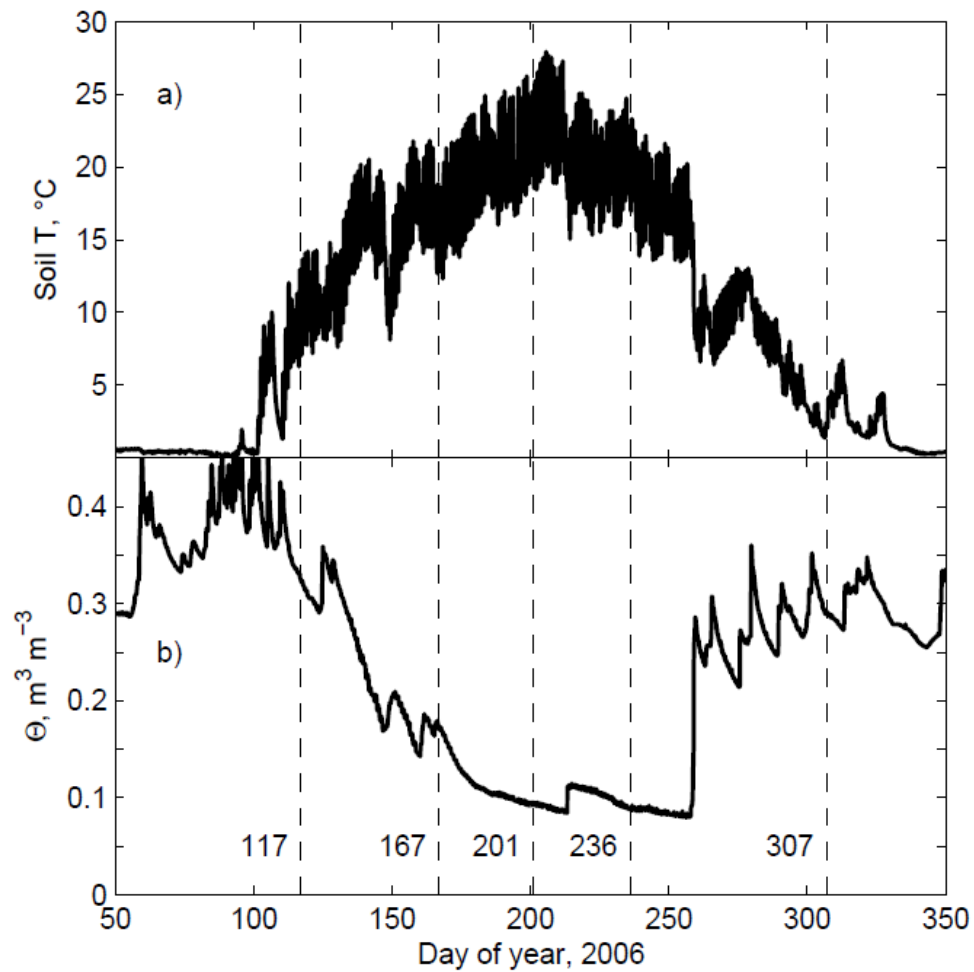


Figure 3.2: Soil temperature (a) and volumetric water content (θ , b) at 10 cm depth within the meadow during 2006. Dates of intensive sampling are shown with vertical dashed lines and day of year of each date is labeled in (b). These dates are representative of each of the five intensive sampling events, which required more than one day to conduct.



Figure 3.3: Photographs taken looking northwest from a central position in the meadow, showing phenological status of trees and meadow vegetation on the five intensive sampling dates in 2006. The day of year appears in the lower left of each image.

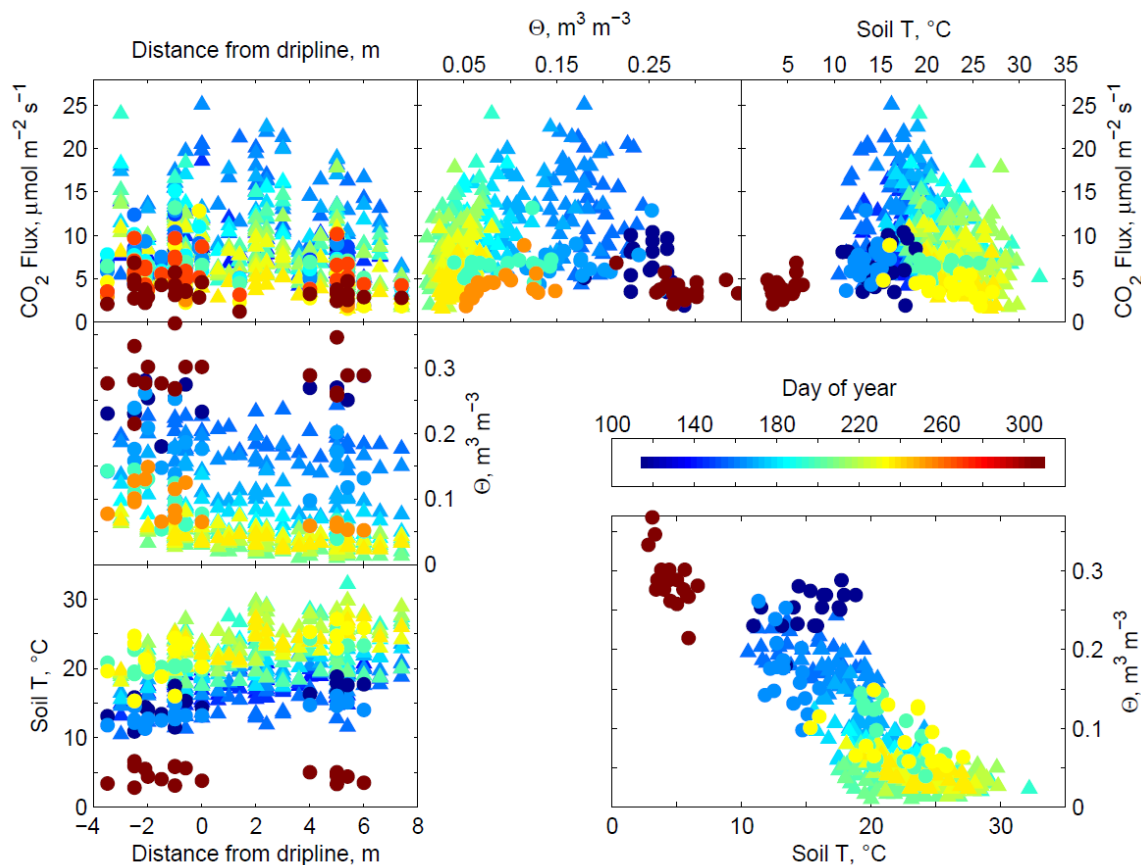


Figure 3.4: Top row: Point measurements of CO₂ fluxes vs. transect position relative to the canopy dripline (see Figure 3.1) of each tree, volumetric water content (θ) over 0-20 cm depth (via moisture probe (2005) or gravimetric measurements (2006)), and soil temperature at 10 cm. Vertical column: CO₂ flux, volumetric water content (as above), and soil temperature at 10 cm plotted vs. transect position relative to the canopy dripline. Lower right panel: relationship between soil moisture and temperature at 10 cm. In all plots data from 2005 are shown as triangles and circles are from 2006. Color represents the date within the season, and progresses from dark blue at day 117 to dark red at day 307 (center right panel).

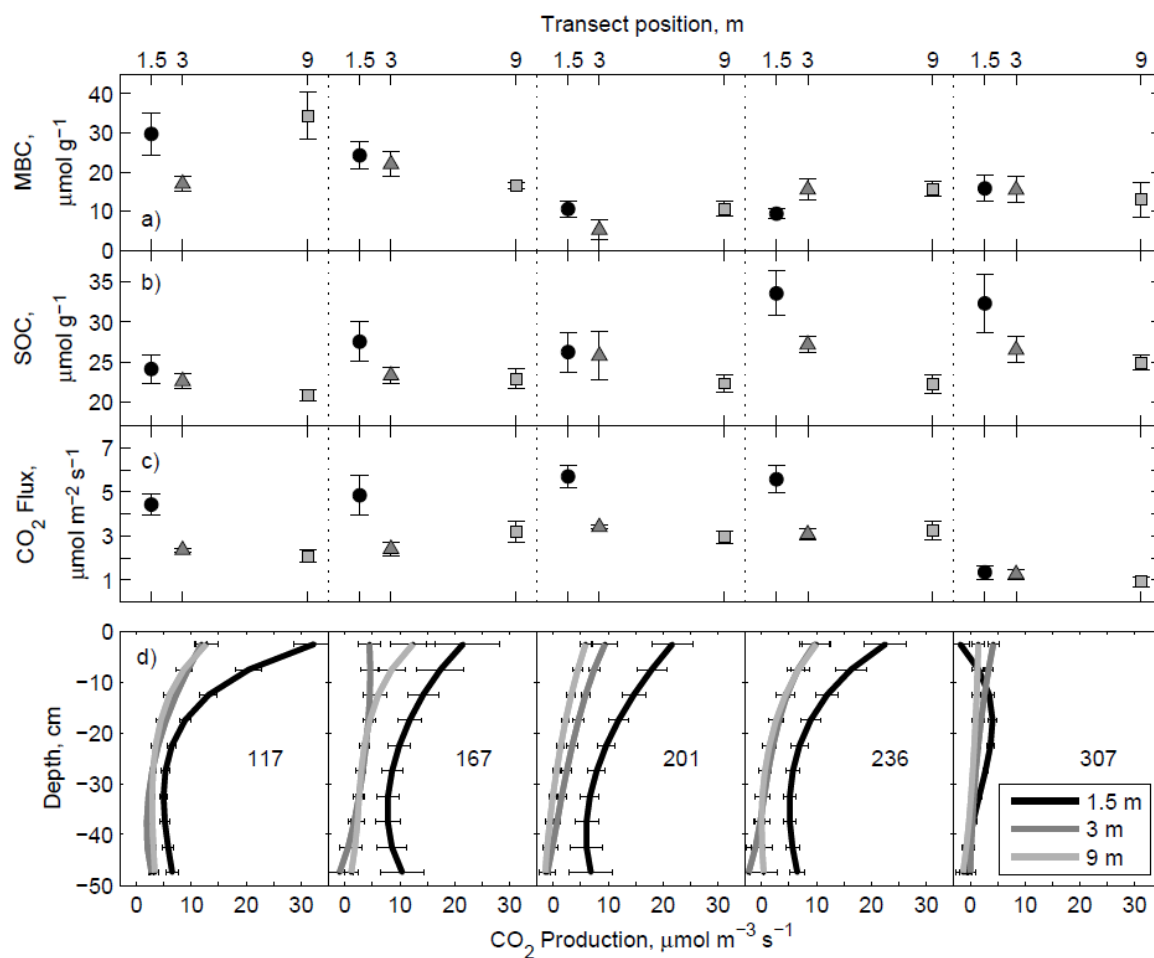


Figure 3.5: Extractable microbial biomass carbon ((a), MBC), extractable soil organic carbon ((b), SOC), and modeled surface CO₂ flux (c) vs. transect position for each of the five intensive sampling periods (separated by vertical dotted lines). (d), model results of CO₂ production with depth for each transect position during each sampling period. All carbon extractions were made from soil collected from the top 10 cm. Symbols in rows (a-c) represent transect positions for consistency with Figures 3.6 and 3.7. Error bars are one standard error of the mean.

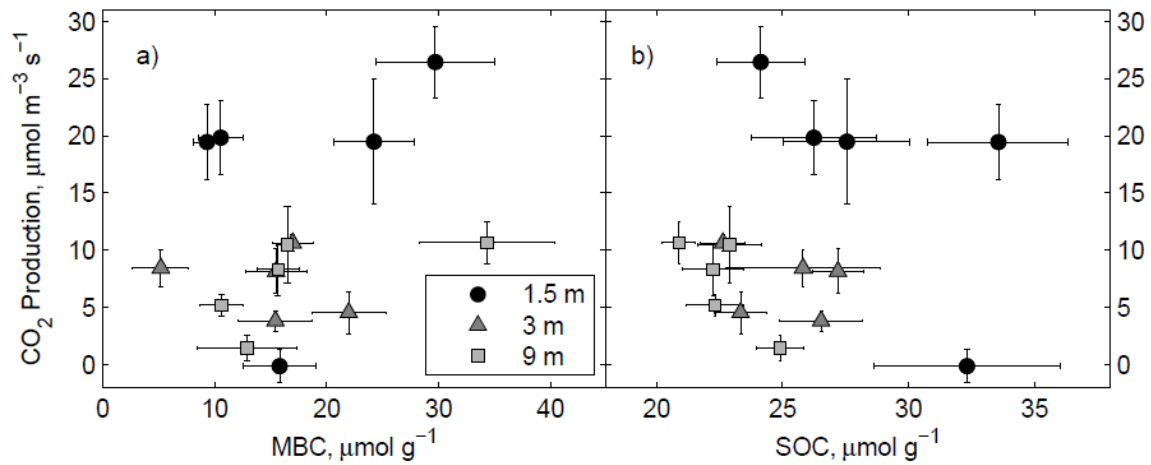


Figure 3.6: Calculated rates of production of CO₂ within the top 10 cm of soil for each transect position vs. extractable microbial biomass carbon (MBC, (a)) and extractable soil organic carbon (SOC, (b)) from 10 cm-deep soil cores.

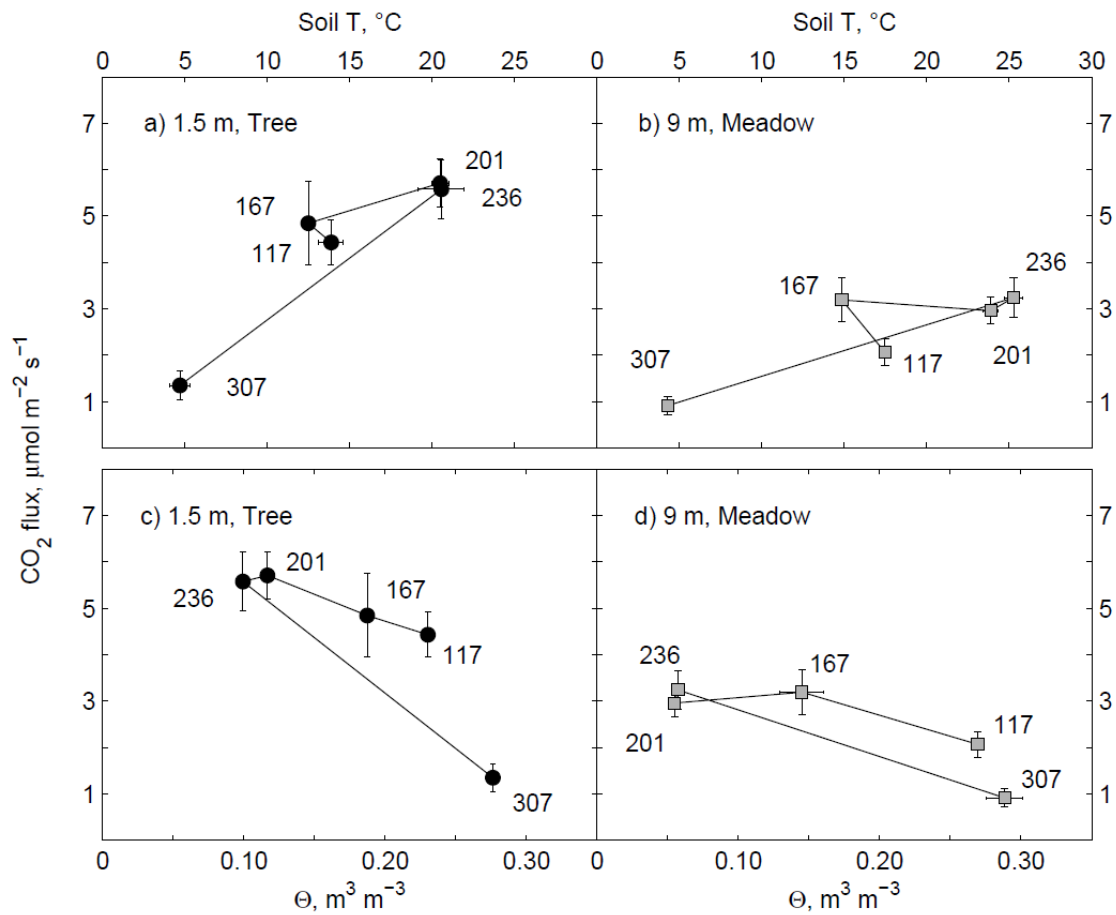


Figure 3.7: Modeled surface CO₂ flux for each of the five intensive sampling dates (numbers) vs. soil temperature ((a), and (b)) and volumetric water content (θ, (c) and (d)) at 10 cm. Plots (a) and (c) are data from 1.5 m transect positions (under tree canopies) and (c) and (d) are data from 9 m positions (in open meadow). Error bars are one standard error of the mean.

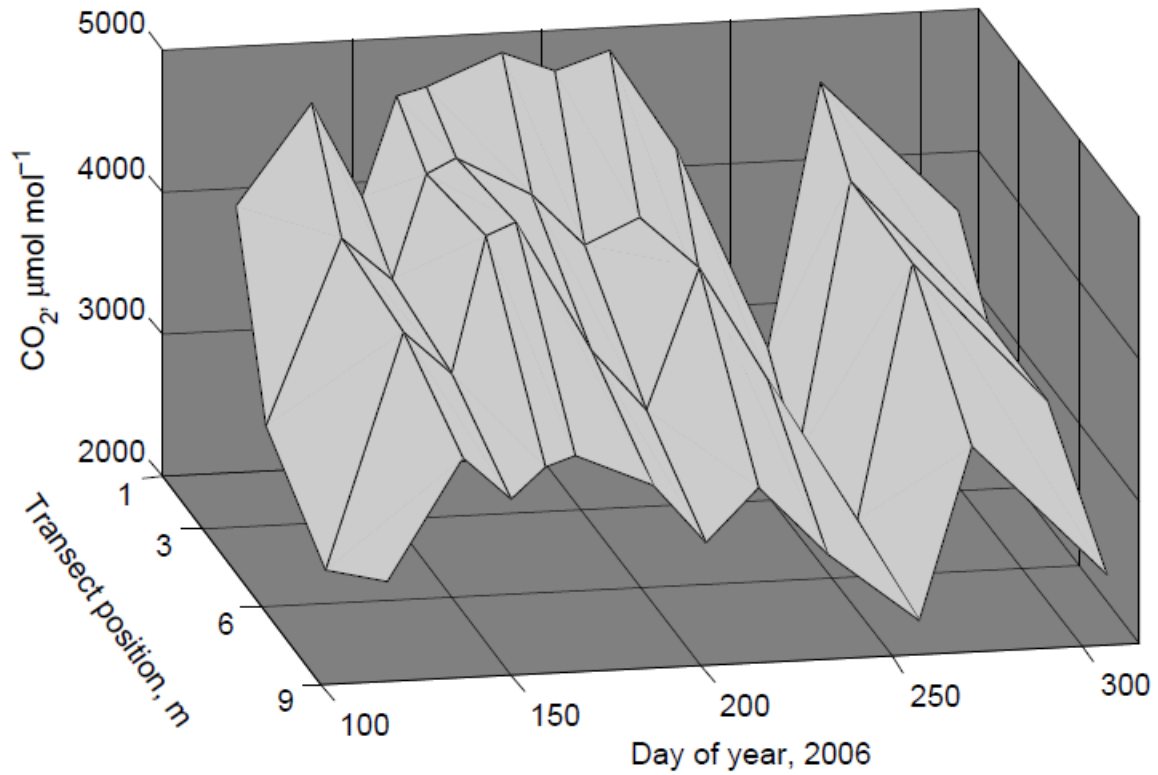


Figure 3.8: Soil carbon dioxide at 20 cm depth vs. transect position over sampling dates throughout the 2006 growing season.

CHAPTER 4

DIFFUSIVE FRACTIONATION COMPLICATES ISOTOPIC

PARTITIONING OF AUTOTROPHIC AND

HETEROTROPHIC SOURCES OF

SOIL RESPIRATION

Abstract

Carbon isotope ratios ($\delta^{13}\text{C}$) of heterotrophic and rhizospheric sources of soil respiration under deciduous trees were evaluated over two growing seasons. Fluxes and $\delta^{13}\text{C}$ of soil respiratory CO_2 on trenched and untrenched plots were calculated from closed chambers, profiles of soil CO_2 mole fraction and $\delta^{13}\text{C}$, and continuous open chambers. $\delta^{13}\text{C}$ of respired CO_2 and bulk carbon were measured from excised leaves and roots and sieved soil cores. Large diel variations ($> 5\text{‰}$) in $\delta^{13}\text{C}$ of soil respiration were observed when diel flux variability was large relative to average daily fluxes, independent of trenching. Soil gas transport modeling supported the conclusion that diel surface flux $\delta^{13}\text{C}$ variation was driven by nonsteady state gas transport effects. Active roots were associated with high summertime soil respiration rates and around 1‰ enrichment in the daily average $\delta^{13}\text{C}$ of the soil surface CO_2 flux. Seasonal $\delta^{13}\text{C}$

variability of about 4‰ (most enriched in summer) was observed on all plots and attributed to the heterotrophic CO₂ source.

Introduction

Soil respiration remains one of the largest sources of uncertainty about carbon cycling within ecosystems because soil biological communities and processes are complex, relatively inaccessible, and highly sensitive to disturbance. Two broad categories of soil organisms can be distinguished by their carbon sources: 1) the bulk soil heterotrophic component feeding on soil organic matter, and 2) the rhizosphere component, which in the present study is taken to include roots, mycorrhizal fungi, and rhizomicrobial heterotrophs feeding on carbon supplied by roots. Simple partitioning of soil respiration into these two components has been achieved by interruption of photosynthate transport belowground to intact soils by methods such as trenching (Hanson et al. 2000) and stem girdling (Högberg et al. 2001). Recent attempts to combine stable carbon isotope ratio ($\delta^{13}\text{C}$) measurements with these approaches have yielded additional information about soil respiration and its components.

The $\delta^{13}\text{C}$ of phloem sugars transported to roots initially depends on photosynthetic discrimination in leaves (Δ). Because root respiration in temperate forests typically represents a large fraction of total soil respiration (Högberg et al. 2001, Subke et al. 2006), environmental variables that drive changes in Δ by affecting assimilation rate or stomatal conductance to CO₂ may be correlated with variability in $\delta^{13}\text{C}$ of soil respiration, possibly with a source-to-sink transport time lag (Ekblad and Högberg 2001, Ekblad et al. 2005). The $\delta^{13}\text{C}$ of CO₂ respired by roots and other rhizosphere

components may also be affected by utilization of fast or slow turnover carbon pools (Schnyder et al. 2003) or allocation between growth vs. maintenance (Ocheltree and Marshall 2004).

The $\delta^{13}\text{C}$ of CO_2 respired by heterotrophic soil microorganisms depends on the substrates within soil organic matter utilized for decomposition. Total soil organic matter is generally enriched in ^{13}C relative to leaf litter, and becomes progressively more enriched with depth (Ehleringer et al. 2000). The CO_2 produced during decomposition can be depleted (Mary et al. 1992, Fernandez et al. 2003) or enriched (Andrews et al. 2000, Böstrom et al. 2007) in ^{13}C relative to bulk soil organic matter.

Total soil respiration tends to be a few ‰ enriched in ^{13}C relative to site-specific bulk leaf $\delta^{13}\text{C}$ (Bowling et al. 2008). However, root respiration has been found to be ^{13}C -depleted relative to leaf and shoot tissues in laboratory studies with herbaceous species (Badeck et al. 2005, Klumpp et al. 2005, Schnyder and Lattanzi 2005). If this relationship extends to woody plants under field conditions, there would be an unknown, putative ^{13}C -enriched soil CO_2 source necessary to account for soil respiration being generally enriched relative to leaf tissues (Bowling et al. 2008). If consistent isotopic differences exist between a ^{13}C -depleted root source and a ^{13}C -enriched heterotroph source, this would be useful for nondisruptive soil respiration partitioning. However, reports from forest trees have shown ^{13}C -enriched respiration from roots (Gessler et al. 2007) and trunks (Brandes et al. 2006) relative to substrates such as water soluble phloem exudates. Studies comparing $\delta^{13}\text{C}$ of root and soil respiration are necessary to identify and define these relationships. Further, application of isotopes to understand the importance of phloem transport to soil respiration and its component sources requires

measurements that extend from isolated roots to include the entire rhizosphere, and a clearer understanding of the processes and conditions that influence the carbon isotope content of belowground respiration.

The present study was conducted to determine the natural abundance $^{13}\text{C}/^{12}\text{C}$ ratio and variability of individual heterotroph (bulk soil) and rhizosphere sources of soil respiration under deciduous boxelder (*Acer negundo*) trees to understand how utilization of these individual carbon sources might vary with phenology and environmental variables. Measurements of rates and $\delta^{13}\text{C}$ of soil respiration were collected on replicated trenched and untrenched plots (without and with active roots) using multiple independent methods. Data from the snow-free periods of two consecutive years are presented, including one entire season (bud burst through leaf senescence) when all methods were applied simultaneously. Comparisons were made between $\delta^{13}\text{C}$ of soil respiration on untrenched and trenched plots; respired CO_2 from sieved soil cores (soils alone), roots, and leaves; and bulk C from soils and root and leaf tissues.

Our continuous open chamber data and experimental treatments provided a unique opportunity to examine the possible causes of diel fluctuations in $\delta^{13}\text{C}$ of the soil surface CO_2 flux. Diel variability in $\delta^{13}\text{C}$ of soil respiration has been observed in some recent studies with high-frequency isotopic flux data (Kodama et al. 2008, Bahn et al. 2009, Marron et al. 2009). In these studies diel $\delta^{13}\text{C}$ variability was generally interpreted to represent variability in source $\delta^{13}\text{C}$ (by implicit assumption of steady state gas transport). In the current study we test the alternative hypothesis that diel variability in the carbon isotope content of the soil respiration surface flux can be driven by nonsteady states of diffusion within the soil profile. Transient diffusive fractionations occur

whenever boundary conditions, production rates, or soil diffusivities change and a system begins to develop towards a new steady state (Amundson et al. 1998, Risk and Kellman 2008, Nickerson and Risk 2009b). Diel variation in surface fluxes is produced when a lighter isotopologue ($^{12}\text{CO}_2$) and a heavier isotopologue ($^{13}\text{CO}_2$) are released from points of respiration simultaneously in a time-varying manner (e.g., with respiratory production driven by changes in soil temperature). Due to the small differences in diffusivities of $^{12}\text{CO}_2$ and $^{13}\text{CO}_2$ in air (Cerling et al. 1991), soils are likely to approach isotopic steady state more slowly than net flux steady state. Thus, daily varying production rates have the potential to perpetuate a transient diffusive state for the isotope ratio of CO_2 , though the net surface CO_2 flux may be near constant equilibrium with production and $\delta^{13}\text{C}$ of respiration may be constant. To further investigate this possibility, an isotopic gas transport model treating production and transport of $^{12}\text{CO}_2$ and $^{13}\text{CO}_2$ independently was run with variable rates and depths of CO_2 production, while maintaining $\delta^{13}\text{C}$ of CO_2 production at a constant value. Model results were compared to continuous chamber data from this and previously published studies.

Methods

Experimental design

This project made use of an experimental garden on the University of Utah campus ($40^\circ45'39.3''\text{N}$, $111^\circ49'48.8''\text{W}$, 1481 m) established for intensive physiological monitoring of boxelder (*Acer negundo*) trees (Hultine et al. 2008). The 100 m by 40 m site was developed in 2001 by transporting in fill material and covering with topsoil from a nearby location, and then planting 36 trees grown from locally collected cuttings along

a six tree by six tree grid. By the time of the present study the trees were mature and had been setting seed for several years. A barrier was installed in 2005 to bisect the study area into two replicate halves by burying 6.35-mm thick PVC sheets vertically to 2 m depth. Artificial streams were then created in each side by pumping water from a nearby natural stream through perforated tubing within excavated gravel-lined streambeds that meandered between the trees. Soils were kept at high moisture content throughout each subsequent year by flowing these streams continuously from just after snow melt in April until rain and snow appeared again in November, when leaves were senescent. For additional site-related details, see Hultine et al. (2008).

For the present study, the central, 2m deep barrier was used to isolate trenched and untrenched (control) plot pairs under individual boxelder trees (Fig. 4.1). Six trees were growing close enough to this barrier to have canopies that extended above it from one side to the other. In March of 2007 “+Roots” (normal, control plots that contained roots and rhizosphere) and “-Roots” (treatment plots with roots severed by trenching at the start of the study) plot pairs were established under each of these trees. One area under each canopy on the same side of the main barrier as the trunk was designated as a “+Roots plot”. An adjacent, approximately 1.5 m² “-Roots” plot was created on the opposite side by trenching on three additional sides to 1 m depth and lining with 1-mm thick polyethylene sheeting. The edges where the two sides of this plot met the main 2-m deep barrier were sealed with a silicone sealant before backfilling. This study coincided with a nitrogen fertilization experiment at the site, in which one half of the study area received a nitrogen addition to the stream water. The arrangement of the trenched/untrenched plots was such that half of each trenching treatment group (three

plots each) was within each nitrogen treatment, allowing for detection of any effects of fertilization on our results.

Understory vegetation within and immediately surrounding all plots was removed weekly throughout the study. Any live roots present within the trenched plots would have been severed by trenching and surface clearing in March of 2007 and represented a potential substrate source for decomposition during the following two growing seasons of the study. However, given that the 2 m root barriers were already isolating these areas from roots of nearby trees, the majority of live roots in these plots would have been from herbaceous understory vegetation (mostly C₃ grasses and forbs), which had only recently begun to germinate at the time of plot installation and clearing.

Meteorological measurements

Air temperature and relative humidity probe measurements (HMP 45 AC, Vaisala, Woburn, MA, USA) were collected every 30 s and stored as 10-min averages during the entire study period by an on-site micrometeorological station described by Hultine et al. (2008). Soil moisture and temperature were measured within a subset of plots to identify any differences associated with the trenching treatment. Soil temperature was measured with thermocouples inserted to 5 cm depth in two plot pairs and soil moisture was recorded with reflectometry probes (CS615, Campbell Scientific, Logan, UT, USA) placed at 15 cm in one plot pair. These were measured at 10-s intervals and stored as 10-min averages by a datalogger (CR10X, Campbell Scientific, Logan, UT, USA), beginning in April 2008.

Soil CO₂ and $\delta^{13}\text{C}$ profile measurements

Gas wells were installed in each of the 12 plots in early April, 2007. The gas wells consisted of individual lengths of stainless steel tubing (6.35 mm OD) with open, buried ends at 1, 2, 4, 7, 10, and 35 cm below the surface and a fittings containing septa (Microsep F-138, Alltech, Deerfield, IL, USA) on the ends protruding above the soil surface. To install the upper 5 wells a small, 10 cm deep hole was excavated near one corner of each plot. Then a 20 cm length of tubing was inserted horizontally through the pit wall at each measurement depth in randomly fanning directions, but generally towards the center of the plot. A metal rod was temporarily placed inside the tube during insertion to prevent clogging. A second piece of tubing with a 90-degree bend was then attached to each horizontal tube, a septum fitting was placed on the aboveground end, and the hole was backfilled. The 35 cm wells consisted of a single length of tubing with a septum fitting and were installed vertically towards the center of each plot, with a metal rod used during installation to prevent clogging.

Gas samples were collected from each gas well in evacuated 12 mL vials (Exetainer, Labco, High Wycombe, Buckinghamshire, UK) using a two-ended needle. Plots were visited for gas well sampling roughly biweekly during the snow-free periods of 2007 and 2008 (March/April – November), which included the entire period from budburst to leaf senescence each year. Mole fraction of CO₂ was measured from each vial by injecting a 0.5 mL sample into CO₂-free air stream, through a port just upstream of an infrared gas analyzer (IRGA, Li-7000, Li-Cor, Lincoln, NE, USA) and integrating the CO₂ peak (Davidson and Trumbore 1995). Peak areas measured from prepared CO₂ standard gases were used to calculate sample CO₂ mole fractions. A second gas sample

was then injected into a tunable diode laser absorption spectrometer (TGA 100A, Campbell Scientific, Logan, UT, USA) for measurement of $\delta^{13}\text{C}$ of CO_2 as described in detail in Moyes et al. (2010). For this measurement the volume of sample injected depended on CO_2 mole fraction, and samples were calibrated using injections from three prepared $\delta^{13}\text{C}$ standard cylinders. Measurement uncertainties were 5% of reading for mole fractions and 0.25‰ for $\delta^{13}\text{C}$.

Closed chamber soil respiration rate measurements

Ten-cm diameter PVC collars were inserted to 4 cm depth in each plot for closed chamber measurements. Soil respiration rates were measured manually using a portable gas exchange system and a closed chamber (Li-6400-09, Li-Cor, Lincoln, NE, USA) on the same days that soil gas wells were sampled.

Determination of rhizosphere and heterotroph

respiration rates and $\delta^{13}\text{C}$

Respiration fluxes on trenched plots were assumed to represent the contribution of heterotrophic soil organisms (soil organic matter-driven) to total soil respiration. This amount was subtracted from the flux measured on untrenched plots to give the contribution of rhizosphere (photosynthate-driven) respiration to total soil respiration. Mole fraction and $\delta^{13}\text{C}$ data from soil gas well profiles were used to calculate $\delta^{13}\text{C}$ of respired CO_2 for each sampling date, using either data from individual profiles or composite data from all +Roots or -Roots replicate plots, via the two-endmember Keeling plot approach (Keeling 1958). Intercepts of lines fit to $\delta^{13}\text{C}$ vs. 1/mole fraction of soil

CO₂ were used, and a steady state, 4.4‰ diffusive enrichment correction was subtracted from each intercept to calculate the δ¹³C of respired CO₂ from each plot or treatment (Cerling et al. 1991, Davidson 1995). The calculated δ¹³C of the soil CO₂ source from trenched plots was taken to represent the δ¹³C of CO₂ respired from soil heterotrophs (δ_{Het}). This source and the δ¹³C of respired CO₂ from the rhizosphere (δ_{Rhiz}) were assumed to combine to produce the δ¹³C of CO₂ respired in untrenched plots (δ_{Tot}). δ_{Rhiz} was calculated as:

$$\delta_{Rhiz} = \frac{(F_{tot} * \delta_{tot}) - (F_{Het} * \delta_{Het})}{F_{tot} - F_{Het}} \quad 4.1$$

where F_{tot} and F_{Het} are the closed chamber flux rate measurements and δ_{tot} and δ_{Het} are the δ¹³C signatures from untrenched and trenched plots, respectively.

Open chamber determination of rates and δ¹³C of

rhizosphere and heterotroph respiration

Four permanent, 30.5-cm diameter PVC collars were inserted 5 cm into the ground in two +Root/-Root plot pairs in early April, 2008. Two flow-through, open chamber lids modeled after Rayment and Jarvis (1997) were used to measure continuous flux rates and δ¹³C of soil respiration with a tunable diode laser absorption spectrometer as described by Moyes et al. (2010). Equipment availability limited measurements to two chambers during a given time (one +Root, one -Root). Chamber lids were moved between pairs of collars approximately every two weeks and immediately following rain events. Lids were sealed to the collars using putty (Terostat VII, Henkel Technologies,

Dusseldorf, Germany) and left in place until they were moved to the other collar pair (lids did not open). Soil respiration flux rates were calculated as:

$$Flux = \frac{(C_o - C_i) * Flow}{A} \quad 4.2$$

where C_o and C_i are the mole fractions of CO_2 in the dry inlet and outlet flows from the chambers, “Flow” is the number of moles of air passing through the chamber per second, and A is the soil surface area enclosed by the chamber. The isotope composition of the soil respiration flux ($\delta^{13}C_{SR}$) was calculated as:

$$\delta^{13}C_{SR} = \frac{(C_o * \delta_o) - (C_i * \delta_i)}{C_o - C_i} \quad 4.3$$

where δ_o and δ_i are the $\delta^{13}C$ of the CO_2 in the inlet and outlet flows in ‰. Flow through each chamber was periodically adjusted between 1 and 4.5 $L \min^{-1}$ to maintain a roughly 50-100 $\mu\text{mol mol}^{-1}$ difference in CO_2 between inlet and outlet flows. This range represented a tradeoff optimum, as smaller gradients limit isotope precision and larger gradients would lead to flux underestimation (Davidson et al. 2002). Prior to field deployment, chambers were tested for differential pressure effects over a range of chamber flow rates with the chamber bottom sealed to a bench top in the laboratory. Flow rates of up to 4.5 $L \min^{-1}$ produced differential pressures smaller than -0.2 Pa (lower within the chamber). Use of a sealed bench top in place of a porous soil medium identified the maximum pressure perturbation associated with each flow rate (Xu et al. 2006). Longdoz et al. (2000) reported that a pressure difference of this magnitude across

a chamber placed in soil increased fluxes by less than 10%, and the chosen maximum flow rate of 4.5 L min^{-1} was below limits reported to produce minimal effects on CO_2 flux measurements with similar chambers (Rayment and Jarvis 1997, Fang and Moncrieff 1998).

Chamber measurements were made every ten minutes, and data are reported as 3-hour and daily averages to reduce noise. The flux and $\delta^{13}\text{C}$ of respired CO_2 from trenched plots was assumed to reflect the heterotrophic contribution to soil respiration, and the rhizosphere-respired CO_2 flux and $\delta^{13}\text{C}$ were calculated from untrenched and trenched CO_2 fluxes and $\delta^{13}\text{C}$ as described above.

$\delta^{13}\text{C}$ of leaves, roots, soil, and respired CO_2 from each

Examination of the diel pattern of bulk $\delta^{13}\text{C}$ of ecosystem components (sun leaf, shade leaf, root, untrenched plot soil, and trenched plot soil), and the $\delta^{13}\text{C}$ of respired CO_2 from each was conducted July 29-30, 2008. Four sets of samples were taken from three trees and their associated “+Roots/-Roots” plots every 6 hours beginning at 9am. At each sampling time, three individual fully expanded leaves, containing 3 leaflets, from the top (sun) and bottom (shade) of each canopy were cut and stored in dark conditions for 10 min before respiration measurements. This consistent delay was chosen to allow leaves to dark-acclimate and avoid transient isotope effects upon darkening (Barbour et al. 2007). At each sampling time, a 5 cm diameter core was taken to a depth of 20 cm from each plot using a bucket auger. Roots, when present, were manually picked from these cores, rinsed with distilled water and patted dry. The soil was then sieved to remove particles larger than 2 mm and the remaining fraction was subsampled. A gas

exchange system composed of a closed loop with an IRGA (Li-820, LiCor, Lincoln, NE, USA), a pump (UNMP830 KVDC-B, KNF, Freiburg, Germany), a glass sample cuvette, and two 100 mL glass flasks in parallel was used to collect samples for analysis of CO₂ and $\delta^{13}\text{C}$. The system was connected to a cylinder containing 400 $\mu\text{mol mol}^{-1}$ (-9.45 ‰) CO₂ in air and flushed before each measurement. Next a leaf, root, or soil sample was placed in the chamber, held in place with glass wool, and the system was flushed from the tank again. The gas cylinder was then disconnected and the pump turned on to circulate the air in the system in a closed loop. Once mixing was adequate, which was apparent in the stability of IRGA measurements and took about 5-10 s, the pump was stopped and the stopcocks on one of the flasks were immediately closed. The pump was started again and CO₂ was allowed to accumulate until the mole fraction had risen by $\sim 50 \mu\text{mol mol}^{-1}$, when the pump was stopped and the second flask was sealed. Mole fraction and $\delta^{13}\text{C}$ of CO₂ in the flasks was measured on a continuous flow isotope ratio mass spectrometer (IRMS, Delta Plus, ThermoFinnigan, Bremen, Germany). $\delta^{13}\text{C}$ of respired CO₂ from the sample was calculated similarly to Eq. 3 (initial and final flasks treated as inlet and outlet). Solid organic samples were immediately placed in drying ovens at 60° C after respiration measurements. Soil samples were acid washed to remove carbonates. Dried samples were milled and measured via continuous flow IRMS coupled with an elemental analyzer (EA 1108, Carlo Erba, Rodano, Italy).

Isotopic diffusion model

To examine the extent to which diel variability in $\delta^{13}\text{C}$ of soil respiration may be produced by diffusive fractionation effects, a model was developed in which $\delta^{13}\text{C}$ of soil

CO₂ production was held constant and production and diffusion of ¹²CO₂ and ¹³CO₂ in the soil were treated independently under varying physical conditions. Model parameters were selected to encompass observed values for those variables that were measured in the current study, and to include realistic values for those which were not. The aim was to include enough variability in model parameters to identify sensitivity of the diel range of modeled δ¹³C of the surface CO₂ flux to variability in each parameter. A total of 320 different simulations were conducted by varying the following parameters in a factorial manner: the shape of the CO₂ production function with depth, the maximum depth of CO₂ production (0.1, 0.2, 0.4, or 0.8 m), the maximum CO₂ production rate at the surface (0.5, 1, 2, 10, or 20 μmoles m⁻³ s⁻¹), Q₁₀ of production of CO₂ (1, 2, 3, or 4), and the volumetric water content profile (0.05, 0.10, 0.15, 0.20, 0.20 m³ m⁻³ (“dry”) or 0.15, 0.30, 0.35, 0.35, 0.40 m³ m⁻³ (“wet”) at 0, 0.1, 0.2, 0.45, and 1 m depth nodes, respectively). In each simulation, 4 days were run at one time. Within each 4 day set, the maximum δ¹³C of the modeled surface CO₂ flux from the second day was compared to the maximum from the first day. Each simulation would continue until these 2 values were within 0.05 ‰ of one another. At that point, the rates and δ¹³C of the modeled surface CO₂ flux from the final day were recorded and a new simulation would start with the next parameter set, using the profiles of ¹²CO₂ and ¹³CO₂ from the last time step of the previous model run as initial conditions.

Within the model a soil column of unit area and a soil depth (L) of 1 m was divided into layers of 2 cm depth increments. Model time steps were 0.002 h (7.2 s). These depth and time increments were found to produce consistent model stability. Total porosity was set to 0.5 m³ m⁻³ throughout the soil profile and volumetric water content (θ,

$\text{m}^3 \text{m}^{-3}$) was linearly interpolated between “dry” or “wet” node values. Air-filled porosity was calculated for each depth by subtracting θ from total porosity.

CO_2 production at 10°C was either input as a decreasing function of depth after Kirkham and Powers (1972):

$$R_{10}(z) = R_{10,z=0} \left(1 - \left(\frac{z}{z_{R=0}} \right)^{1/4} \right) \quad 4.4$$

where $R_{10,z=0}$ is the CO_2 production rate at 10°C at the surface in $\mu\text{mol m}^{-3} \text{s}^{-1}$, and $z_{R=0}$ is the depth where production goes to zero; or represented by a constant value over a depth interval:

$$R_{10}(z) = \begin{cases} R_{10,z=0} & z < z_{R=0} \\ 0 & z \geq z_{R=0} \end{cases} \quad 4.5$$

The CO_2 production profile was then adjusted for changing soil temperature with depth and time. Soil temperature was modeled after Campbell and Norman (1998) with surface temperature set to vary between 10 and 25°C :

$$T(z, t) = T_{ave} + A_o * \exp(-z/d) * \sin[\omega(t - 8) - z/d] \quad 4.6$$

where T_{ave} is the average surface temperature, A_o is half the amplitude of diel surface temperature variation, d is a damping depth, and ω is $\pi/12$ and sets the period to 24 h. Damping depth was set to 0.05 for dry, and 0.1 for wet soil conditions (Campbell and Norman 1998). CO_2 production in each layer and time step was adjusted according to temperature at each depth following the Q_{10} equation (Curiel Yuste et al. 2005a):

$$R(z, t) = R_{10}(z) * Q_{10}^{((T(z, t) - 10) / 10)} \quad 4.7$$

where Q_{10} is a coefficient defining the temperature sensitivity of CO_2 production.

Individual production rates for $^{12}\text{CO}_2$ and $^{13}\text{CO}_2$ were then calculated to reflect a constant $\delta^{13}\text{C}$ of total production of -25 ‰. The number of moles of CO_2 produced within a given layer over each time step was calculated as:

$$R_{i, j-1} = R(z, t) * \Delta z * \Delta t \quad 4.8$$

where subscripts i and j reflect vertical layers and model time steps, respectively, Δz is the difference in depth (m) between successive layers, and Δt is the length of each time step (s).

Diffusion coefficients of CO_2 were calculated for each soil layer and time step following:

$$D(z, t) = D_o(z, t) * \xi(z) \quad 4.9$$

with $D_o(z, t)$ being the diffusivity of CO_2 in air, given by:

$$D_o(z, t) = D_{ao} * \left(\frac{T(z, t)}{293.15} \right)^{1.75} * \left(\frac{101.3}{P} \right) \quad 4.10$$

where P is 86 kPa (local atmospheric pressure for Salt Lake City) and D_{ao} is $15.7 \text{ mm}^2 \text{ s}^{-1}$, the reference value for CO_2 diffusivity in air at 293.15 K and 101.3 kPa (Campbell and Norman 1998). $\xi(z)$ is a tortuosity factor, which was calculated based on air-filled (ϵ) and total (ϕ) porosities following Millington (1959):

$$\xi(z) = \frac{\varepsilon(z)^{\frac{10}{3}}}{\phi^2} \quad 4.11$$

The diffusion coefficients for $^{12}\text{CO}_2$ and $^{13}\text{CO}_2$ for each layer and time were then calculated from the corresponding total CO_2 value to maintain a ratio ($D_{12\text{CO}_2}/D_{13\text{CO}_2}$) of 1.0044 (Cerling et al. 1991).

Vertical fluxes of $^{12}\text{CO}_2$ and $^{13}\text{CO}_2$ between layers were calculated as:

$$F_{ij} = \left(\frac{C_{i,j-1} - C_{i-1,j-1}}{\Delta z} \right) * \left(\frac{D_{i,j-1} + D_{i-1,j-1}}{2} \right) * \Delta t \quad 4.12$$

where C is the isotopologue molar density in $\mu\text{mol}/\text{m}^3$. The new molar density of CO_2 in each layer after each model time step ($C_{i,j}$) was then calculated as the sum of the molar density in the previous time step ($C_{i,j-1}$), the flux out through the upper boundary (F_{out}), the flux in through the lower boundary (F_{in}) and the amount produced within the layer ($R_{i,j-1}$) following Nickerson and Risk (2009b):

$$C_{i,j} = \frac{C_{i,j-1} * \varepsilon * \Delta z - F_{\text{out}} + F_{\text{in}} + R_{i,j-1}}{\varepsilon * \Delta z} \quad 4.13$$

To maintain a constant surface boundary condition and calculate surface fluxes of $^{12}\text{CO}_2$ ($F_{12\text{CO}_2}$) and $^{13}\text{CO}_2$ ($F_{13\text{CO}_2}$), the uppermost “soil” layer was maintained at CO_2 mole fraction of $385 \mu\text{mol mol}^{-1}$ and $\delta^{13}\text{C}$ of -8.5‰ . Calculated fluxes of $^{12}\text{CO}_2$ and $^{13}\text{CO}_2$ across the upper boundary of the uppermost layer were summed to produce the total surface CO_2 flux, and used to calculate the surface flux $\delta^{13}\text{C}$ ($\delta^{13}\text{C}_F$) following

$$\delta^{13}C_F = \left(\frac{F_{13CO_2} / F_{12CO_2}}{R_{std}} - 1 \right) * 1000 \quad 4.14$$

where R_{std} is the $^{13}C/^{12}C$ ratio of the Vienna PDB scale (0.01124) (Craig 1957).

Results

Soil respiration fluxes in plots with roots followed the seasonal pattern of air and soil temperature, being highest in midsummer when leaves were on the trees, and lowest in winter while trees were dormant (Fig. 4.2). Seasonal variability in soil respiration on plots without roots was much smaller, leading to a calculated relative contribution of rhizosphere respiration of up to ~75% to the total CO_2 flux on plots with roots in the summer. $\delta^{13}C$ of soil respiration from open chambers (Fig. 4.2f) and soil gas profiles grouped by treatment (Keeling plots constructed with all measurements from a particular treatment and sampling date, Fig. 4.2c) were enriched in ^{13}C in summer by about 4‰ relative to winter on all plots, independent of trenching. During peak flux rates in midsummer, $\delta^{13}C$ of soil respiration calculated from soil gas Keeling plots (Fig. 4.2c) and from daily averages of open chamber data (Fig. 4.2f) was more enriched in plots with live roots (~ -25.5‰) than in trenched plots (~ -26.5‰). Because the majority of soil respiration on plots with roots during summer was associated with rhizosphere respiration (Fig. 4.2b.), the calculated rhizosphere-respired $\delta^{13}C$ endmember was only slightly more enriched (< 1‰) in $^{13}CO_2$ than the total soil flux on these plots (Fig. 4.2c).

Data from open chambers compared well with gas well profiles from the same individual plots (Fig. 4.3), with both methods showing consistent seasonal patterns of summertime enrichment in $\delta^{13}\text{C}$ of soil respiration, and isotopically heavier respired CO_2 from plots with roots. These patterns were apparent in a comparison of $\delta^{13}\text{C}$ of soil respiration vs. fluxe rates for the two method combinations (Fig. 4.4a,b), where high summer fluxes associated with the +Roots treatment were generally more enriched in $^{13}\text{CO}_2$ compared to low cold season fluxes from both treatments.

No strong diel patterns of $\delta^{13}\text{C}$ of respiration were observed in the overnight gas exchange measurements from leaves, roots, or soils, and so averages from all replicates and sampling times are presented (Fig. 4.4c). Only the bulk samples from the 3:00 am sampling are presented. $\delta^{13}\text{C}$ of respiration from sieved soil samples was more enriched from plots with roots than without roots, consistent with chamber and profile measurements of intact soil (Fig. 4.4a,b). This contrasted with the difference between $\delta^{13}\text{C}$ of bulk soil carbon between treatments, which was most enriched in samples from plots without roots. Measurements of $\delta^{13}\text{C}$ of respiration from root samples were more enriched than all other measured respiration sources and plant tissues. Sun leaf biomass and respiration were enriched in ^{13}C relative to shade leaves, and leaf respiration was enriched relative to leaf biomass for both sun and shade leaves.

Large diel variation was observed in open chamber measurements of $\delta^{13}\text{C}$ of the soil CO_2 surface flux during some periods from some plots (Fig. 4.3, 4.5). In Figure 4.3, data with large peak-to-peak variability appearing as random noise were in fact regular, diel fluctuations, as presented in Figure 4.5. When observed, this variation was generally in phase with 5 cm soil temperatures (Fig. 4.6), being most enriched in the afternoon and

most depleted in the early morning (Fig. 4.5, 4.6). The magnitude of diel variation in respiration $\delta^{13}\text{C}$ was highest when surface flux rates were low (Fig. 4.6, 4.7a). Diel variability in $\delta^{13}\text{C}$ of soil respiration was positively correlated with the coefficient of variation (CV) of the respiration flux (standard deviation of diel flux/average diel flux), but not the total amplitude of flux variability (Fig. 4.6, 4.7b). This distinction is highlighted in data from a ten-day period from a +Roots and –Roots plot pair presented in Figure 4.6: although the amplitude of flux variability in the +Roots plot was greater (panel c), the CV and the diel variability in $\delta^{13}\text{C}$ of soil respiration (panel b) were larger in the –Roots plot. These trends were consistent throughout the season regardless of the presence or absence of active roots (Fig. 4.7).

Model results supported the relationship presented in Fig. 4.7a, as the diel range of $\delta^{13}\text{C}$ exiting the surface layer was largest when fluxes were small (Fig. 4.8a). Modeled variability in surface flux $\delta^{13}\text{C}$ was not as directly associated with flux variability (coefficient of variation, Fig. 4.8b) as was measured in the current study (Fig. 4.7b). However, model simulations consistently produced maximum variability in $\delta^{13}\text{C}$ of the surface flux when CO_2 production was concentrated near the soil surface, such as within the top 10 cm (Fig. 4.8c). The diel phase of the $\delta^{13}\text{C}$ of the surface flux produced by the model varied slightly, depending on input parameters, but generally modeled flux $\delta^{13}\text{C}$ peaked just before midday.

Soils at 5 cm depth reached higher afternoon temperatures by a few degrees during summer in the two measured trenched plots than in the two untrenched plots (Fig. 4.2d). Water content at 15 cm in the instrumented trenched plot remained relatively constant throughout the measured period in the absence of transpiration (data not shown).

While a seasonal pattern was apparent in the 15 cm water content of the irrigated untrenched plot, minimum water content remained fairly high (>20%) and similar to the water content measured in the trenched plot during summer. During coring for soil samples on July 30, 2008, tree roots were found to have grown through a seam in the plastic sheeting and into one trenched plot. No data from this plot were used for “+ Roots/- Roots” treatment comparisons, but chamber data from this plot were plotted in Figure 4.7 as “+ Roots”. The open soil chamber collar was moved to another trenched (- Roots) plot where measurements resumed. Effects of the trenching treatment overshadowed any effects of the coincident nitrogen addition treatment at the site on the soil respiration fluxes and $\delta^{13}\text{C}$ of CO_2 , so we pooled data according to trenching only.

Discussion

Measurements of soil respiration $\delta^{13}\text{C}$

This study examined the $\delta^{13}\text{C}$ of soil respiration using soil gas Keeling plots and open soil chambers, including an entire season of concurrent measurements. While laboratory experiments have demonstrated comparability and accuracy of these two methods with measurement of a controlled CO_2 source (Moyes et al. 2010), this level of agreement between the two methods in a field study (Fig. 4.2, 4.3, 4.4a,b) was encouraging. It is worth stressing that all current methods to measure $\delta^{13}\text{C}$ of soil respiration are wrought with methodological challenges because of the requirement for minute diffusive gradients to remain undisturbed (Nickerson and Risk 2009a). This is why we applied two independent approaches to measure soil flux $\delta^{13}\text{C}$, and sought to evaluate our results with a diffusive transport model. Open soil chambers were chosen

because they induce minimal lateral diffusion (Nickerson and Risk 2009a) and remain in place long after diffusive re-equilibration should occur, operating near steady state. Soil gas profiles were selected for comparison with the expectation that gas wells would equilibrate more slowly with changes in soil gas conditions, and thus be less sensitive to short-term disturbances and provide measurements representing flux variability over slightly longer time scales.

Diel flux $\delta^{13}\text{C}$ variability was observed with both open soil chambers in a manner similar to other published studies, and which agreed with model simulations (Fig. 4.8). Further, maximum $\delta^{13}\text{C}$ variability was measured while flow through the chamber (and thus the induced pressure gradient) was lowest to maintain a minimum mole fraction difference between inlet and outlet flows during low flux periods. Two sets of overnight measurements of gas wells were conducted and results (data not shown) suggested that Keeling intercepts followed the diel cycle observed with chambers, but this variability was dampened. This difference would be expected because changes in soil gas measurements require equilibration of the soil gas profile and gas well volume. For analysis of seasonal and trenching treatment effects, average daily values of soil respiration $\delta^{13}\text{C}$ from the soil chambers were compared to afternoon gas well Keeling plot values. From these data some strong biotic effects were evident. While the application of consistent methods should have rendered the relative seasonal and trenching effects largely neutral to any measurement artifacts, confidence in the absolute values of these effects comes from the similarity of results obtained with both methods.

Trenching treatment effects

The trenching treatment produced one set of plots with an entirely heterotrophic CO₂ source, which we compared to adjacent plots with a seasonal shift from a heterotrophic winter source to a primarily autotrophic (photosynthate-driven) summer CO₂ source. Trenching reduced summer soil respiration rates by about 75%, which provides an estimate of the seasonal maximum contribution from the rhizosphere to soil respiration at this site (Fig. 4.2b). This value is larger than the 31-65% reductions observed after girdling in North American (Scott-Denton et al. 2006) and European (Högberg et al. 2001, Bhupinderpal-Singh et al. 2003, Subke et al. 2004) coniferous forest stands, and similar to the 71% maximum summertime reduction of soil respiration seen in trenched plots in a Japanese mixed deciduous forest (Lee et al. 2003). Calculated rhizosphere respiration approached zero during the cold seasons when leaves were absent from the trees. Seasonal variation in soil respiration on trenched plots was small and decoupled from patterns on adjacent plots with roots. This is evidence that the trenching treatments in the current study were deep enough to exclude lateral diffusion of CO₂ beneath trench walls and root in-growth, which can lead to underestimation of rhizosphere respiration (Jassal and Black 2006). Additional factors that were not accounted for in our rhizosphere respiration estimates were the possible flux of CO₂ in the xylem stream (Aubrey and Teskey 2009) and priming of decomposition of soil organic matter.

During the growing season, soil respiration on plots with roots was predominantly more enriched in ¹³CO₂ than respiration from trenched plots (Fig. 4.2-4.5). This difference of about 1‰ was attributed to enriched respiration from the rhizosphere,

which represents a flux-weighted mean of root and mycorrhizal respiration and consumption of root exudates or root tissues by microorganisms. Root-stimulated mineralization of soil organic matter was assumed to produce a $\delta^{13}\text{C}$ of respiration matching that on root-free plots. Enrichment of rhizosphere respiration is supported by the enriched $\delta^{13}\text{C}$ of respiration measured directly from roots relative to soil sampled from trenched or untrenched plots (Fig. 4.4b). The large difference observed between $\delta^{13}\text{C}$ of root tissue and root-respired CO_2 is higher in magnitude than has been previously reported. Accumulation of carbon dioxide during our root respiration gas exchange measurements was slow, potentially indicating low or altered metabolic activity within the excised and washed roots sampled, and/or enhancing the possibility for measurement errors. While the magnitude of enrichment of root respiration observed in the current study is unprecedented, this result is qualitatively consistent with our soil flux $\delta^{13}\text{C}$ measurements. The same directional influence of roots on soil respiration $\delta^{13}\text{C}$ was also found in a recent evaluation of soil CO_2 sources in a *Fagus sylvatica* forest (Marron et al. 2009). Those authors found that $\delta^{13}\text{C}$ from root respiration was more enriched than CO_2 respired in soil or litter incubations. Studies involving *Eucalyptus delegatensis* (Gessler et al. 2007), *Fagus sylvatica* (Damesin and Lelarge 2003), *Quercus petraea* (Maunoury et al. 2007), and *Pinus sylvestris* (Brandes et al. 2006) trees have additionally found CO_2 respired from trunks and/or roots to be enriched in ^{13}C relative to phloem carbon or bulk stem tissue.

Our observations from soil profiles and open soil chambers of a ^{13}C -depletion effect of root exclusion by trenching contrast with a girdling study in a Swedish boreal *Picea abies* forest, which showed no effect of girdling on the $\delta^{13}\text{C}$ of soil respiration

(Betson et al. 2007). However, our observations are consistent with results reported by Subke et al. (2004) showing consistently ^{13}C -depleted CO_2 respired in girdled plots relative to controls in a German stand of the same species. Prévost-Bouré et al. (2009) found mixed isotopic results from trenching treatments in three separate broadleaf forests, but with occasionally significant differences pointing to ^{13}C depletion with trenching. The observed treatment effect of ^{13}C -depleted respiration from trenched plots was also apparent in the midsummer measurements of respired CO_2 from sieved soil core samples with visible roots removed (Fig. 4.4b). This suggests that carbon from roots was likely distributed to the soil surrounding roots in untrenched plots as a substrate for microbial respiration, such as in the form of exudates or mycorrhizal fungal biomass. This carbon transfer might also explain the low respiration rates observed from root tissues despite high soil respiration rates on untrenched plots (Fig. 4.2; 4.4a,b), and the difference in bulk soil carbon $\delta^{13}\text{C}$ between treatments (Fig. 4.4c). Bulk soil organic carbon $\delta^{13}\text{C}$, particularly from soil in trenched plots, was more enriched than expected for a primarily C_3 -vegetated area. Because the site was developed from transported local topsoil without complete records of vegetation composition or history of the source area, we cannot exclude the possibility of a mixed C_3/C_4 history affecting the isotope content of soil organic matter at the site. Additionally, though soil samples were tested for complete acidification, the enriched bulk soil values could be explained by the presence of residual soil carbonates in the samples.

Seasonal variation in $\delta^{13}\text{C}$ of soil respiration

The seasonal $\delta^{13}\text{C}$ variability of soil respiration in the absence of active roots in the current study (Fig. 4.2c, f; 4.3c, d) supports the conclusion that heterotrophic processes were responsible for seasonal variability in $\delta^{13}\text{C}$ of soil respiration. A similar pattern of enrichment between spring and summer $\delta^{13}\text{C}$ of decomposition substrates was seen in both girdled and ungirdled plots in a *Picea abies* forest (Ekberg et al. 2007). This seasonal change was attributed to decomposition of more recalcitrant, ^{13}C -enriched compounds in summer, possibly due to priming in ungirdled plots and increased substrate supply in girdled plots. Marron et al. (2009) argued that summer ^{13}C -enrichment of soil respiration in a *Fagus sylvatica* stand was likely a combined effect of the seasonal contribution of enriched root respiration and seasonal variability in litter respiration $\delta^{13}\text{C}$. Alternatively, a seasonal change towards an enriched winter respiration source was observed in root exclusion plots in a Japanese larch forest (Takahashi et al. 2008). In the current study involving deciduous trees, a winter-depleted seasonal pattern was observed in plots with and without active roots, and low fluxes on trenched plots provided no evidence of increased decomposition of root litter associated with trenching.

Heterotrophically-driven variability in soil respiration $\delta^{13}\text{C}$ is in contrast to a general emphasis on the importance of weather conditions on photosynthetic discrimination (Δ) as a driver of regional and temporal variability of $\delta^{13}\text{C}$ of soil (Ekblad and Högberg 2001, Ekblad et al. 2005) and ecosystem respiration (Bowling et al. 2002a, McDowell et al. 2004a, Scartazza et al. 2004, Knohl et al. 2005, Chen and Chen 2007). For example, a largely seasonal shift towards ^{13}C -depleted soil respiration in cold seasons was observed in a pine and spruce dominated forest in Sweden (Ekblad and

Högberg 2001), which was attributed to seasonal changes in evaporative demand and consequent stomatal limitation to Δ . This connection between environmental variables affecting Δ and $\delta^{13}\text{C}$ of soil respiration assumes that sugars transported to the soil via the phloem provide a continuous link between above- and belowground $\delta^{13}\text{C}$ variability. This connection has been supported by demonstrating a dependence of the $\delta^{13}\text{C}$ of phloem sugars on stomatal conductance (Keitel et al. 2003, Gessler et al. 2004). Given that a large proportion of forest soil respiration appears to be derived from recent assimilation (Högberg et al. 2001), some degree of coupling of Δ and $\delta^{13}\text{C}$ of ecosystem respiration is expected. While some field measurements have supported strong correlations between $\delta^{13}\text{C}$ of assimilation and respiration on the ecosystem scale (Bowling et al. 2002a, Scartazza et al. 2004, Knohl and Buchmann 2005), others have shown a more nuanced or contingent relationship (McDowell et al. 2004b, Barbour et al. 2005, Riveros-Iregui et al. in review). Though summers during the present study were relatively warm and dry, the irrigated boxelder trees were maintained in continuously moist soil, and leaf tissue $\delta^{13}\text{C}$ did not reflect a strong stomatal limitation to photosynthesis (Fig. 4.4c). Relationships between seasonal or synoptic VPD variations and $\delta^{13}\text{C}$ of rhizosphere respiration were not strongly apparent in this data set, with the possible exception of a single storm event in late August, 2008 (Fig. 4.3a, days ~245, VPD data not shown).

The explanation for the changes in heterotrophic substrate utilization and possibly microbial community composition responsible for the consistent seasonal pattern observed in $\delta^{13}\text{C}$ of respired CO_2 in the current study in 2007 and 2008 is unknown. Although annual turnover of root litter was limited to untrenched plots, leaf litter fell onto

all plots in each fall and was not removed, representing a seasonal pulse of new carbon for decomposition. Soil microbial communities, and the activity of their associated extracellular decomposing enzymes, have been found to alternate between cold and warm season assemblages where soil temperature varies strongly over the year (Schadt et al. 2003, Monson et al. 2006, Lipson 2007, Weintraub et al. 2007, Wallenstein et al. 2009). Incubating soils at different temperatures has been shown to induce changes in $\delta^{13}\text{C}$ of respired CO_2 along with community composition (Andrews et al. 2000). Dry summer conditions may restrict heterotrophic activity to deeper soil layers retaining more moisture and where soil organic matter tends to be enriched in ^{13}C , producing a seasonal pattern (Steinmann et al. 2004a, Theis et al. 2007). Thus, in addition to the effects of weather conditions on Δ , many seasonally-dependent environmental variables have the potential to cause or coincide with variability in heterotrophic respiration sources independently, highlighting the importance of considering these sources individually.

Diel variation in $\delta^{13}\text{C}$ of soil respiration

The largest diel variations in the $\delta^{13}\text{C}$ of soil respiration ($> 5\text{‰}$) were observed on plots with and without roots during the low flux period immediately prior to the growing season, when soils were cooler than midsummer on average, but with strong diel fluctuations in soil temperature. These are the largest diel $\delta^{13}\text{C}$ ranges of soil respiration reported to date. Throughout the growing season, smaller daily cycles in the $\delta^{13}\text{C}$ of soil respiration were occasionally apparent (e.g., Fig. 4.5c, d) with amplitudes similar to those reported by Kodama et. al (2008), Marron et. al (2009), and Bahn et. al(2009), or were absent (e.g., Fig. 4.5a, b) as seen by Betson et. al (2007). The surface flux $\delta^{13}\text{C}$ has

generally been assumed to reflect that of respiratory CO₂ production, even when flux $\delta^{13}\text{C}$ has been found to vary on a diel basis. Such fluctuations have been previously attributed to variability in $\delta^{13}\text{C}$ of phloem sugars supplied to roots or proportions of autotrophic and heterotrophic sources throughout the day. However, within the current study diel variability in flux $\delta^{13}\text{C}$ was observed on plots with and without active roots and thus could not have been due to these differences in carbon sources. Substrate $\delta^{13}\text{C}$ variability would only explain the observed flux $\delta^{13}\text{C}$ variability if large apparent fractionations occurred during oxidation of soil organic matter with a strong soil temperature dependence.

Throughout the current study, the amplitude of diel variability in flux $\delta^{13}\text{C}$ was consistently correlated with the coefficient of variation of the flux, a measure of flux variability relative to average flux magnitude (Fig. 4.6, 4.7b). The independence of this relationship from potential source variations (e.g., seasonal substrate pulses, roots vs. heterotrophs) and its dependence on changing flux rates point to soil gas transport-related diffusive isotope effects as a likely cause of observed diel variability in flux $\delta^{13}\text{C}$. Measurements from the current study fit within the variability of model results, suggesting that all observed diel variability in surface flux $\delta^{13}\text{C}$ could be explained by diffusive transient effects in soil gas transport with a *constant* $\delta^{13}\text{C}$ of respiratory production. Model support for this conclusion was particularly strong if CO₂ production was low and concentrated near the surface (Fig. 4.8a,c), which is likely to reflect the activity and distribution of microbial communities during the early and late seasons when measured fluxes were smallest and isotopic variability was highest. While isotopic measurements of low respiration rates from sources localized near the surface might be

especially susceptible to chamber influences on diffusive mole fraction gradients, the convergence of chamber data and model predictions (Fig. 4.8) does not highlight any measurement errors. On the contrary, if diel flux $\delta^{13}\text{C}$ variability reflects diffusive transient effects rather than changes in source substrate, as suggested here, this variability complicates the application of $\delta^{13}\text{C}$ of soil respiration to understanding soil respiratory source dynamics.

Data from the current study were compared with other reports of diel variations of $\delta^{13}\text{C}$ of soil respiration. Average soil respiration fluxes and diel amplitudes of fluxes and their isotope ratio were estimated visually from figures published in Betson et. al (2007), Kodama et. al (2008), Marron et. al (2009), and Bahn et. al (2009). Flux means and amplitudes were used to generate sine function curves from which the coefficient of variation was calculated for one day. For a more direct comparison, data from the current study were treated in the same way, using a sine curve fitted to an average daily flux pattern made from each consecutive 3-day period to calculate a flux CV. Data from the four studies above were consistent with the observation of decreasing $\delta^{13}\text{C}$ variability with increasing fluxes seen in the current study and produced by the model (Fig. 4.8a). In addition, data from these four studies showed a similar correlation between the diel range of $\delta^{13}\text{C}$ and the CV of the soil CO_2 flux (Fig. 4.8b). Differences in the relationship between flux CV and isotopic variability across this study and those cited (especially Kodama et al. (2008)) might have been due to a uniquely shallow depth of production at our study site (Fig. 4.8c), methodological differences between chamber measurement techniques, or differences in sampling frequency. The consistency of patterns across the studies evaluated in Fig. 4.8a, b with the current study and results from our constant

source model suggests that, contrary to diel variations in $\delta^{13}\text{C}$ of respiration substrates, diel flux $\delta^{13}\text{C}$ variability could have been caused by physical processes alone.

Recent work by Bathellier et al. (2009) has suggested that $\delta^{13}\text{C}$ of root respiration may be less variable diurnally than $\delta^{13}\text{C}$ of leaf-respiration. Those authors found a constant $\delta^{13}\text{C}$ of root respiration during starvation-induced decrease in respiratory quotient (RQ), in contrast to the pattern of positive correlation between RQ and $\delta^{13}\text{C}$ of leaf respiration shown for the same species (*Phaseolus vulgaris*) by Tcherkez et al. (2003). The RQ-associated mechanism entails a shift in the proportion of pyruvate decarboxylation and Krebs cycle decarboxylation, which have opposing effects on $\delta^{13}\text{C}$ of respired CO_2 . This mechanism was suggested by Hymus et al. (2005) to account for large observed diurnal variation in oak leaf-respired $\delta^{13}\text{C}$, which corresponded with daily cumulative assimilation rather than variability in $\delta^{13}\text{C}$ of leaf sugars. The disconnection between $\delta^{13}\text{C}$ of root respiration and substrate availability to roots observed by Bathellier et al. (2009) would support the interpretation that diel variability in $\delta^{13}\text{C}$ of soil respiration is more likely driven by transient diffusive transport effects than $\delta^{13}\text{C}$ of root-respired CO_2 . In the current study, the observations of 1) identical relationships between variability in soil respiration rate and $\delta^{13}\text{C}$ regardless of presence or absence of roots (Fig. 4.7), 2) absence of diel $\delta^{13}\text{C}$ variability in soil respiration when rhizosphere respiration was highest, and 3) no diel variability in the $\delta^{13}\text{C}$ of respired CO_2 from soils or roots measured separately point to this same conclusion.

Conclusions

In an analysis of $\delta^{13}\text{C}$ of soil-respired CO_2 in trenched and untrenched plots under deciduous trees, we found short-term (diel) variability, which appeared to be associated with abiotic processes, and longer-term (seasonal) differences associated with biotic processes. Diel variability in $\delta^{13}\text{C}$ of soil respiration ranged from 0-12‰, and was related to flux variability and average magnitude (small, variable fluxes produced maximum $\delta^{13}\text{C}$ variability). A diffusive transport model with a constant respiratory source $\delta^{13}\text{C}$ supported the conclusion that diel flux $\delta^{13}\text{C}$ variability was due to transient diffusive fractionations. Seasonal and treatment effects were analyzed from soil chamber data averaged for each day to remove diel fluctuations, and slower-equilibrating soil gas profiles. Both methods showed that trenching reduced summertime soil respiration rates by 75% and $\delta^{13}\text{C}$ of soil respiration by ~1‰. A seasonal pattern of ~4‰ ^{13}C -enrichment in summer vs. spring and fall soil respiration was observed on all plots and attributed to seasonal variability of heterotrophic processes. This conclusion points to the need to consider heterotrophic processes in addition to photosynthetic discrimination as a potentially dominant driver of soil respiration $\delta^{13}\text{C}$.

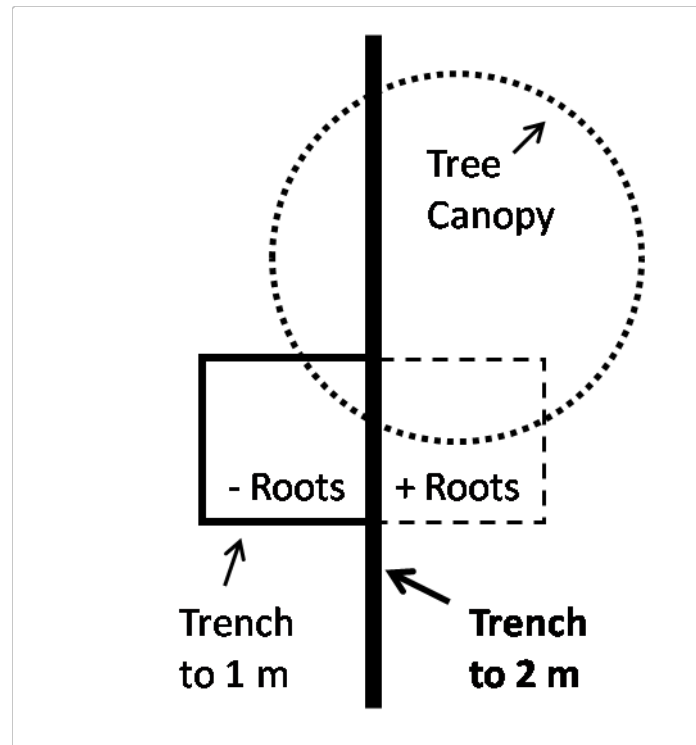


Figure 4.1: Overhead view of plot setup showing one of six replicate plot pairs under individual boxelder trees. A 2 m deep trenched root barrier runs through the center of the site with trees (canopy shown by dotted circle) positioned on alternating sides. On the opposite side of this trench a 1 m deep trenched barrier excluded understory roots from trenched (- Roots) plots. The dashed line on the + Roots side indicates an untrenched plot boundary, with no associated soil disturbance.

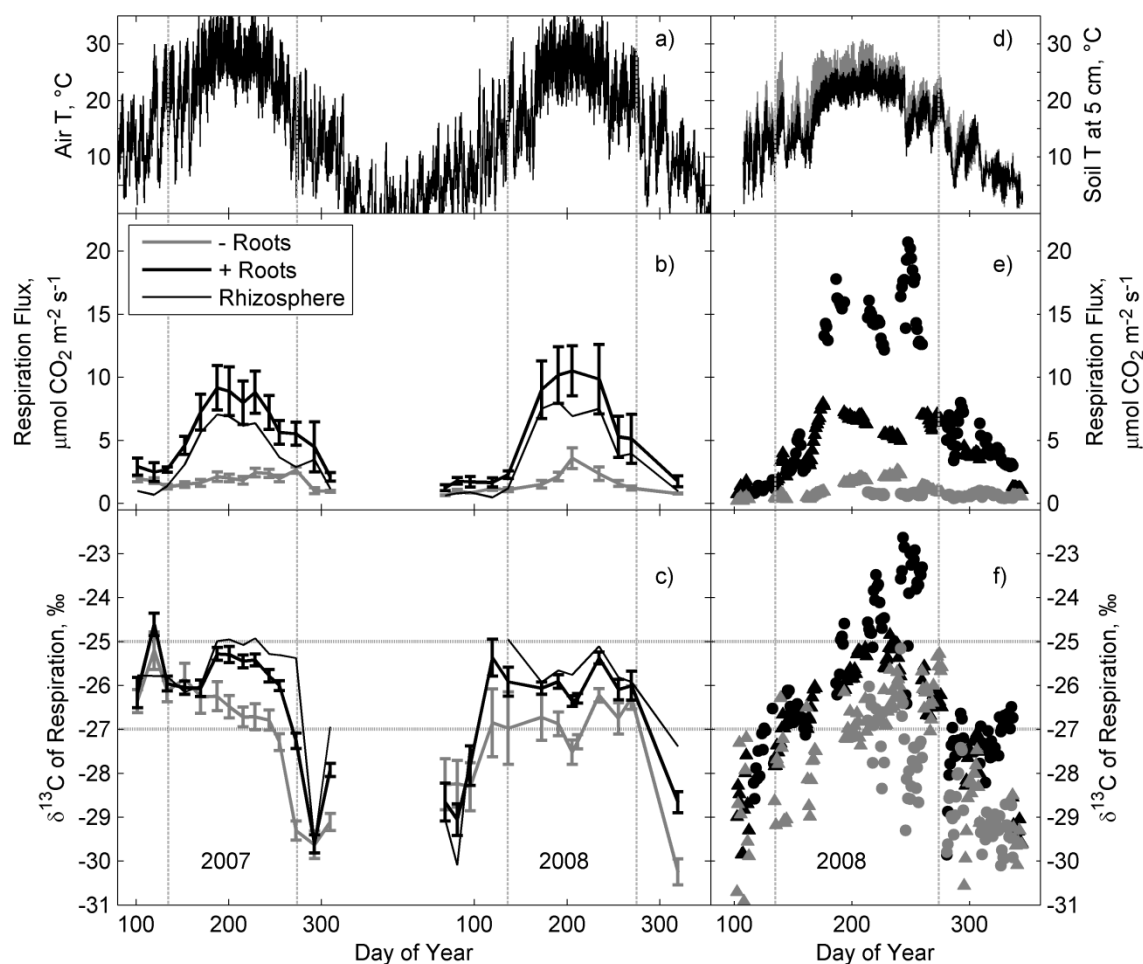


Figure 4.2: Temperature, soil respiration fluxes, and $\delta^{13}\text{C}$ of soil respiration for trencend and untrencend plots during the study period. (a) Air temperature for the 2007 and 2008 study periods. (b) Average soil respiration fluxes by treatment measured with the closed soil chamber and the calculated average rhizosphere contribution to soil respiration rates. Error bars are one standard error of the mean. (c) $\delta^{13}\text{C}$ of respiration from Keeling plots generated from composite soil gas profile data by treatment and the calculated $\delta^{13}\text{C}$ of rhizosphere-respired CO_2 . Error bars are one standard error of the intercept. (d) Average soil temperatures at 5 cm depth from two trencend (gray) and two untrencend (black) plots in 2008. (e) Average daily soil respiration fluxes measured with the open chambers from two trencend (gray) and two untrencend (black) plots (plot 1: circles, plot 2: triangles). (f) Average daily $\delta^{13}\text{C}$ of respiration measured with the open soil chambers from two trencend (gray) and two untrencend (black) plots (plot 1: circles, plot 2: triangles). Dotted vertical lines in all plots show the approximate dates of bud burst (May 15) and leaf senescence (Oct. 1) of trees for the two growing seasons. Horizontal lines in the bottom panel highlight $\delta^{13}\text{C}$ values of -25 and -27 ‰ for comparison to Figures 4.3-4.5.

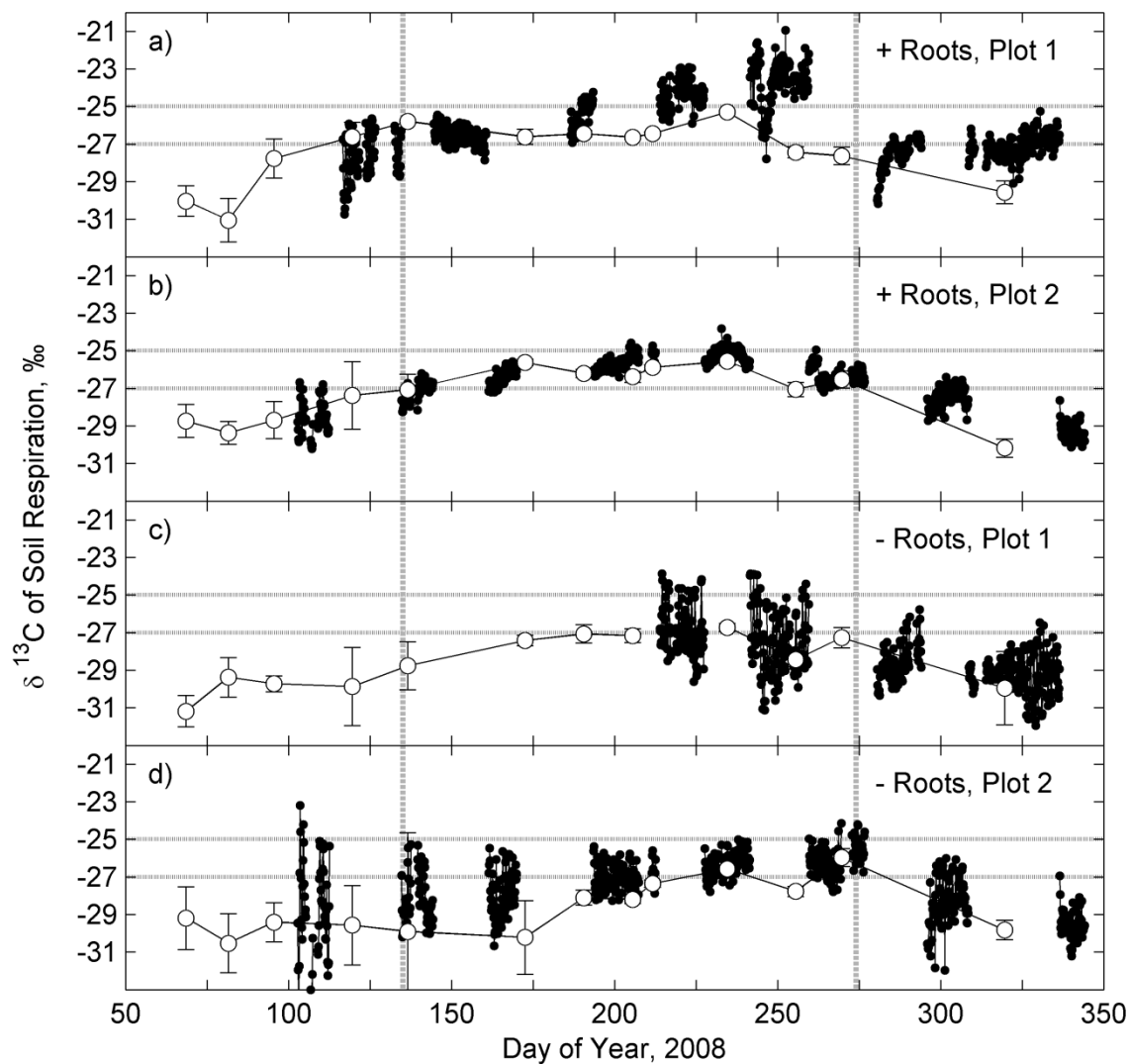


Figure 4.3: Carbon isotope ratio of soil-respired CO₂ derived from soil gas profiles (○) and three-hour means from open chambers (●) on individual plots with (top two panels) and without (bottom two panels) roots during 2008. Dotted vertical lines show approximate dates of bud burst (May 15) and leaf senescence (Oct. 1) of trees. Horizontal lines highlight δ¹³C values of -25 and -27‰. Error bars are 1 standard error of the intercept. Periods with high variability in open chamber measurements of flux δ¹³C are due to regular, diel patterns (see Figure 4.5).

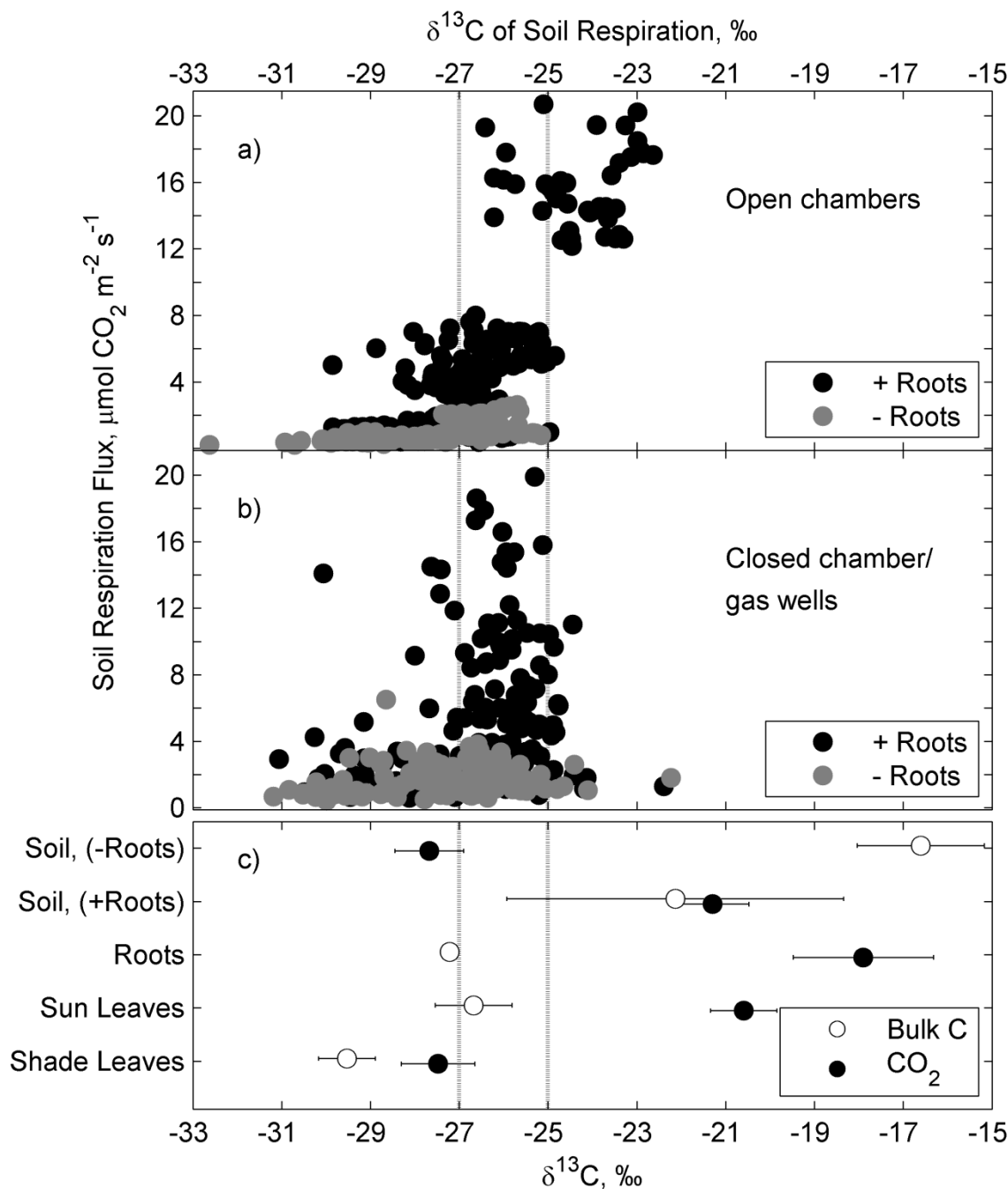


Figure 4.4: Comparison of fluxes and $\delta^{13}\text{C}$ of soil-respired CO_2 using two method combinations: afternoon closed chamber flux measurements vs. $\delta^{13}\text{C}$ of soil respired CO_2 from gas profile-derived Keeling plots (a), and daily average fluxes vs. $\delta^{13}\text{C}$ of soil-respired CO_2 from open chambers (b). (c) Bulk $\delta^{13}\text{C}$ values from sieved soils (soil with roots and rock pieces removed, from the +Roots or the -Roots plots) and plant tissues (open symbols) and the $\delta^{13}\text{C}$ of their respired CO_2 (closed symbols). Diel variation was not observed in $\delta^{13}\text{C}$ of respired CO_2 , so measurements from all sampling times were averaged. Error bars are 1 SEM. Vertical lines highlight -25 and -27‰.

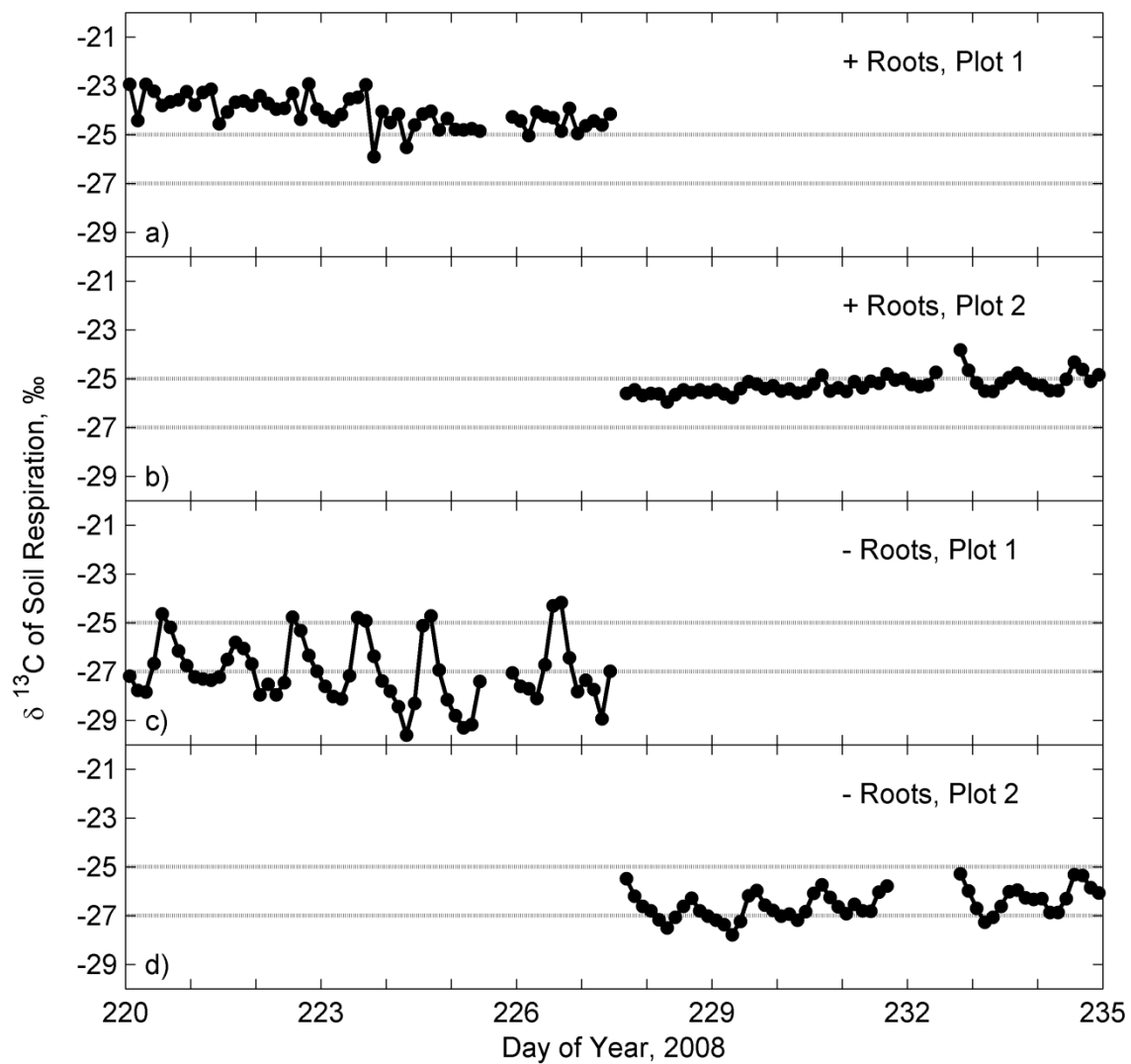


Figure 4.5: $\delta^{13}\text{C}$ of soil respiration from open chamber measurements from each of the four collars during days 220 – 235 of 2008, showing differences in diel $\delta^{13}\text{C}$ variability. Dotted lines highlight -25 and -27‰.

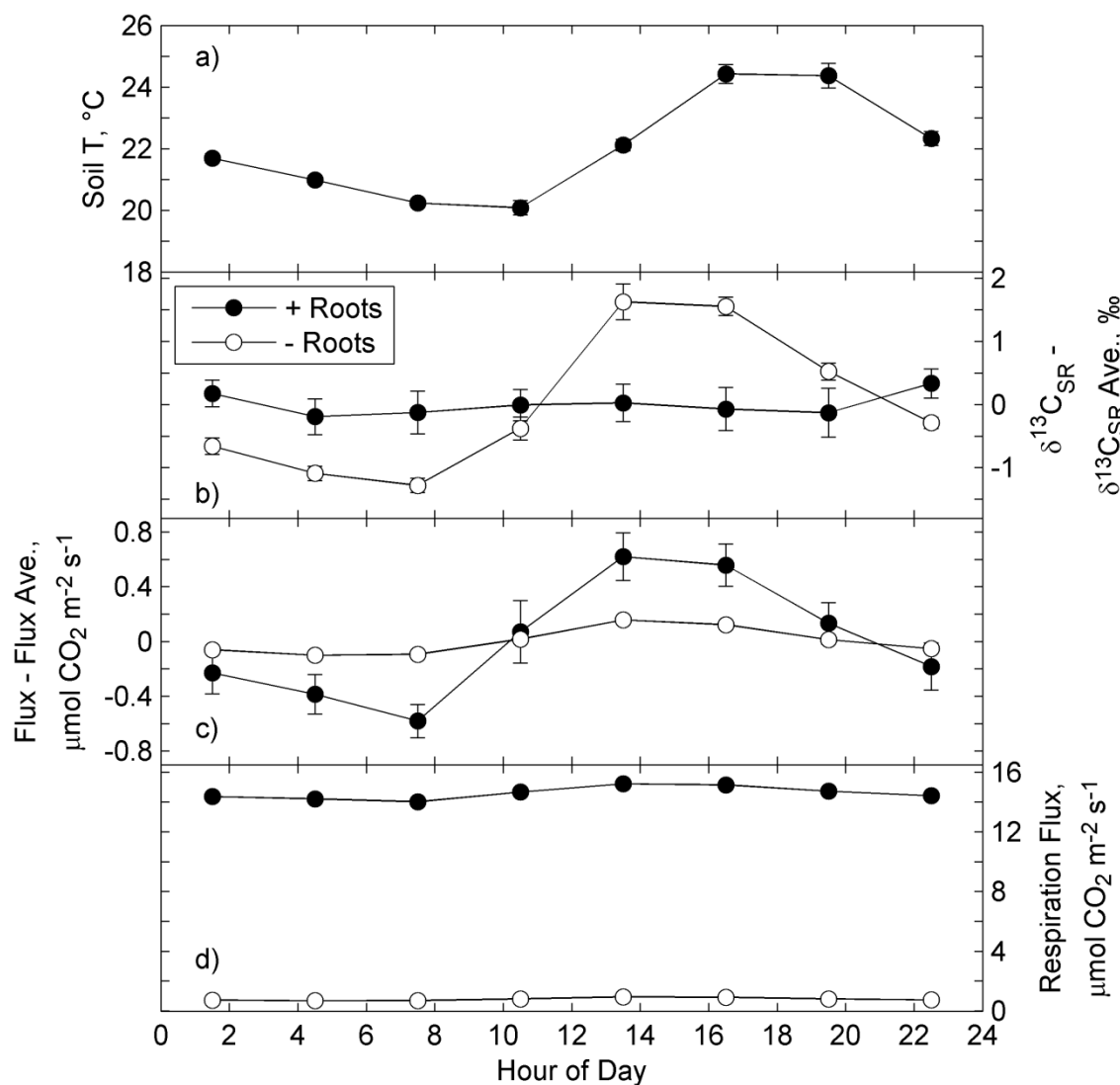


Figure 4.6: Open chamber data from the plot 1 pair of untrenched (+ Roots) and trenched (- Roots) treatments, averaged from days 215–224, 2008. Error bars are 1 SEM and are smaller than symbols where not visible. (a) Average 3-hourly soil temperatures at 5 cm. (b) Diel variation in $\delta^{13}\text{C}$ of soil respiration ($\delta^{13}\text{C}_{\text{SR}}$) from the daily mean. (c) Diel variation from the mean soil respiration flux. (d) Diel flux magnitudes during the averaged period.

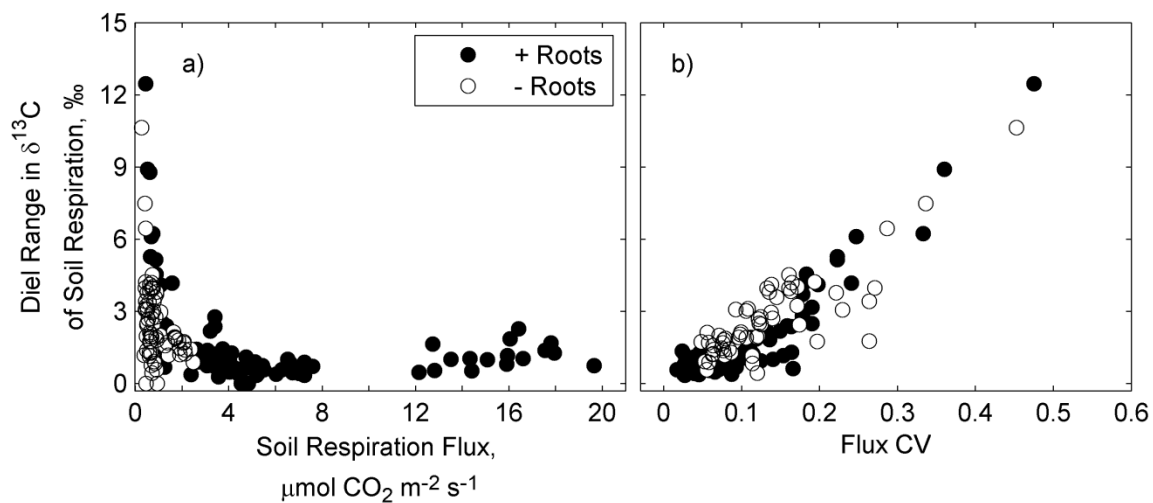


Figure 4.7: Diel variation in $\delta^{13}\text{C}$ of soil respiration plotted against soil respiration flux (a) and the coefficient of variation of the respiration flux (b) *see Figure 4.6*. Each data point was calculated from an average of 3 consecutive days of open chamber data from the entire 2008 study period.

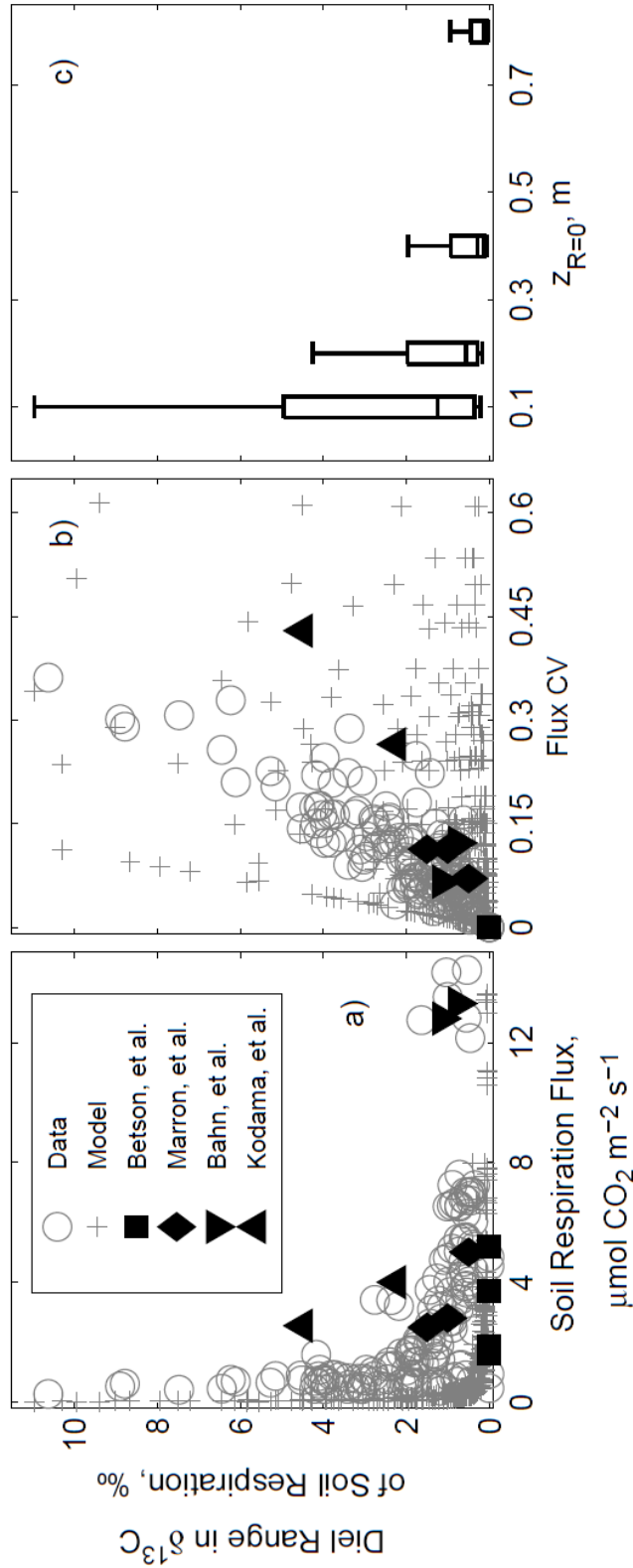


Figure 4.8: Diel variation in $\delta^{13}\text{C}$ of soil respiration plotted against soil respiration flux (a), the coefficient of variation of the respiration flux (b), and depth of zero production ($z_{R=0}$, c). Panels (a) and (b) contain data from the current study, model results, and results from 4 published studies for comparison. Model results on all panels were obtained from 320 model simulations (including data beyond the axes limits of (a) and (b)). For flux CV calculation in (b), average fluxes were taken as the center of the flux range, and the coefficient of variation for each flux was calculated by fitting a sine function to the flux average and diel amplitude and calculating its CV. (c), box and whisker plots from 320 model simulations (including data beyond the axes limits of (a) and (b)) showing diel variability in soil flux $\delta^{13}\text{C}$ produced by the model for different input values of depth of zero production ($z_{R=0}$). Boxes depict quartiles above and below the median and contain 50 percent of observations centered on the median, and whiskers show 75 percent of observations centered on the median for each parameter category. For all model simulations $\delta^{13}\text{C}$ of CO_2 production was constant with depth and time at -25‰ .

APPENDIX

AN INJECTION METHOD FOR MEASURING THE CARBON

ISOTOPE CONTENT OF SOIL CARBON DIOXIDE AND

SOIL RESPIRATION WITH A TUNABLE DIODE

LASER ABSORPTION SPECTROMETER

Reprinted from Rapid Communications in Mass Spectrometry, Vol 24: 894-900, A.B. Moyes, A.J. Schauer, R.T. Siegwolf, and D.R. Bowling “An injection method for measuring the carbon isotope content of soil carbon dioxide and soil respiration with a tunable diode laser absorption spectrometer”, copyright 2010, with permission from John Wiley and Sons Limited.

An injection method for measuring the carbon isotope content of soil carbon dioxide and soil respiration with a tunable diode laser absorption spectrometer

Andrew B. Moyes^{1*}, Andrew J. Schauer^{1†}, Rolf T. W. Siegwolf² and David R. Bowling¹

¹Department of Biology, University of Utah, 257 South 1400 East, Salt Lake City, UT 84112, USA

²Paul Scherrer Institut, 5232 Villigen PSI, Switzerland

Received 24 November 2009; Revised 14 January 2010; Accepted 15 January 2010

We present a novel technique in which the carbon isotope ratio ($\delta^{13}\text{C}$) of soil CO_2 is measured from small gas samples (<5 mL) injected into a stream of CO_2 -free air flowing into a tunable diode laser absorption spectrometer (TDL). This new method extends the dynamic range of the TDL to measure CO_2 mole fractions ranging from ambient to pure CO_2 , reduces the volume of sample required to a few mL, and does not require field deployment of the instrument. The measurement precision of samples stored for up to 60 days was 0.23‰. The new TDL method was applied with a simple gas well sampling technique to obtain and measure gas samples from shallow soil depth increments for CO_2 mole fraction and $\delta^{13}\text{C}$ analysis, and subsequent determination of the $\delta^{13}\text{C}$ of soil-respired CO_2 . The method was tested using an artificial soil system containing a controlled CO_2 source and compared with an independent method using the TDL and an open soil chamber. The profile and chamber estimates of $\delta^{13}\text{C}$ of an artificially produced CO_2 flux were consistent and converged to the $\delta^{13}\text{C}$ of the CO_2 source at steady state, indicating the accuracy of both methods under controlled conditions. The new TDL method, in which a small pulse of sample is measured on a carrier gas stream, is analogous for the TDL technique to the development of continuous-flow configurations for isotope ratio mass spectrometry. While the applications presented here are focused on soil CO_2 , this new TDL method could be applied in a number of situations requiring measurement of $\delta^{13}\text{C}$ of CO_2 in small gas samples with ambient to high CO_2 mole fractions. Copyright © 2010 John Wiley & Sons, Ltd.

Tunable diode laser (TDL) absorption spectrometers have been utilized for a variety of ecosystem stable isotope applications due to their portability, fast response, and relatively low cost compared with mass spectrometers.^{1–6} However, most TDL-based methods reported to date have required enough volume of sample to flow through the instrument to flush the sample cell and for measurements to remain stable during an averaging period. This typically requires flow rates of 100–400 sccm, which limits the potential applications of the instrument. Tunable diode laser-based applications for CO_2 isotopes have also been restricted by poor instrument performance when the CO_2 mole fractions are outside the range of 350–700 $\mu\text{mol mol}^{-1}$.⁶

We have developed a new TDL-based method in which the carbon isotope content ($\delta^{13}\text{C}$) of CO_2 is calculated from independent, time-varying $^{12}\text{CO}_2$ and $^{13}\text{CO}_2$ peaks produced by a small injection of sample gas into a flow of CO_2 -free air. Engel *et al.*⁷ recently presented a method in which CO_2 -free air flowed through small (<60 mL) arthropod chambers and mixed with respired CO_2 for TDL measurement of $\delta^{13}\text{C}$. They showed how the carbon isotope ratio of a pulse of CO_2

could be measured with the instrument by averaging the ratios of $^{13}\text{CO}_2$ and $^{12}\text{CO}_2$ over a period of a few seconds while the CO_2 mole fractions were within an acceptable measurement range. In contrast, the method presented in the current study entails calculation of $\delta^{13}\text{C}$ from a specific moment within a CO_2 peak produced by a manual syringe injection of sample gas through a septum port. With this configuration, gas samples of a few mL or smaller can be sampled, stored, and measured on the TDL instrument at a later date. This method extends the measurement capability of the TDL to include CO_2 mole fractions from 350 $\mu\text{mol mol}^{-1}$ to pure CO_2 without additional dilution, and has the potential to expand TDL isotope applications in a way similar to the development of continuous-flow isotope ratio mass spectrometry.

Tunable diode laser instruments have been used to measure the isotopic content of soil respiration with open soil chambers,^{4,5} by sampling air during nocturnal accumulation just above ground,^{4,8,9} or from diluted flows from above and within snow and soil.¹⁰ The injection method described here enables a new soil respiration measurement application for the TDL which was previously limited to mass spectrometers: measurement of $\delta^{13}\text{C}$ of CO_2 in small gas samples collected from soil pore spaces.

Profiles of CO_2 mole fraction and $\delta^{13}\text{C}$ within the soil pore space have been used to calculate the carbon isotope content of

*Correspondence to: A. B. Moyes, Department of Biology, University of Utah, 257 South 1400 East, Salt Lake City, UT 84112, USA. E-mail: moyes@biology.utah.edu

†Present address: Department of Earth and Space Sciences, University of Washington, Seattle, WA 98195, USA.

soil-respired CO_2 using a two-source mixing model.¹¹ This approach assumes that the CO_2 in the soil column is composed of a diffusively mixed combination of (1) atmospheric CO_2 and (2) a weighted mean of CO_2 produced by all soil sources. Under these circumstances, a plot of $\delta^{13}\text{C}$ vs. $1/[\text{CO}_2]$ (a Keeling plot¹²) from soil profile measurements will be linear, with an intercept that reflects the $\delta^{13}\text{C}$ of the soil surface CO_2 flux (net $\delta^{13}\text{C}$ from all soil sources) plus a $\sim 4.4\%$ offset caused by diffusive enrichment.^{13,14} The 4.4% enrichment is theoretically based, and advection within the soil may mean enrichment of the soil gas profile is somewhat less than the theoretical value under some conditions.¹⁰

In biologically and/or geologically active soils a steep $\delta^{13}\text{C}$ gradient typically exists near the soil surface, as the CO_2 mole fraction increases with the composite soil source over the first few cm to m of depth.^{13,15,16} In the absence of geological sources, localization of biological activities near the surface frequently leads to little variation in $\delta^{13}\text{C}$ below approximately 10 cm depth. Thus, to obtain maximum biologically driven CO_2 and $\delta^{13}\text{C}$ measurement ranges for isotopic analysis with the Keeling plot method, multiple measurements from the upper 10 cm of soil depth are often ideal, with the use of additional deeper measurements as needed.

The central objective of the present study was to test the TDL injection technique for the analysis of soil gas samples collected from shallow depth increments, for use in determination of the $\delta^{13}\text{C}$ of the soil surface CO_2 flux using the Keeling plot approach. Breecker and Sharp¹⁷ developed a method to obtain high-resolution profiles of CO_2 mole fractions and $\delta^{13}\text{C}$ in shallow soil depths by inserting gas wells horizontally into the soil, accessible by lengths of 2 mm diameter tubing which extended above the surface. Sample collection required initially purging this volume of tubing by drawing gas up from the gas well with a syringe. A secondary objective of the present study was to test a modified approach in which the gas well tubing (0.64 cm o.d.) extends above the soil surface, allowing for immediate sample collection (no purging necessary). This approach may reduce disturbance to diffusive soil profiles, but requires that the entire gas well volume remains equilibrated with the CO_2 mole fraction and isotope content at the depth of the open gas well end. We evaluated this assumption and the performance of the TDL injection method in two laboratory experiments with an artificial soil. In the first experiment, samples from vertically inserted gas wells were compared with gas from perforated, horizontally buried tubes as CO_2 diffused from a reservoir through an artificial soil medium. In the second experiment we compared the Keeling plot based soil profile method with an independent method where the carbon isotope ratio and rate of an artificially induced CO_2 efflux were measured continuously using the TDL with an open, flow-through soil respiration chamber.

EXPERIMENTAL

Tunable diode laser injection technique

Three CO_2 isotope standard cylinders were prepared by spiking empty compressed-gas cylinders with variable amounts of pure CO_2 having $\delta^{13}\text{C}$ values of -31.63 and $+12.15\%$, and using an air compressor to pressurize and

Carbon isotope content of soil CO_2 and soil respiration 895

dilute the cylinders with air from outside our laboratory. The cylinders were spiked to achieve a final CO_2 mole fraction of approximately $3000 \mu\text{mol mol}^{-1}$ and carbon isotope ratios across the range of values typically observed in soils (~ -8 to -25%). Standard cylinders were measured for the $\delta^{13}\text{C}$ of CO_2 by purifying approximately $150 \mu\text{mol}$ of CO_2 away from all other cylinder constituents for subsequent dual-inlet IRMS analysis (DeltaPlus Advantage, ThermoFinnigan, Bremen, Germany). Cylinder air was moved at a known flow rate through a dry ice/ethanol slush trap for water removal and a liquid nitrogen trap for CO_2 collection under high vacuum. The contents of the liquid nitrogen trap were inserted into a helium stream for CO_2 and N_2O separation via gas chromatography (GC). A thermal conductivity detector was monitored for peak elution. The CO_2 was collected in a second liquid nitrogen trap downstream of the GC column. Once the CO_2 peak had completely eluted, the helium carrier was routed to vent. The CO_2 was vacuum-transferred to a glass cold finger, which was then flame-sealed. The CO_2 was introduced into a dual-inlet IRMS instrument for analysis against NIST-traceable CO_2 isotope standards (OzTech Trading Corporation, Safford, AZ, USA) that had previously been standardized to the Vienna Pee Dee Belemnite (VPDB) scale by measurement against the calcite standard NBS19. The $\delta^{13}\text{C}$ values of CO_2 in the cylinders from three repeated cryogenic extractions and analyses were -7.576 ± 0.002 , -19.560 ± 0.006 , and $-31.275 \pm 0.023\%$.

The tunable diode laser (TDL, model TGA100A, Campbell Scientific, Logan, UT, USA) was described in detail by Bowling *et al.*⁹ The absorption lines used for $^{12}\text{CO}_2$ and $^{13}\text{CO}_2$ in this study were 2299.642 and 2299.795 cm^{-1} , respectively. The TDL was configured with a continuous flow of CO_2 -free air (ambient air chemically scrubbed of CO_2 with soda lime) at a flow rate of 50 sccm (Fig. 1). At this flow rate, the sample cell pressure was 2.3 kPa. Samples were injected manually through a septum (Microsep F-138, Alltech, Deerfield, IL, USA) placed within a union tee fitting (316L-400-3, Swagelok, Solon, OH, USA) downstream of the CO_2 trap, but upstream of a $15 \mu\text{m}$ filter (SS-4FW-15, Nupro, Willoughby, OH, USA) and mass flow controller (1179A, MKS, Andover, MA, USA). Injections were performed using gas-tight syringes with capacities ranging from 0.5 to 5.0 mL (Pressure-Lok, VICI, Baton Rouge, LA, USA). Before entering the TDL system, water vapor was removed from the sample and carrier stream with a Nafion membrane counterflow system (PD 625, Campbell Scientific).

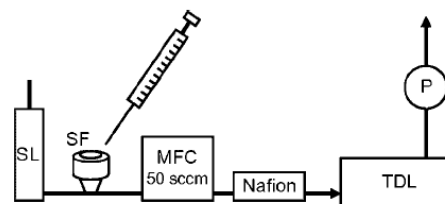


Figure 1. Schematic of syringe injection plumbing for the tunable diode laser (TDL). SL = soda lime, SF = septum fitting, MFC = mass flow controller, Nafion = a counterflow drying assembly to remove water vapor, and P = pump.

To achieve appropriately sized $^{12}\text{CO}_2$ and $^{13}\text{CO}_2$ peaks using our method, measurement of CO_2 mole fraction was required prior to sample injection into the TDL. The CO_2 mole fraction of all gas samples was determined a few minutes to one hour prior to TDL measurement, using an infrared gas analyzer (IRGA, Li-7000, Licor, Lincoln, NE, USA) as described by Davidson and Trumbore.¹⁸ From each sample 0.5 mL of gas at ambient pressure was injected using a gas-tight syringe into a closed, CO_2 -free air stream, just upstream of the IRGA. The integrated voltage peak from the injected sample was used to calculate the mole fraction of CO_2 in the sample by applying a calibration produced from injections of standard gases from custom-prepared cylinders or flasks. Standard cylinders for CO_2 mole fraction calibration were prepared using an air compressor as described above. Standard flasks were prepared as volumetric combinations of CO_2 -free air and pure CO_2 by (1) flushing glass flasks of precisely known volume (nominally 2 to 2.5 L) in a loop containing a soda lime trap, (2) disconnecting the flask and attaching a septum fitting, and then (3) removing a calculated volume of gas with a syringe and replacing the same volume with pure CO_2 .

The volumes of sample injected into the CO_2 -free carrier stream for TDL measurement were adjusted based on CO_2 mole fraction to consistently introduce 0.88 nmol of CO_2 . A factorial examination of variable injection volumes and CO_2 mole fractions showed that measurement precision was optimized when the amount of CO_2 injected was near this value. During a routine sample run, gas samples were injected into the TDL every 2 min. Calibration gas from each of the three standard cylinders was injected in the same manner between sets of 3–5 unknown samples. This frequency of calibration was required to correct for instrumental drift of unknown origin. The $^{12}\text{CO}_2$ and $^{13}\text{CO}_2$ peaks were measured individually by the TDL at a frequency of 10 Hz (Fig. 2(a)). The slope of the change in mole fraction vs. time was calculated for successive 0.5-s windows (Fig. 2(b)). The maximum and

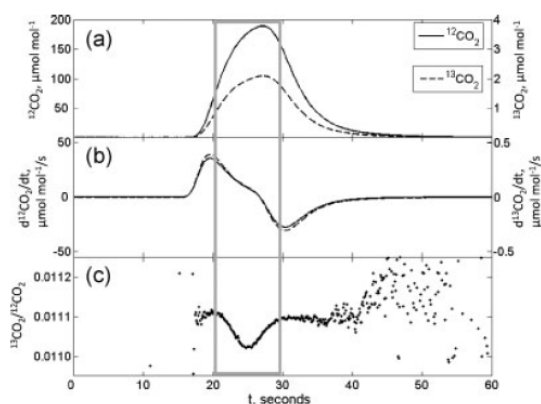


Figure 2. 10-Hz data from one representative injection into the TDL inlet stream. $^{12}\text{CO}_2$ and $^{13}\text{CO}_2$ peaks were measured by the instrument (a), within which the maximum and minimum slopes vs. time were identified (b), and used to find and define (grey lines) a persistent local minimum feature within the ratio of $^{13}\text{CO}_2/^{12}\text{CO}_2$ vs. time (c).

minimum slopes were found and used to define a highly repeatable, local minimum feature apparent in the molar ratio of $^{13}\text{CO}_2/^{12}\text{CO}_2$ vs. time (Fig. 2(c), grey window). A second-order polynomial was fitted to the data within this feature and the minimum value of the fit line was used to calculate a raw carbon isotope ratio ($\delta^{13}\text{C}$, ‰) following convention:

$$\delta^{13}\text{C} = \left(\frac{R_{\text{sample}}}{R_{\text{std}}} - 1 \right) * 1000 \quad (1)$$

where R_{sample} is the minimum value of a line fitted to the $^{13}\text{CO}_2/^{12}\text{CO}_2$ feature and R_{std} is 0.01124, the ratio of $^{13}\text{C}/^{12}\text{C}$ in PDB carbonate.¹⁹ The shape of this feature is probably determined by a kinetic fractionation of CO_2 isotopologues during gas flow from the injection port to the TDL. However, calculating a ratio based on either an average or minimum value for this feature within peaks consistently produced better precision than using a ratio determined from individual $^{12}\text{CO}_2$ and $^{13}\text{CO}_2$ peak maxima or integrated peak areas (data not shown). The advantage of using a $^{13}\text{CO}_2/^{12}\text{CO}_2$ ratio calculated from a specific point within the peaks, rather than a ratio of integrated $^{13}\text{CO}_2$ and $^{12}\text{CO}_2$ peak areas, may be due to the limitations of TDL performance at very low mole fractions (with fewer IR-absorbing molecules).

A linear fit between isotope measurements of the calibration standard cylinders and known $\delta^{13}\text{C}$ of CO_2 in each cylinder was used to calibrate all samples within a run to the VPDB scale. Instrument drift within each run was then identified by interpolating between the average difference between measured and known tank isotope ratios of each calibration set vs. injection number. This interpolated offset function was subtracted from the calibrated measurements to correct for changes in instrument response during a run.

Gas sample collection and storage

When not sampled with a syringe immediately before injection into the TDL, gas well samples were collected in 12-mL, septum-capped, evacuated vials (Exetainer, Labco, High Wycombe, UK) using a two-ended blood-collection needle (22G1 Vacutainer, Becton Dickinson, Franklin Lakes, NJ, USA). Storage in vials was tested for the isotope effects of leaking or CO_2 exchange with septum polymer material. Vials were filled from two of the isotope standard cylinders (-7.58 and -31.28 ‰) and an additional gas preparation mixed from a cylinder of pure CO_2 at $+12.15$ ‰ and laboratory air to a CO_2 mole fraction of $3000 \mu\text{mol mol}^{-1}$. The vials were stored at room temperature. Subsets of vials from each source were randomly selected and measured on the day of filling and then at various intervals for up to 60 additional days (each vial was measured only once).

Laboratory experiments

A method based on the design of Pumpanen *et al.*²⁰ was used to generate an artificial soil respiration source in the laboratory (an alternate design was recently used for a soil CO_2 isotope study by Kayler *et al.*¹¹). An artificial soil was prepared using oven-dry desert sand derived from the Cedar Mesa sandstone formation of southern Utah containing very low organic content,²¹ sieved to remove particles larger than $500 \mu\text{m}$ diameter. A 17-cm column of this medium was suspended on a perforated platform within an 89 cm tall,

RCM

58 cm wide polyethylene barrel. The surface of the sand was open to air in the laboratory and the bottom of the barrel was plumbed to allow a flow of pure CO₂ with a $\delta^{13}\text{C}$ value of -31.63% from a gas cylinder, using a mass flow controller (1179A, MKS, Andover, MA, USA).

Two parallel lengths of 0.64 cm diameter tubing (Bev-A-Line IV, Cole-Parmer, Vernon Hills, IL, USA) were perforated by piercing multiple times with a needle and laid horizontally through the sand medium at 1, 7.5, and 13 cm depths. These tubes were accessible by septum fittings on the outside of the barrel. A second set of gas-sampling wells was installed vertically in the sand from the surface. These were 15-cm lengths of 0.64-cm diameter stainless steel tubing inserted to 0.5, 1, 2, 3, 4, 5, and 7.5 cm, with straight unions (SS-400-6, Swagelok) containing septa on the protruding ends.

In the first laboratory experiment, mole fraction and isotope gradients were initially produced in the sand medium by flowing pure CO₂ into the lower portion of the barrel. The rise in the CO₂ mole fraction inside the barrel was monitored with a solid-state CO₂ analyzer (GMT222, Vaisala, Woburn, MA, USA). The flow was stopped when the CO₂ mole fraction in the gas below the sand column reached $12\,000\ \mu\text{mol mol}^{-1}$, and the flow then remained off. Gas samples were collected from both sets of gas wells approximately 2 h later, and again on the following day. Gas from the vertically inserted tubes was sampled directly with syringes immediately before measurement of CO₂ mole fraction and carbon isotope content, whereas gas from the horizontal tubes was collected in evacuated vials before measurement.

The second laboratory experiment began with the barrel and soil medium at ambient CO₂ mole fraction and $\delta^{13}\text{C}$. Profile and chamber measurements were made over a period of about 3 days after a continuous, 5 sccm flow of pure CO₂ of -31.63% was initiated into the lower barrel compartment from a gas cylinder. The open chamber was run continuously and gas samples were collected from the inserted and buried tubes into evacuated vials at 0.5, 2, 6, 23, 36, 58, and 70 h after the start of CO₂ flow into the barrel.

Chamber measurements of soil surface CO₂ flux

During the second laboratory experiment, an open, flow-through soil chamber²² was plumbed to the TDL (Fig. 3) and inserted about 3 cm into the barrel sand column from the

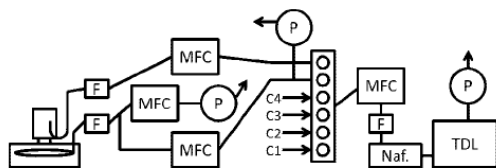


Figure 3. Plumbing diagram of soil chamber measurement with the tunable diode laser (TDL). Mass flow controllers (MFCs) regulated (from left to right) total chamber flow, inlet and outlet sampling flows, and TDL sampling flow, using three separate pumps (P). A solenoid manifold selected between the calibration tanks (C1–4) and the chamber inlet and outlet flows. All flows were filtered (F) and samples entering the TDL were dried using Nafion (Naf.).

Carbon isotope content of soil CO₂ and soil respiration 897

surface. The chamber was made of transparent acrylic, 33 cm tall and 26 cm in diameter, with a specialized lid assembly²² containing a funneled aluminum inlet tube. The chamber design allowed measured pressure differentials (inside to outside the chamber) to remain below 0.2 Pa at flow rates of up to 5000 sccm. These low-pressure differentials at particular flow rates were verified by direct measurement of the differential pressure (PX653-0.05BD5V, Omega Engineering Inc., Stamford, CT, USA) with the chamber attached to an impermeable slate laboratory bench, as recommended by Xu *et al.*²³

A continuous flow through the chamber was driven by a pump and controlled by a mass flow controller (1179A, MKS). A second pump pulled sample flows of gas continuously from the chamber inlet and outlet flows, each set to 300 sccm with an additional mass flow controller. A solenoid valve manifold was used to select between sampling chamber inlet and outlet flows and four calibration gas cylinders. A datalogger (CR5000, Campbell Scientific) controlled measurement cycling between these six flows, with each cycle (inlet, outlet, and 4 calibration tanks) lasting 10 min. The flow to the TDL was maintained at 150 sccm by an additional mass flow controller and dried with a Nafion counterflow system (PD 625, Campbell Scientific). All flows were filtered to 15 μm . Standard gases were prepared and calibrations conducted as described by Schaeffer *et al.*²⁴ Soil surface flux rates were calculated from the chamber using:

$$\text{Flux} = \frac{(\text{CO}_{2o} - \text{CO}_{2i}) \times \text{Flow}}{\text{Area}} \quad (2)$$

where CO_{2o} and CO_{2i} are the mole fractions of CO₂ in the outlet and inlet flows from the chamber, Flow is the number of moles of air passing through the chamber per second, and Area is the soil surface area enclosed by the chamber. The carbon isotope ratio of the soil surface CO₂ flux in the chamber ($\delta^{13}\text{C}_F$) was calculated as:

$$\delta^{13}\text{C}_F = \frac{(\text{CO}_{2o} \times \delta_o) - (\text{CO}_{2i} \times \delta_i)}{\text{CO}_{2o} - \text{CO}_{2i}} \quad (3)$$

where δ_o and δ_i are the $\delta^{13}\text{C}$ values, respectively, of the CO₂ in the outlet and inlet flows in ‰. The chamber flow was adjusted periodically to keep the mole fraction difference between inlet and outlet flows around $50\ \mu\text{mol mol}^{-1}$. The chamber data were averaged for 3-h periods.

RESULTS AND DISCUSSION

The injection method for the TDL

Vials filled with $\sim 3000\ \mu\text{mol mol}^{-1}$ CO₂ spanning a range of $\delta^{13}\text{C}$ values and stored at room temperature showed no directional drift for up to 60 days of storage time after filling (Fig. 4). This lack of drift represents an improvement over similar tests performed with the same commercial vials.^{25,26} This improvement is probably due in part to the higher mole fraction of CO₂ in our samples of about $3000\ \mu\text{mol mol}^{-1}$. For the calculation of a Keeling plot intercept from soil CO₂, this suggests that any effect of storage on the calculated intercept will be reduced when the sample mole fractions are at least $3000\ \mu\text{mol mol}^{-1}$. In soil gas profiles collected in the field, this mole fraction is likely to be reached within the first few

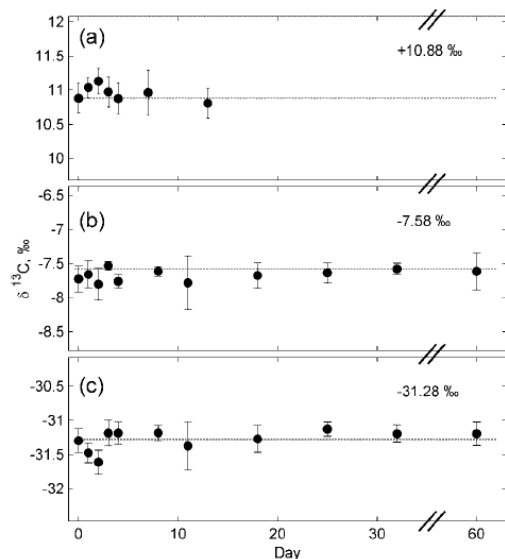


Figure 4. Repeated measurements of sample vials filled on day 0 with one of three prepared gases containing $\sim 3000 \mu\text{mol mol}^{-1}$ CO_2 at different carbon isotope ratios (labeled on each panel). Points are means and standard deviations of 5–11 randomly selected vials from each group.

centimeters of soil depth. The standard deviation of the $\delta^{13}\text{C}$ value of the CO_2 of all the vials sampled during the storage test (calculated on the population of measured – known values for each vial) was 0.23‰. This value incorporates errors associated with the collection, storage, measurement, and calibration of samples and represents a good indication of the overall performance of this method as it applies to field studies. While this measurement uncertainty is larger than typical precision associated with mass spectrometry, the small sample volumes required may enable repeated measurements, and the error of Keeling plot intercepts is usually more dependent on the range of CO_2 mole fractions of each sample population.²⁷ Estimates of precision and accuracy of the TDL measurement alone (without sampling and storage errors) were obtained by injecting gas directly from standard cylinders into the TDL and treating some standard gas injections as unknowns. In these tests the accuracy was within $\pm 0.1\%$ of the $\delta^{13}\text{C}$ value of the CO_2 in the cylinder, with standard deviations of 0.15‰ or less.

The new TDL measurement capability made possible by this method is analogous to the extended capabilities brought to isotope ratio mass spectrometry (IRMS) by continuous-flow (CF) configurations. In both cases a small sample is introduced into a carrier stream and peak measurements are used to calculate an isotope ratio, enabling a larger range of potential applications.²⁸ For example, CF-IRMS techniques have been developed to measure the carbon isotope ratios of atmospheric CO_2 ²⁹ and methane,³⁰ oxygen isotope ratios in dissolved and gaseous O_2 ,³¹ sulfur isotope ratios in mineral sulfides and sulfates,³² and nitrogen and

oxygen isotope ratios of N_2O .³³ Similarly, the new TDL method described in this paper could be directly applied to measure the $\delta^{13}\text{C}$ of CO_2 in a variety of research situations, such as gas exchange studies with plants,³⁴ animals,³⁵ or microbial incubations;³⁶ analysis of gases processed by reacting acid with fossil teeth³⁷ or pedogenic carbonates;³⁸ or measurement of samples collected from volcanic emissions in remote areas.³⁹ In addition, modifications of this method could probably be developed for TDL instruments configured to measure isotopologues of other trace gases.

Laboratory experiments

The CO_2 profiles in the sand 2 and 24 h after turning off the pure CO_2 source in the first experiment were linear (Fig. 5(a)), reflecting a diffusive flux through a homogeneous medium that did not contain any source activity. As CO_2 diffused out of the barrel through the sand over the course of the experiment, the CO_2 gradient decreased and the $\delta^{13}\text{C}$ profile became more enriched (Fig. 5(b)). Without a CO_2 source, the system underwent an isotopic distillation as the lighter $^{12}\text{CO}_2$ molecules left the barrel at a slightly higher rate than the heavier $^{13}\text{CO}_2$ molecules. Because the room was large and ventilated, the atmospheric boundary condition was held relatively constant, which was apparent in the isotope mixing lines that reflected a progressively enriched flux from the sand (Figs. 5(c) and 5(d)). The Keeling plot intercept from samples collected at 2 h (Fig. 5(d)) was -29.03% , reflecting a CO_2 surface flux $\delta^{13}\text{C}$ of -33.43% (subtracting 4.4‰ from -29.03%) and the intercept from the 24-h sample set was -23.16% , indicating a CO_2 surface flux $\delta^{13}\text{C}$ of -27.56% .

Samples collected with evacuated 12-mL vials from the horizontal tubing wells and with gas-tight syringes from the vertical tubing wells produced the same relationships of CO_2 mole fractions and carbon isotope content with depth (Fig. 5). This indicates that the gas within the volume of the vertically inserted tubing was effectively equilibrated with the CO_2 at the depth of the open end, although the profiles were changing over time. Numerous measurements spanning relatively large gradients of CO_2 mole fraction and $\delta^{13}\text{C}$ within the top 10 cm of sand were made possible by the small gas well design, enabling relatively precise calculations of Keeling intercepts. In the Keeling plot calculation from the profiles sampled 2 h after flow was stopped, the standard error of the intercept was 0.11‰, smaller than the errors associated with the individual isotope measurements in the regression (typically 0.25‰). In the profiles collected at 24 h, the measured ranges of CO_2 mole fraction and $\delta^{13}\text{C}$ were smaller and the standard error of the intercept was 0.28‰.

In the second laboratory experiment a CO_2 flux began to develop from the sand surface shortly after initiation of the flow of pure CO_2 into the space below the sand (Fig. 6(a)). The $\delta^{13}\text{C}$ of the flux quickly became about 4‰ more depleted in $^{13}\text{CO}_2$ than the source in both chamber and profile estimates, followed by a gradual, asymptotic increase towards the source value of -31.63% (Fig. 6(b)). This transient increase towards a steady-state flux $\delta^{13}\text{C}$ followed theoretical predictions based on isotopic diffusion¹⁵ and lasted approximately 3 days. The equilibration time for this

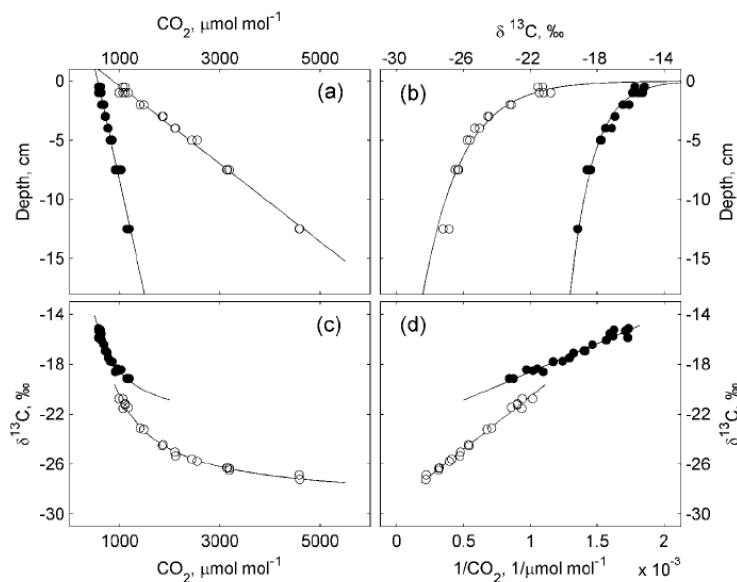


Figure 5. Combined data from vertical (at 0.5, 1, 2, 3, 4, 5, and 7.5 cm) and horizontal (at 1, 7.5, and 13 cm) gas wells from within 17 cm of sand 2 h (open symbols) and 24 h (closed symbols) after stopping flow of pure CO₂ into an air space below the sand layer. Fit lines are: (a) linear, (b) calculated from a linear fit of δ¹³C vs. log depth, and (c) calculated from the linear Keeling plot fit shown in (d).

system was so long because of the large storage volume of air beneath the sand platform (~150 L). The calculated δ¹³C of the CO₂ flux produced in the medium over time was similar for the Keeling plot approach using combined data from

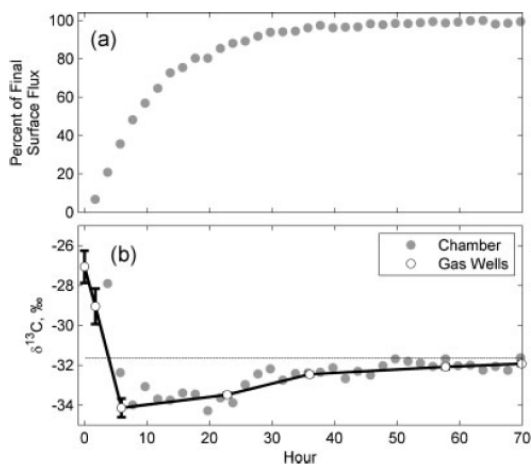


Figure 6. (a) Open chamber surface flux of CO₂ and (b) δ¹³C of CO₂ in the soil surface flux measured using open chamber and gas well methods, plotted vs. time since initiation of pure CO₂ flow under 17 cm of sand. The dashed line is the δ¹³C of CO₂ in the source tank (-31.63‰). Gas well derived flux isotope ratios were adjusted by 4.4‰ for diffusive enrichment and error bars are 1 standard error of the intercept (smaller than symbols in some cases).

vertical and horizontal gas well samples and the open chamber approach (Fig. 6(b)). This agreement, and the convergence towards a steady-state CO₂ flux δ¹³C matching the measured value for the tank CO₂ source, provide evidence of the accuracy of both methods for determining the δ¹³C of soil-respired CO₂ under these controlled conditions, and a measure of confidence for the use of these methods in the field.

For this experiment evacuated 12-mL vials were used for the collection of sample gas from the vertical and horizontal gas wells, although the internal volume of the vertical gas wells was only ~3.5 mL. This means that gas in the pore spaces surrounding the open end of the gas well was drawn into the sample. Because the CO₂ mole fraction and δ¹³C profiles were a result of diffusive mixing of two sources, the use of horizontal gas wells equilibrated at precise depths or vertical gas wells drawing from a volume of pore spaces surrounding the gas well ends produced the same calculated Keeling plot intercepts.

CONCLUSIONS

This paper outlines a new syringe injection approach for a tunable diode laser absorption spectrometer, and its application to measure the δ¹³C of soil-respired CO₂. With this injection method, small volumes of soil gas with high CO₂ mole fractions can be delivered to the TDL and measured every 2 min with approximately 0.25‰ precision. The injection technique was applied to measure profiles of mole fractions and the δ¹³C of CO₂ in an artificial soil medium in laboratory experiments using a known, con-

trolled CO₂ source. Keeling plot derived $\delta^{13}\text{C}$ measurements of the induced CO₂ flux from depth profile samples compared well with expectations based on theory and with a second TDL method, which employed an open chamber on the surface of the medium. Keeling plot intercept calculations were unaffected by the gas-sampling methods including (1) drawing gas from within vertical gas wells with a small syringe, (2) drawing gas from the vertical gas well plus pore spaces around the submerged end of tubing using an evacuated vial and a double-ended needle, and (3) sampling gas from within horizontal perforated tubing.

Soil profile samples can be collected, transported, and stored for later measurement for the calculation of the $\delta^{13}\text{C}$ of soil-respired CO₂, but this method offers limited temporal resolution. Alternatively, the open chamber method has an advantage of providing continuous measurements of the $\delta^{13}\text{C}$ and rates of CO₂ efflux, but with limited spatial replication and requiring field deployment of the instrument. The independence of the profile and chamber methods, while making use of the same instrument, provides a unique validation opportunity for researchers with access to a tunable diode laser. We encourage researchers reporting open chamber $\delta^{13}\text{C}$ data in future studies to take such a validation step.

Acknowledgements

We thank Suzanne Bethers, Tim Anglin, Timothy Jackson, Jim Ehleringer, Thure Cerling, and Jukka Pumpanen for help with planning, construction, and/or use of the barrel system. We also thank Lisa Wingate, John Moncrieff, and John Miller for lending soil chambers. This research was supported by the Office of Science (BER), U.S. Department of Energy (Grant No. DE-FG02-04ER63904), the University of Utah, and the A. Herbert and Marian W. Gold Scholarship.

REFERENCES

- Zhang J, Griffis TJ, Baker JM. *Plant Cell Environ.* 2006; 29: 483.
- Lee XH, Kim K, Smith R. *Global Biogeochem. Cycles* 2007; 21: DOI: 10.1029/2006GB002871.
- Griffis TJ, Sargent SD, Baker JM, Lee X, Tanner BD, Greene J, Swiatek E, Billmark K. *J. Geophys. Res. Atmospheres* 2008; 113: DOI: 10.1029/2007JD009297.
- Marron N, Plain C, Longdoz B, Epron D. *Plant Soil* 2009; 318: 137.
- Bahn M, Schmitt M, Siegwolf R, Richter A, Brüggemann N. *New Phytologist* 2009; 182: 451.
- Bowling DR, Sargent SD, Tanner BD, Ehleringer JR. *Agric. Forest Meteorol.* 2003; 118: 1.
- Engel S, Lease HM, McDowell NG, Corbett AH, Wolf BO. *Rapid Commun. Mass Spectrom.* 2009; 23: 1281.
- Drewitt G, Wagner-Riddle C, Warland J. *Agric. Forest Meteorol.* 2009; 149: 614.
- Schaeffer SM, Anderson DE, Burns SP, Monson RK, Sun J, Bowling DR. *Agric. Forest Meteorol.* 2008; 148: 592.
- Bowling DR, Massman WJ, Schaeffer SM, Burns SP, Monson RK, Williams MW. *Biogeochemistry* 2009; 95: 37.
- Kayler ZE, Sulzman EW, Marshall JD, Mix A, Rugh WD, Bond BJ. *Rapid Commun. Mass Spectrom.* 2008; 22: 2533.
- Keeling CD. *Geochim. Cosmochim. Acta* 1958; 13: 322.
- Cerling TE, Solomon DK, Quade J, Bowman JR. *Geochim. Cosmochim. Acta* 1991; 55: 3403.
- Davidson GR. *Geochim. Cosmochim. Acta* 1995; 59: 2485.
- Amundson R, Stern L, Baisden T, Wang Y. *Geoderma* 1998; 82: 83.
- Keller CK, Bacon DH. *Global Biogeochem. Cycles* 1998; 12: 361.
- Breecker D, Sharp ZD. *Rapid Commun. Mass Spectrom.* 2008; 22: 449.
- Davidson EA, Trumbore SE. *Tellus* 1995; 47: 550.
- Craig H. *Geochim. Cosmochim. Acta* 1957; 12: 133.
- Pumpanen J, Kolari P, Ilvesniemi H, Minkinen K, Vesala T, Niinisto S, Lohila A, Larmola T, Morero M, Pihlatie M, Janssens I, Yuste JC, Grunzweig JM, Reth S, Subke JA, Savage K, Kutsch W, Ostreng G, Ziegler W, Anthoni P, Lindroth A, Hari P. *Agric. Forest Meteorol.* 2004; 123: 159.
- Neff JC, Reynolds R, Sanford RL, Fernandez D, Lamothe P. *Ecosystems* 2006; 9: 879.
- Rayment MB, Jarvis PG. *J. Geophys. Res. Atmospheres* 1997; 102: 28779.
- Xu LK, Furtaw MD, Madsen RA, Garcia RL, Anderson DJ, McDermitt DK. *J. Geophys. Res. Atmospheres* 2006; 111: D08S10.
- Schaeffer SM, Miller JB, Vaughn BH, White JWC, Bowling DR. *Atmos. Chem. Phys.* 2008; 8: 5263.
- Tu KP, Brooks PD, Dawson TE. *Rapid Commun. Mass Spectrom.* 2001; 15: 952.
- Knohl A, Werner RA, Geilmann H, Brand WA. *Rapid Commun. Mass Spectrom.* 2004; 18: 1663.
- Zobitz JM, Keener JP, Schnyder H, Bowling DR. *Agric. Forest Meteorol.* 2006; 136: 56.
- Brand WA. *J. Mass Spectrom.* 1996; 31: 225.
- Lai C-T, Ehleringer JR, Schauer AJ, Tans PP, Hollinger DY, Paw UKT, Munger JW, Wofsy SC. *Global Change Biol.* 2005; 11: 633.
- Miller JB, Mack KA, Dissly R, White JWC, Dlugokencky EJ, Tans PP. *J. Geophys. Res. Atmospheres* 2002; 107: DOI: 10.1029/2001JD000630.
- Wassenaar LI, Koehler G. *Anal. Chem.* 1999; 71: 4965.
- Grassineau NV, Matthey DP, Lowry D. *Anal. Chem.* 2000; 73: 220.
- Komatsu DD, Ishimura T, Nakagawa F, Tsunogai U. *Rapid Commun. Mass Spectrom.* 2008; 22: 1587.
- Priault P, Wegener F, Werner C. *New Phytologist* 2009; 181: 400.
- Passey BH, Robinson TF, Ayliffe LK, Cerling TE, Sponheimer M, Dearing MD, Roeder BL, Ehleringer JR. *J. Archaeol. Sci.* 2005; 32: 1459.
- Anesio AM, Theil-Nielsen J, Graneli W. *Microbial Ecol.* 2000; 40: 200.
- Morgan ME, Behrensmeyer AK, Badgley C, Barry JC, Nelson S, Pilbeam D. *Geology* 2009; 37: 103.
- Takeuchi A, Goodwin AJ, Moravec BG, Larson PB, Keller CK. *Quat. Res.* 2009; 72: 198.
- Sato M, Mori T, Shimoike Y, Nagao K, Notsu K. *Earth, Planets Space* 2002; 54: 257.

REFERENCES

- Amundson, R., L. Stern, T. Baisden, and Y. Wang. 1998. The isotopic composition of soil and soil-respired CO₂. *Geoderma* **82**:83-114.
- Andrews, J. A., R. Matamala, K. M. Westover, and W. H. Schlesinger. 2000. Temperature effects on the diversity of soil heterotrophs and the $\delta^{13}\text{C}$ of soil-respired CO₂. *Soil Biology & Biochemistry* **32**:699-706.
- Aubrey, D. P. and R. O. Teskey. 2009. Root-derived CO₂ efflux via xylem stream rivals soil CO₂ efflux. *New Phytologist* **184**:35-40.
- Austin, A. T., L. Yahdjian, J. M. Stark, J. Belnap, A. Porporato, U. Norton, D. A. Ravetta, and S. M. Schaeffer. 2004. Water pulses and biogeochemical cycles in arid and semiarid ecosystems. *Oecologia* **141**:221-235.
- Badeck, F. W., G. Tcherkez, S. Nogues, C. Piel, and J. Ghashghaie. 2005. Post-photosynthetic fractionation of stable carbon isotopes between plant organs - a widespread phenomenon. *Rapid Communications in Mass Spectrometry* **19**:1381-1391.
- Bahn, M., M. Schmitt, R. Siegwolf, A. Richter, and N. Brüggemann. 2009. Does photosynthesis affect grassland soil-respired CO₂ and its carbon isotope composition on a diurnal timescale? *New Phytologist* **182**:451-460.
- Barbour, M. M., J. E. Hunt, R. J. Dungan, M. H. Turnbull, G. W. Brailsford, G. D. Farquhar, and D. Whitehead. 2005. Variation in the degree of coupling between $\delta^{13}\text{C}$ of phloem sap and ecosystem respiration in two mature *Nothofagus* forests. *New Phytologist* **166**:497-512.
- Barbour, M. M., N. G. McDowell, G. Tcherkez, C. P. Bickford, and D. T. Hanson. 2007. A new measurement technique reveals rapid post-illumination changes in the carbon isotope composition of leaf-respired CO₂. *Plant, Cell, and Environment* **30**:469-482.
- Bardgett, R. D., W. D. Bowman, R. Kaufmann, and S. K. Schmidt. 2005. A temporal approach to linking aboveground and belowground ecology. *Trends in Ecology & Evolution* **20**:634-641.
- Bathellier, C., G. Tcherkez, R. Bligny, E. Gout, G. Cornic, and J. Ghashghaie. 2009. Metabolic origin of the delta C-13 of respired CO₂ in roots of *Phaseolus vulgaris*. *New Phytologist* **181**:387-399.

- Betson, N. R., S. G. Gottlicher, M. Hall, G. Wallin, A. Richter, and P. Högberg. 2007. No diurnal variation in rate or carbon isotope composition of soil respiration in a boreal forest. *Tree Physiology* **27**:749-756.
- Bhupinderpal-Singh, A. Nordgren, M. O. Lofvenius, M. N. Högberg, P. E. Mellander, and P. Högberg. 2003. Tree root and soil heterotrophic respiration as revealed by girdling of boreal Scots pine forest: extending observations beyond the first year. *Plant Cell and Environment* **26**:1287-1296.
- Bond-Lamberty, B. and A. Thomson. 2010. Temperature-associated increases in the global soil respiration record. *Nature* **464**:579-582.
- Bond-Lamberty, B., C. K. Wang, and S. T. Gower. 2004. A global relationship between the heterotrophic and autotrophic components of soil respiration? *Global Change Biology* **10**:1756-1766.
- Boone, R. D., K. J. Nadelhoffer, J. D. Canary, and J. P. Kaye. 1998. Roots exert a strong influence on the temperature sensitivity of soil respiration. *Nature* **396**:570-572.
- Borken, W. and E. Matzner. 2009. Reappraisal of drying and wetting effects on C and N mineralization and fluxes in soils. *Global Change Biology* **15**:808-824.
- Borken, W., K. Savage, E. A. Davidson, and S. E. Trumbore. 2006. Effects of experimental drought on soil respiration and radiocarbon efflux from a temperate forest soil. *Global Change Biology* **12**:177-193.
- Borken, W., Y. J. Xu, R. Brumme, and N. Lamersdorf. 1999. A climate change scenario for carbon dioxide and dissolved organic carbon fluxes from a temperate forest soil: Drought and rewetting effects. *Soil Science Society of America Journal* **63**:1848-1855.
- Borken, W., Y. J. Xu, E. A. Davidson, and A. Beese. 2002. Site and temporal variation of soil respiration in European beech, Norway spruce, and Scots pine forests. *Global Change Biology* **8**:1205-1216.
- Böstrom, B., D. Comstedt, and A. Ekblad. 2007. Isotope fractionation and ^{13}C enrichment in soil profiles during the decomposition of soil organic matter. *Oecologia* **153**:89-98.
- Bowling, D. R., N. G. McDowell, B. J. Bond, B. E. Law, and J. R. Ehleringer. 2002a. ^{13}C content of ecosystem respiration is linked to precipitation and vapor pressure deficit. *Oecologia* **131**:113-124.
- Bowling, D. R., N. G. McDowell, B. J. Bond, B. E. Law, and J. R. Ehleringer. 2002b. C-13 content of ecosystem respiration is linked to precipitation and vapor pressure deficit. *Oecologia* **131**:113-124.

- Bowling, D. R., D. E. Pataki, and J. T. Randerson. 2008. Carbon isotopes in terrestrial ecosystem pools and CO₂ fluxes. *New Phytologist* **178**:24-40, doi: 10.1111/j.1469-8137.2007.02342.x.
- Brandes, E., N. Kodama, K. Whittaker, C. Weston, H. Rennenberg, C. Keitel, M. A. Adams, and A. Gessler. 2006. Short-term variation in the isotopic composition of organic matter allocated from the leaves to the stem of *Pinus sylvestris*: effects of photosynthetic and postphotosynthetic carbon isotope fractionation. *Global Change Biology* **12**:1922-1939.
- Bremer, D. J., J. M. Ham, C. E. Owensby, and A. K. Knapp. 1998. Responses of soil respiration to clipping and grazing in a tallgrass prairie. *Journal of Environmental Quality* **27**:1539-1548.
- Brooks, P. D., D. McKnight, and K. Elder. 2005. Carbon limitation of soil respiration under winter snowpacks: potential feedbacks between growing season and winter carbon fluxes. *Global Change Biology* **11**:231-238.
- Burke, M. K. and D. J. Raynal. 1994. Fine root growth phenology, production, and turnover in a northern hardwood forest ecosystem. *Plant and Soil* **162**:135-146.
- Campbell, G. S. and J. M. Norman. 1998. *An Introduction to Environmental Biophysics*. Springer.
- Campbell, J. L., O. J. Sun, and B. E. Law. 2004. Supply-side controls on soil respiration among Oregon forests. *Global Change Biology* **10**:1857-1869.
- Canadell, J., R. B. Jackson, J. R. Ehleringer, H. A. Mooney, O. E. Sala, and E. D. Schulze. 1996. Maximum rooting depth of vegetation types at the global scale. *Oecologia* **108**:583-595.
- Cerling, T. E., D. K. Solomon, J. Quade, and J. R. Bowman. 1991. On the isotopic composition of carbon in soil carbon dioxide. *Geochimica et Cosmochimica Acta* **55**:3403-3405.
- Chapin, F. S., III. 2003. Effects of Plant Traits on Ecosystem and Regional Processes: a Conceptual Framework for Predicting the Consequences of Global Change. *Annals of Botany* **91**:455-463.
- Chen, B. and J. M. Chen. 2007. Diurnal, seasonal and interannual variability of carbon isotope discrimination at the canopy level in response to environmental factors in a boreal forest ecosystem. *Plant, Cell & Environment* **30**:1223-1239.
- Chen, S., G. Lin, J. Huang, and G. D. Jenerette. 2009. Dependence of carbon sequestration on the differential responses of ecosystem photosynthesis and

- respiration to rain pulses in a semiarid steppe. *Global Change Biology* **15**:2450-2461.
- Coxson, D. S. and D. Parkinson. 1987. Winter respiratory activity in aspen woodland forest floor litter and soils. *Soil Biology & Biochemistry* **19**:49-59.
- Craig, H. 1957. Isotopic standards for carbon and oxygen and correction factors for mass-spectrometric analysis of carbon dioxide. *Geochimica et Cosmochimica Acta* **12**:133-149.
- Craine, J. M., W. G. Lee, W. J. Bond, R. J. Williams, and L. C. Johnson. 2005. Environmental Constraints on a Global Relationship among Leaf and Root Traits of Grasses. *Ecology* **86**:12-19.
- Craine, J. M., D. A. Wedin, and F. S. Chapin. 1998. Predominance of ecophysiological controls on soil CO₂ flux in a Minnesota grassland. *Plant and Soil* **207**:77-86.
- Craine, J. M., D. A. Wedin, and F. S. Chapin. 1999. Predominance of ecophysiological controls on soil CO₂ flux in a Minnesota grassland. *Plant and Soil* **207**:77-86.
- Curiel Yuste, J., D. D. Baldocchi, A. Gershenson, A. Goldstein, L. Misson, and S. Wong. 2007. Microbial soil respiration and its dependency on carbon inputs, soil temperature and moisture. *Global Change Biology* **13**:2018-2035.
- Curiel Yuste, J., I. A. Janssens, A. Carrara, and R. Ceulemans. 2004. Annual Q(10) of soil respiration reflects plant phenological patterns as well as temperature sensitivity. *Global Change Biology* **10**:161-169.
- Curiel Yuste, J., I. A. Janssens, and R. Ceulemans. 2005a. Calibration and validation of an empirical approach to model soil CO₂ efflux in a deciduous forest. *Biogeochemistry*:209-230.
- Curiel Yuste, J., M. Nagy, I. A. Janssens, A. Carrara, and R. Ceulemans. 2005b. Soil respiration in a mixed temperate forest and its contribution to total ecosystem respiration. *Tree Physiology* **25**:609-619.
- Damesin, C. and C. Lelarge. 2003. Carbon isotope composition of current-year shoots from *Fagus sylvatica* in relation to growth, respiration and use of reserves. *Plant Cell and Environment* **26**:207-219.
- Davidson, E. A., E. Belk, and R. D. Boone. 1998. Soil water content and temperature as independent or confounded factors controlling soil respiration in a temperate mixed hardwood forest. *Global Change Biology* **4**:217-227.
- Davidson, E. A. and I. A. Janssens. 2006. Temperature sensitivity of soil carbon decomposition and feedbacks to climate change. *Nature* **440**:165-173.

- Davidson, E. A., I. A. Janssens, and Y. Luo. 2006. On the variability of respiration in terrestrial ecosystems: Moving beyond Q_{10} . *Global Change Biology* **12**:154-164.
- Davidson, E. A., K. Savage, L. V. Verchot, and R. Navarro. 2002. Minimizing artifacts and biases in chamber-based measurements of soil respiration. *Agricultural and Forest Meteorology* **113**:21-37.
- Davidson, E. A. and S. E. Trumbore. 1995. Gas diffusivity and production of CO_2 in deep soils of the eastern Amazon. *Tellus* **47**:550-565.
- Davidson, E. A., S. E. Trumbore, and R. Amundson. 2000. Biogeochemistry - Soil warming and organic carbon content. *Nature* **408**:789-790.
- Davidson, G. R. 1995. The stable isotopic composition and measurement of carbon in soil CO_2 . *Geochimica et Cosmochimica Acta* **59**:2485-2489.
- Dawson, T. E. and J. R. Ehleringer. 1991. Streamside trees that do not use stream water. *Nature* **350**:335-337.
- de Dato, G., P. De Angelis, C. Sirca, and C. Beier. 2010. Impact of drought and increasing temperatures on soil CO_2 emissions in a Mediterranean shrubland (gariga). *Plant and Soil* **327**:153-166.
- De Deyn, G. B., J. H. C. Cornelissen, and R. D. Bardgett. 2008. Plant functional traits and soil carbon sequestration in contrasting biomes. *Ecology Letters* **11**:516-531.
- Del Grosso, S. J., W. J. Parton, A. R. Mosier, E. A. Holland, E. Pendall, D. S. Schimel, and D. S. Ojima. 2005. Modeling soil CO_2 emissions from ecosystems. *Biogeochemistry*:71-91.
- Dijkstra, F. A., S. E. Hobbie, and P. B. Reich. 2006. Soil Processes Affected by Sixteen Grassland Species Grown under Different Environmental Conditions. *Soil Science Society of America Journal* **70**:770-777.
- Ehleringer, J. R., L. A. Arnow, T. Arnow, I. B. McNulty, and N. C. Negus. 1992. Red Butte Canyon Research Natural Area: history, flora, geology, climate, and ecology. *Great Basin Naturalist* **52**:95-121.
- Ehleringer, J. R., N. Buchmann, and L. B. Flanagan. 2000. Carbon isotope ratios in belowground carbon cycle processes. *Ecological Applications* **10**:412-422.
- Ekberg, A., N. Buchmann, and G. Gleixner. 2007. Rhizospheric influence on soil respiration and decomposition in a temperate Norway spruce stand. *Soil Biology & Biochemistry* **39**:2103-2110.

- Ekblad, A., B. Bostrom, A. Holm, and D. Comstedt. 2005. Forest soil respiration rate and $\delta^{13}\text{C}$ is regulated by recent above ground weather conditions. *Oecologia* **143**:136-142.
- Ekblad, A. and P. Högberg. 2001. Natural abundance of ^{13}C in CO_2 respired from forest soils reveals speed of link between tree photosynthesis and root respiration. *Oecologia* **127**:305-308.
- Epron, D., V. Le Dantec, E. Dufrene, and A. Granier. 2001. Seasonal dynamics of soil carbon dioxide efflux and simulated rhizosphere respiration in a beech forest. *Tree Physiology* **21**:145-152.
- Fahey, T. J. and J. W. Hughes. 1994. Fine Root Dynamics in a Northern Hardwood Forest Ecosystem, Hubbard Brook Experimental Forest, NH. *The Journal of Ecology* **82**:533-548.
- Fang, C. and J. B. Moncrieff. 1998. An open-top chamber for measuring soil respiration and the influence of pressure difference on CO_2 efflux measurement. *Functional Ecology* **12**:319-325.
- Fang, C. and J. B. Moncrieff. 2001. The dependence of soil CO_2 efflux on temperature. *Soil Biology & Biochemistry* **33**:155-165.
- Fernandez, I., N. Mahieu, and G. Cadisch. 2003. Carbon isotopic fractionation during decomposition of plant materials of different quality. *Global Biogeochemical Cycles* **17**:1075, doi:10.1029/2001GB001834.
- Fierer, N., O. A. Chadwick, and S. E. Trumbore. 2005. Production of CO_2 in soil profiles of a California annual grassland. *Ecosystems* **8**:412-429.
- Fierer, N. and J. P. Schimel. 2003. A proposed mechanism for the pulse in carbon dioxide production commonly observed following the rapid rewetting of a dry soil. *Soil Science Society of America Journal* **67**:798-805.
- Gessler, A., C. Keitel, N. Kodama, C. Weston, A. J. Winters, H. Keith, K. Grice, R. Leuning, and G. D. Farquhar. 2007. $\delta^{13}\text{C}$ of organic matter transported from the leaves to the roots in *Eucalyptus delegatensis*: short-term variations and relation to respired CO_2 . *Functional Plant Biology* **34**:692-706.
- Gessler, A., H. Rennenberg, and C. Keitel. 2004. Stable isotope composition of organic compounds transported in the phloem of European beech - Evaluation of different methods of phloem sap collection and assessment of gradients in carbon isotope composition during leaf-to-stem transport. *Plant Biology* **6**:721-729.

- Goulden, M. L., J. W. Munger, S.-M. Fan, B. C. Daube, and S. C. Wofsy. 1996. Measurements of carbon sequestration by long-term eddy covariance: methods and a critical evaluation of accuracy. *Global Change Biology* **2**:169-182.
- Goulden, M. L., S. C. Wofsy, J. W. Harden, S. E. Trumbore, P. M. Crill, S. T. Gower, T. Fries, B. C. Daube, S. M. Fan, D. J. Sutton, A. Bazzaz, and J. W. Munger. 1998. Sensitivity of boreal forest carbon balance to soil thaw. *Science* **279**:214-217.
- Griffiths, R. P., J. A. Entry, E. R. Ingham, and W. H. Emmingham. 1997. Chemistry and microbial activity of forest and pasture riparian-zone soils along three Pacific Northwest streams. *Plant and Soil* **190**:169-178.
- Grime, J. P. 1997. *ECOLOGY: Biodiversity and Ecosystem Function: The Debate Deepens*. *Science* **277**:1260-1261.
- Hanson, P. J., N. T. Edwards, C. T. Garten, and J. A. Andrews. 2000. Separating root and soil microbial contributions to soil respiration: A review of methods and observations. *Biogeochemistry* **48**:115-146.
- Hendrick, R. L. and K. S. Pregitzer. 1996. Temporal and Depth-Related Patterns of Fine Root Dynamics in Northern Hardwood Forests. *Journal of Ecology* **84**:167-176.
- Hirsch, A. I., S. E. Trumbore, and M. L. Goulden. 2002a. Direct measurement of the deep soil respiration accompanying seasonal thawing of a boreal forest soil. *Journal of Geophysical Research-Atmospheres* **108**:8221, doi:8210.1029/2001JD000921, 002003.
- Hirsch, A. I., S. E. Trumbore, and M. L. Goulden. 2002b. Direct measurement of the deep soil respiration accompanying seasonal thawing of a boreal forest soil. *Journal of Geophysical Research-Atmospheres* **108**:-
- Hobbie, S., J. Oleksyn, D. Eissenstat, and P. Reich. 2010. Fine root decomposition rates do not mirror those of leaf litter among temperate tree species. *Oecologia* **162**:505-513.
- Hogberg, P., A. Nordgren, N. Buchmann, A. F. S. Taylor, A. Ekblad, M. N. Hogberg, G. Nyberg, M. Ottosson-Lofvenius, and D. J. Read. 2001. Large-scale forest girdling shows that current photosynthesis drives soil respiration. *Nature* **411**:789-792.
- Högberg, P., A. Nordgren, N. Buchmann, A. F. S. Taylor, A. Ekblad, M. N. Högberg, G. Nyberg, M. Ottosson-Lofvenius, and D. J. Read. 2001. Large-scale forest girdling shows that current photosynthesis drives soil respiration. *Nature* **411**:789-792.
- Howard, D. M. and P. J. A. Howard. 1993. Relationships between CO₂ evolution, moisture content and temperature for a range of soil types. *Soil Biology and Biochemistry* **25**:1537-1546.

- Hubbard, R. M., M. G. Ryan, K. Elder, and C. C. Rhoades. 2005. Seasonal patterns in soil surface CO₂ flux under snow cover in 50 and 300 year old subalpine forests. *Biogeochemistry*:93-107.
- Hultine, K. R., S. E. Bush, A. G. West, and J. R. Ehleringer. 2007. Population structure, physiology and ecohydrological impacts of dioecious riparian tree species of western North America. *Oecologia* **154**:85-93.
- Hultine, K. R., T. L. Jackson, K. G. Burtch, S. M. Schaeffer, and J. R. Ehleringer. 2008. Elevated stream inorganic nitrogen impacts on a dominant riparian tree species: Results from an experimental riparian stream system. *Journal of Geophysical Research-Biogeosciences* **113**:doi:10.1029/2008JG000809.
- Hymus, G. J., K. Maseyk, R. Valentini, and D. Yakir. 2005. Large daily variation in ¹³C-enrichment of leaf-respired CO₂ in two *Quercus* forest canopies. *New Phytologist* **167**:377-384.
- Irvine, J., B. E. Law, and M. R. Kurpius. 2005. Coupling of canopy gas exchange with root and rhizosphere respiration in a semi-arid forest. *Biogeochemistry*:271-282.
- Irvine, J., B. E. Law, J. G. Martin, and D. Vickers. 2008. Interannual variation in soil CO₂ efflux and the response of root respiration to climate and canopy gas exchange in mature ponderosa pine. *Global Change Biology* **14**:2848-2859.
- Jackson, R. B., J. Canadell, J. R. Ehleringer, H. A. Mooney, O. E. Sala, and E. D. Schulze. 1996. A global analysis of root distributions for terrestrial biomes. *Oecologia* **108**:389-411.
- Janssens, I. A., H. Lankreijer, G. Matteucci, A. S. Kowalski, N. Buchmann, D. Epron, K. Pilegaard, W. Kutsch, B. Longdoz, T. Grunwald, L. Montagnani, S. Dore, C. Rebmann, E. J. Moors, A. Grelle, U. Rannik, K. Morgenstern, S. Oltchev, R. Clement, J. Gudmundsson, S. Minerbi, P. Berbigier, A. Ibrom, J. Moncrieff, M. Aubinet, C. Bernhofer, N. O. Jensen, T. Vesala, A. Granier, E. D. Schulze, A. Lindroth, A. J. Dolman, P. G. Jarvis, R. Ceulemans, and R. Valentini. 2001. Productivity overshadows temperature in determining soil and ecosystem respiration across European forests. *Global Change Biology* **7**:269-278.
- Janssens, I. A. and K. Pilegaard. 2003. Large seasonal changes in Q₁₀ of soil respiration in a beech forest. *Global Change Biology* **9**:911-918.
- Jassal, R., A. Black, M. Novak, K. Morgenstern, Z. Nestic, and D. Gaumont-Guay. 2005. Relationship between soil CO₂ concentrations and forest-floor CO₂ effluxes. *Agricultural and Forest Meteorology* **130**:176-192.

- Jassal, R. S. and T. A. Black. 2006. Estimating heterotrophic and autotrophic soil respiration using small-area trenched plot technique: Theory and practice. *Agricultural and Forest Meteorology* **140**:193-202.
- Jassal, R. S., T. A. Black, M. D. Novak, D. Gaumont-Guay, and Z. Nestic. 2008. Effect of soil water stress on soil respiration and its temperature sensitivity in an 18-year-old temperate Douglas-fir stand. *Global Change Biology* **14**:1305-1318.
- Jiang, L. F., F. C. Shi, B. Li, Y. Q. Luo, J. Q. Chen, and J. K. Chen. 2005. Separating rhizosphere respiration from total soil respiration in two larch plantations in northeastern China. *Tree Physiology* **25**:1187-1195.
- Jones, D. L., A. Hodge, and Y. Kuzyakov. 2004. Plant and mycorrhizal regulation of rhizodeposition. *New Phytologist* **163**:459-480.
- Keeling, C. D. 1958. The concentration and isotopic abundances of atmospheric carbon dioxide in rural areas. *Geochimica et Cosmochimica Acta* **13**:322-334.
- Keeling, C. D., T. P. Whorf, M. Wahlen, and J. van der Plicht. 1995. Interannual extremes in the rate of rise of atmospheric carbon dioxide since 1980. *Nature* **375**:666-670.
- Keitel, C., M. A. Adams, T. Holst, A. Matzarakis, H. Mayer, H. Rennenberg, and A. Gessler. 2003. Carbon and oxygen isotope composition of organic compounds in the phloem sap provides a short-term measure for stomatal conductance of European beech (*Fagus sylvatica* L.). *Plant, Cell and Environment* **26**:1157-1168.
- Kelliher, F. M., J. Lloyd, A. Arneth, B. Luhker, J. N. Byers, T. M. McSeveny, I. Milukova, S. Grigoriev, M. Panfyorov, A. Sogatchev, A. Varlargin, W. Ziegler, G. Bauer, S. C. Wong, and E. D. Schulze. 1999. Carbon dioxide efflux density from the floor of a central Siberian pine forest. *Agricultural and Forest Meteorology* **94**:217-232.
- King, J. S., T. J. Albaugh, H. L. Allen, M. Buford, B. R. Strain, and P. Dougherty. 2002. Below-ground carbon input to soil is controlled by nutrient availability and fine root dynamics in loblolly pine. *New Phytologist* **154**:389-398.
- Kirkham, D. and W. L. Powers. 1972. *Advanced Soil Physics*. John Wiley and Sons, Inc., New York.
- Klumpp, K., R. Schäufele, M. Lötscher, F. A. Lattanzi, W. Feneis, and H. Schnyder. 2005. C-isotope composition of CO₂ respired by shoots and roots: fractionation during dark respiration? *Plant Cell and Environment* **28**:241-250.

- Knohl, A. and N. Buchmann. 2005. Partitioning the net CO₂ flux of a deciduous forest into respiration and assimilation using stable carbon isotopes. *Global Biogeochemical Cycles* **19**:GB4008, doi:4010.1029/2004GB002301.
- Knohl, A., R. A. Werner, W. A. Brand, and N. Buchmann. 2005. Short-term variations in $\delta^{13}\text{C}$ of ecosystem respiration reveals link between assimilation and respiration in a deciduous forest. *Oecologia* **142**:70-82.
- Knorr, W., I. C. Prentice, J. I. House, and E. A. Holland. 2005. Long-term sensitivity of soil carbon turnover to warming. *Nature* **433**:298-301.
- Kodama, N., R. Barnard, Y. Salmon, C. Weston, J. Ferrio, J. Holst, R. Werner, M. Saurer, H. Rennenberg, N. Buchmann, and A. Gessler. 2008. Temporal dynamics of the carbon isotope composition in a *Pinus sylvestris* stand: from newly assimilated organic carbon to respired carbon dioxide. *Oecologia* **156**:737-750.
- Kueppers, L. M. and J. Harte. 2005. Subalpine forest carbon cycling: Short- and long-term influence of climate and species. *Ecological Applications* **15**:1984-1999.
- Kuzyakov, Y. 2006. Sources of CO₂ efflux from soil and review of partitioning methods. *Soil Biology & Biochemistry* **38**:425-448.
- Kuzyakov, Y. and W. Cheng. 2004. Photosynthesis controls of CO₂ efflux from maize rhizosphere. *Plant and Soil* **263**:85-99.
- Kuzyakov, Y., J. K. Friedel, and K. Stahr. 2000. Review of mechanisms and quantification of priming effects. *Soil Biology and Biochemistry* **32**:1485-1498.
- Lavigne, M. B., R. Boutin, R. J. Foster, G. Goodine, P. Y. Bernier, and G. Robitaille. 2003. Soil respiration responses to temperature are controlled more by roots than by decomposition in balsam fir ecosystems. *Canadian Journal of Forest Research- Revue Canadienne De Recherche Forestiere* **33**:1744-1753.
- Lee, M. S., K. Nakane, T. Nakatsubo, and H. Koizumi. 2003. Seasonal changes in the contribution of root respiration to total soil respiration in a cool-temperate deciduous forest. *Plant and Soil* **255**:311-318.
- Lipson, D. A. 2007. Relationships between temperature responses and bacterial community structure along seasonal and altitudinal gradients. *FEMS Microbiology Ecology* **59**:418-427.
- Lloyd, J. and J. A. Taylor. 1994. On the Temperature Dependence of Soil Respiration. *Functional Ecology* **8**:315-323.

- Longdoz, B., M. Yernaux, and M. Aubinet. 2000. Soil CO₂ efflux measurements in a mixed forest: impact of chamber disturbances, spatial variability and seasonal evolution. *Global Change Biology* **6**:907-917.
- Luo, Y. Q., S. Q. Wan, D. F. Hui, and L. L. Wallace. 2001. Acclimatization of soil respiration to warming in a tall grass prairie. *Nature* **413**:622-625.
- Marron, N., C. Plain, B. Longdoz, and D. Epron. 2009. Seasonal and daily time course of the ¹³C composition in soil CO₂ efflux recorded with a tunable diode laser spectrophotometer (TDLS). *Plant and Soil* **318**:137-151.
- Mary, B., A. Mariotti, and J. L. Morel. 1992. Use of ¹³C variations at natural abundance for studying the biodegradation of root mucilage, roots and glucose in soil. *Soil Biology & Biochemistry* **24**:1065-1072.
- Massman, W. J. 1998. A review of the molecular diffusivities of H₂O, CO₂, CH₄, CO, O-3, SO₂, NH₃, N₂O, NO, AND NO₂ in air, O-2 AND N-2 near STP. *Atmospheric Environment* **32**:1111-1127.
- Maunoury, F., D. Berveiller, C. Lelarge, J. Y. Pontailler, L. Vanbostal, and C. Damesin. 2007. Seasonal, daily and diurnal variations in the stable carbon isotope composition of carbon dioxide respired by tree trunks in a deciduous oak forest. *Oecologia* **151**:268-279.
- McDowell, N. G., D. R. Bowling, B. J. Bond, J. Irvine, B. E. Law, P. Anthoni, and J. R. Ehleringer. 2004a. Response of the carbon isotopic content of ecosystem, leaf, and soil respiration to meteorological and physiological driving factors in a *Pinus ponderosa* ecosystem. *Global Biogeochemical Cycles* **18**:GB1013, doi:10.1029/1203GB00249.
- McDowell, N. G., D. R. Bowling, A. Schauer, J. Irvine, B. J. Bond, B. E. Law, and J. R. Ehleringer. 2004b. Associations between carbon isotope ratios of ecosystem respiration, water availability and canopy conductance. *Global Change Biology* **10**:1767-1784.
- Millington, R. J. 1959. Gas diffusion in porous media. *Science* **130**:100-102.
- Misson, L., A. Gershenson, J. W. Tang, M. McKay, W. X. Cheng, and A. Goldstein. 2006. Influences of canopy photosynthesis and summer rain pulses on root dynamics and soil respiration in a young ponderosa pine forest. *Tree Physiology* **26**:833-844.
- Monson, R. K., D. L. Lipson, S. P. Burns, A. A. Turnipseed, A. C. Delany, M. W. Williams, and S. K. Schmidt. 2006. Winter forest soil respiration controlled by climate and microbial community composition. *Nature* **439**:711-714.

- Monson, R. K., J. P. Sparks, T. N. Rosenstiel, L. E. Scott-Denton, T. E. Huxman, P. C. Harley, A. A. Turnipseed, S. P. Burns, B. Backlund, and J. Hu. 2005. Climatic influences on net ecosystem CO₂ exchange during the transition from wintertime carbon source to springtime carbon sink in a high-elevation, subalpine forest. *Oecologia* **146**:130-147.
- Moren, A. S. and A. Lindroth. 2000. CO₂ exchange at the floor of a boreal forest. *Agricultural and Forest Meteorology* **101**:1-14.
- Moyes, A. B. and D. R. Bowling. in prep-a. Plant phenology regulates seasonal variation of soil respiration along Rocky Mountain tree-meadow transects
- Moyes, A. B. and D. R. Bowling. in prep-b. Seasonality of temperature, moisture, and substrate controls on soil respiration in a rocky mountain meadow.
- Moyes, A. B., S. J. Gaines, R. Siegwolf, and D. R. Bowling. in review. Diffusive fractionation complicates isotopic partitioning of autotrophic and heterotrophic sources of soil respiration.
- Moyes, A. B., A. J. Schauer, R. T. W. Siegwolf, and D. R. Bowling. 2010. An injection method for measuring the carbon isotope content of soil carbon dioxide and soil respiration with a tunable diode laser absorption spectrometer. *Rapid Communications in Mass Spectrometry* **24**:894-900.
- Nakayama, F. S. 1990. Soil Respiration. *Remote Sensing Reviews* **5**:311-321.
- Nickerson, N. and D. Risk. 2009a. A numerical evaluation of chamber methodologies used in measuring the $\delta^{13}\text{C}$ of soil respiration. *Rapid Communications in Mass Spectrometry* **23**:2802-2810.
- Nickerson, N. and D. Risk. 2009b. Physical controls on the isotopic composition of soil-respired CO₂. *Journal of Geophysical Research-Biogeosciences* **114**:doi:10.1029/2008JG000766.
- Ocheltree, T. W. and J. D. Marshall. 2004. Apparent respiratory discrimination is correlated with growth rate in the shoot apex of sunflower (*Helianthus annuus*). *Journal of Experimental Botany* **55**:2599-2605.
- Ohashi, M., K. Gyokusen, and A. Saito. 2000. Contribution of root respiration to total soil respiration in a Japanese cedar (*Cryptomeria japonica* D. Don) artificial forest. *Ecological Research* **15**:323-333.
- Olsen, H. R. and H. Van Miegroet. 2009. Factors Affecting Carbon Dioxide Release from Forest and Rangeland Soils in Northern Utah. *Soil Sci Soc Am J* **74**:282-291.

- Palmroth, S., C. A. Maier, H. R. McCarthy, A. C. Oishi, H. S. Kim, K. H. Johnsen, G. G. Katul, and R. Oren. 2005. Contrasting responses to drought of forest floor CO₂ efflux in a Loblolly pine plantation and a nearby Oak-Hickory forest. *Global Change Biology* **11**:421-434.
- Paterson, E., A. J. Midwood, and P. Millard. 2009. Through the eye of the needle: a review of isotope approaches to quantify microbial processes mediating soil carbon balance. *New Phytologist* **184**:19-33.
- Petit, J. R., J. Jouzel, D. Raynaud, N. I. Barkov, J. M. Barnola, I. Basile, M. Bender, J. Chappellaz, M. Davis, G. Delaygue, M. Delmotte, V. M. Kotlyakov, M. Legrand, V. Y. Lipenkov, C. Lorius, L. Pepin, C. Ritz, E. Saltzman, and M. Stievenard. 1999. Climate and atmospheric history of the past 420,000 years from the Vostok ice core, Antarctica. *Nature* **399**:429-436.
- Phillips, S. L. and J. R. Ehleringer. 1995. Limited uptake of summer precipitation by bigtooth maple (*Acer grandidentatum* Nutt) and Gambel's oak (*Quercus gambelii* Nutt). *Trees* **9**:214-219.
- Prevost-Boure, N. C., J. Ngao, D. Berveiller, D. Bonal, C. Damesin, E. Dufréne, J. C. Lata, V. Le Dantec, B. Longdoz, S. Ponton, K. Soudani, and D. Epron. 2009. Root exclusion through trenching does not affect the isotopic composition of soil CO₂ efflux. *Plant and Soil*:1-13.
- Raich, J. W. 1992. The global carbon dioxide flux in soil respiration and its relationship to vegetation and climate. *Tellus* **44B**:81-99.
- Raich, J. W. and A. Tufekcioglu. 2000. Vegetation and soil respiration: Correlations and controls. *Biogeochemistry* **48**:71-90.
- Rayment, M. B. and P. G. Jarvis. 1997. An improved open chamber system for measuring soil CO₂ effluxes in the field. *Journal of Geophysical Research-Atmospheres* **102**:28779-28784.
- Rayment, M. B. and P. G. Jarvis. 2000. Temporal and spatial variation of soil CO₂ efflux in a Canadian boreal forest. *Soil Biology & Biochemistry* **32**:35-45.
- Reichstein, M., A. Rey, A. Freibauer, J. Tenhunen, R. Valentini, J. Banza, P. Casals, Y. F. Cheng, J. M. Grunzweig, J. Irvine, R. Joffre, B. E. Law, D. Loustau, F. Miglietta, W. Oechel, J. M. Ourcival, J. S. Pereira, A. Peressotti, F. Ponti, Y. Qi, S. Rambal, M. Rayment, J. Romanya, F. Rossi, V. Tedeschi, G. Tirone, M. Xu, and D. Yakir. 2003. Modeling temporal and large-scale spatial variability of soil respiration from soil water availability, temperature and vegetation productivity indices. *Global Biogeochemical Cycles* **17**:-

- Risk, D. and L. Kellman. 2008. Isotopic fractionation in non-equilibrium diffusive environments. *Geophysical Research Letters* **35**:-.
- Riveros-Iregui, D. A., J. Hu, D. R. Bowling, and R. K. Monson. in review. Variability in the relation between the stable isotopic composition of ecosystem respiration and climate in a high elevation subalpine forest.
- Ryan, M. G. and B. E. Law. 2005. Interpreting, measuring, and modeling soil respiration. *Biogeochemistry* **73**:3-27.
- Saetre, P. and J. M. Stark. 2005. Microbial dynamics and carbon and nitrogen cycling following re-wetting of soils beneath two semi-arid plant species. *Oecologia* **142**:247-260.
- Savage, K., E. A. Davidson, A. D. Richardson, and D. Y. Hollinger. 2009. Three scales of temporal resolution from automated soil respiration measurements. *Agricultural and Forest Meteorology* **149**:2012-2021.
- Savage, K. E. and E. A. Davidson. 2001. Interannual Variation of Soil Respiration in Two New England Forests. *Global Biogeochem. Cycles* **15**:337-350.
- Scartazza, A., C. Mata, G. Matteucci, D. Yakir, S. Moscatello, and E. Brugnoli. 2004. Comparisons of $\delta^{13}\text{C}$ of photosynthetic products and ecosystem respiratory CO_2 and their response to seasonal climate variability. *Oecologia* **140**:340-351.
- Schadt, C. W., A. P. Martin, D. A. Lipson, and S. K. Schmidt. 2003. Seasonal dynamics of previously unknown fungal lineages in tundra soils. *Science* **301**:1359-1361.
- Schimel, D. S. 1995. Terrestrial ecosystems and the carbon cycle. *Global Change Biology* **1**:77-91.
- Schimel, D. S., J. I. House, K. A. Hibbard, P. Bousquet, P. Ciais, P. Peylin, B. H. Braswell, M. J. Apps, D. Baker, A. Bondeau, J. Canadell, G. Churkina, W. Cramer, A. S. Denning, C. B. Field, P. Friedlingstein, C. Goodale, M. Heimann, R. A. Houghton, J. M. Melillo, B. Moore, D. Murdiyarso, I. Noble, S. W. Pacala, I. C. Prentice, M. R. Raupach, P. J. Rayner, R. J. Scholes, W. L. Steffen, and C. Wirth. 2001. Recent patterns and mechanisms of carbon exchange by terrestrial ecosystems. *Nature* **414**:169-172.
- Schlesinger, W. H. and J. A. Andrews. 2000. Soil respiration and the global carbon cycle. *Biogeochemistry* **48**:7-20.
- Schnyder, H. and F. A. Lattanzi. 2005. Partitioning respiration of C_3 - C_4 mixed communities using the natural abundance ^{13}C approach - testing assumptions in a controlled environment. *Plant Biology* **7**:592-600.

- Schnyder, H., R. Schauffele, M. Lotscher, and T. Gebbing. 2003. Disentangling CO₂ fluxes: direct measurements of mesocosm-scale natural abundance ¹³CO₂/¹²CO₂ gas exchange, ¹³C discrimination, and labelling of CO₂ exchange flux components in controlled environments. *Plant Cell and Environment* **26**:1863-1874.
- Schubert, K. R. and H. J. Evans. 1976. Hydrogen evolution: A major factor affecting the efficiency of nitrogen fixation in nodulated symbionts. *Proceedings of the National Academy of Sciences of the United States of America* **73**:1207-1211.
- Schulze, E.-D. 2006. Biological control of the terrestrial carbon sink. *Biogeosciences* **3**:147-166.
- Scott-Denton, L. E., T. N. Rosenstiel, and R. K. Monson. 2005. Differential controls by climate and substrate over the heterotrophic and rhizospheric components of soil respiration. *Global Change Biology* **12**:205-216.
- Scott-Denton, L. E., T. N. Rosenstiel, and R. K. Monson. 2006. Differential controls by climate and substrate over the heterotrophic and rhizospheric components of soil respiration. *Global Change Biology* **12**:205-216.
- Scott-Denton, L. E., K. L. Sparks, and R. K. Monson. 2003. Spatial and temporal controls of soil respiration rate in a high-elevation, subalpine forest. *Soil Biology & Biochemistry* **35**:525-534.
- Silver, W. and R. Miya. 2001. Global patterns in root decomposition: comparisons of climate and litter quality effects. *Oecologia* **129**:407-419.
- Skopp, J., M. D. Jawson, and J. W. Doran. 1990. Steady-State Aerobic Microbial Activity as a Function of Soil Water Content. *Soil Science Society of America Journal* **54**:1619-1625.
- Sperry, J. S. 2000. Hydraulic constraints on plant gas exchange. *Agricultural and Forest Meteorology* **104**:13-23.
- Sponseller, R. A. 2007. Precipitation pulses and soil CO₂ flux in a Sonoran Desert ecosystem. *Global Change Biology* **13**:426-436.
- Steinmann, K., R. T. W. Siegwolf, M. Saurer, and C. Korner. 2004a. Carbon fluxes to the soil in a mature temperate forest assessed by ¹³C isotope tracing. *Oecologia* **141**:489-501.
- Steinmann, K. T. W., R. Siegwolf, M. Saurer, and C. Korner. 2004b. Carbon fluxes to the soil in a mature temperate forest assessed by C-13 isotope tracing. *Oecologia* **141**:489-501.

- Subke, J.-A., I. Inglima, and M. F. Cotrufo. 2006. Trends and methodological impacts in soil CO₂ efflux partitioning: A metaanalytical review. *Global Change Biology* **12**:921-943.
- Subke, J. A., V. Hahn, G. Battipaglia, S. Linder, N. Buchmann, and M. F. Cotrufo. 2004. Feedback interactions between needle litter decomposition and rhizosphere activity. *Oecologia* **139**:551-559.
- Sulzman, E. W., J. B. Brant, R. D. Bowden, and K. Lajtha. 2005. Contribution of aboveground litter, belowground litter, and rhizosphere respiration to total soil CO₂ efflux in an old growth coniferous forest. *Biogeochemistry* **73**:231-256.
- Takahashi, Y., N. Liang, R. Hirata, T. Machida, and Y. Fujinuma. 2008. Variability in carbon stable isotope ratio of heterotrophic respiration in a deciduous needle-leaf forest. *Journal of Geophysical Research-Biogeosciences* **113**:doi:10.1029/2007JG000478.
- Tang, J. W. and D. D. Baldocchi. 2005. Spatial-temporal variation in soil respiration in an oak-grass savanna ecosystem in California and its partitioning into autotrophic and heterotrophic components. *Biogeochemistry* **73**:183-207.
- Tang, J. W., D. D. Baldocchi, and L. Xu. 2005. Tree photosynthesis modulates soil respiration on a diurnal time scale. *Global Change Biology* **11**:1298-1304.
- Tcherkez, G., S. Nogues, J. Bleton, G. Cornic, F. Badeck, and J. Ghashghaie. 2003. Metabolic origin of carbon isotope composition of leaf dark-respired CO₂ in French bean. *Plant Physiology* **131**:237-244.
- Theis, D. E., M. Jaeggi, D. Aeschlimann, H. Blum, E. Frossard, and R. T. W. Siegwolf. 2007. Dynamics of soil organic matter turnover and soil respired CO₂ in a temperate grassland labelled with ¹³C. *European Journal of Soil Science* **58**:1364-1372.
- Tilman, D., P. B. Reich, J. Knops, D. Wedin, T. Mielke, and C. Lehman. 2001. Diversity and Productivity in a Long-Term Grassland Experiment. *Science* **294**:843-845.
- Van Miegroet, H., J. L. Boettinger, M. A. Baker, J. Nielsen, D. Evans, and A. Stum. 2005. Soil carbon distribution and quality in a montane rangeland-forest mosaic in northern Utah. *Forest Ecology and Management* **220**:284-299.
- Van Miegroet, H., M. T. Hysell, and A. D. Johnson. 2000. Soil Microclimate and Chemistry of Spruce-Fir Tree Islands in Northern Utah. *Soil Science Society of America Journal* **64**:1515-1525.

- Vitousek, P. M., L. R. Walker, L. D. Whiteaker, D. Mueller-Dombois, and P. A. Matson. 1987. Biological Invasion by *Myrica faya* Alters Ecosystem Development in Hawaii. *Science* **238**:802-804.
- Wallenstein, M. D., S. K. McMahon, and J. P. Schimel. 2009. Seasonal variation in enzyme activities and temperature sensitivities in Arctic tundra soils. *Global Change Biology* **15**:1631-1639.
- Wan, S. Q. and Y. Q. Luo. 2003. Substrate regulation of soil respiration in a tallgrass prairie: Results of a clipping and shading experiment. *Global Biogeochemical Cycles* **17**:-.
- Wardle, D. A., R. D. Bardgett, J. N. Klironomos, H. Setälä, W. H. v. d. Putten, and D. H. Wall. 2004. Ecological Linkages between Aboveground and Belowground Biota. *Science* **304**:1629-1633.
- Weintraub, M. N., L. E. Scott-Denton, S. K. Schmidt, and R. K. Monson. 2007. The effects of tree rhizodeposition on soil exoenzyme activity, dissolved organic carbon, and nutrient availability in a subalpine forest ecosystem. *Oecologia* **154**:327-338.
- Wieser, G. 2004. Seasonal variation of soil respiration in a *Pinus cembra* forest at the upper timberline in the Central Austrian Alps. *Tree Physiology* **24**:475-480.
- Xu, L. K., D. D. Baldocchi, and J. W. Tang. 2004. How soil moisture, rain pulses, and growth alter the response of ecosystem respiration to temperature. *Global Biogeochemical Cycles* **18**:GB4002, doi:4010.1029/2004GB002281.
- Xu, L. K., M. D. Furtaw, R. A. Madsen, R. L. Garcia, D. J. Anderson, and D. K. McDermitt. 2006. On maintaining pressure equilibrium between a soil CO₂ flux chamber and the ambient air. *Journal of Geophysical Research-Atmospheres* **111**:D08S10, doi:10.1029/2005JD006435.
- Xu, M. and Y. Qi. 2001. Soil-surface CO₂ efflux and its spatial and temporal variations in a young ponderosa pine plantation in northern California. *Global Change Biology* **7**:667-677.